HOST DEFENCE PEPTIDE (HDP) HUMAN BETA DEFENSIN 9 (HBD9)

Nazri Omar, MD

Submitted to the University of Nottingham for the degree of Doctor of Philosophy

Table of content

List of figures

List of tables

Abbreviation

Acronym	Definition
AM	Amniotic membrane
AMPs	Antimicrobial peptides
Ara-B	Arabinosa B
araBAD	L-arabinose operon
ATP	Adenosine triphosphate
Bin1b	rat epididymis-specific beta-defensin
BisTris	organic tertiary amine for buffering agent
BLAST	Basic Local Alignment Search Tool
BlastN	Basic Local Alignment Search Tool - Nucleotide
BNBD12	Bovine beta defensin 12
BNBD2	Bovine beta defensin 2
BP	Base pair
BSA	Bovine serum albumin
CA	Chromosomal aberration
CAP-18	Cathelicidin
CCR6	Chemokine receptor 6 gene
cDNA	Complementary deoxyribonucleic acid
CFU	Colony forming unit
CFU/ml	Colony forming unit/ml
CNV	Copy number variance
Co-NTA	Cobalt-nitralo-triacetic acid
CT	Computed tomography
CV	Column volume
DEFA	Alpha defensin gene
DEFB	Beta defensin gene
DEFT	Theta defensin gene
DNA	Deoxyribonucleic Acid
dNTP	Deoxy-nucleotide tripeptide
DS	Double strand
DTT	Dithiothreitol
EDTA	Ethylene-diamine-tetraacetic Acid
EK	Enterokinase
ESBL	Extended spectrum beta-lactamase
EtBr	Ethidium bromide
ExPasy	SIB Bioinformatics Resource Portal, databases and softwares
FISH	Fluorescence In Situ Hybridization
FPLC	Fast Protein Liquid Chromatography
FPRL1	Formyl peptide receptor 1
hBD	Human beta defensin
hBD1	Human beta defensin 1
hBD9	Human beta defensin 9
hCAP-18	Human cathelicidin
HD	Human Defensin
HD5	Human Defensin 5

Acronym	Definition
HD6	Human Defensin 5
HDP	Human Defence Peptide
HDPs	Human Defence Peptides
HGPRT	Hypoxanthine-guanine phosphoribosyl transferase
HisPur	Histidine purification
HisTag	Histidine tag
HIV-1	Human immunodeficiency virus
HMM	Hidden Markov Model
HNP1	Human Neutrophils Peptide 1
HNP2	Human Neutrophils Peptide 2
HNP3	Human Neutrophils Peptide 3
HPLC	High-Performance Liquid Chromatography
HPRT1	Hypoxanthine phosphoribosyl transferase 1
IEC	Ion-Exchange Chromatography
IFN	Interferon
IgA	Immunoglobulin A
IGF-1	Inhibitory Growth Factor
IgG	Immunoglobulin G
IL-1	Interleukin 1
IL-11	Interleukin 11
IL-1β	Interleukin 1-β
IL-6	Interleukin 6
IMAC	Immobilized Metal Ion Affinity Chromatography
Image J	Gel analysis software, NCBI
IPTG	Isopropyl thio-β-D-galactoside
JNK	C-Jun N-Terminal Kinase
K12	K12 Escherichia coli
lacUV5	Lac promoter
LB	Luria Bertani
LB/Amp	Luria Bertani/ampicillin
LD	Lethal Dose
LEAP	Liver-expressed antimicrobial peptide
LL37	Synonym for hCAP18
LPS	Lipopolysaccharide
MBL	Nitrogen-limiting culture medium for fungus
MBP	Maltose-Binding Protein
MCP1	Monocyte chemo-attractant peptide 1
MCP2	Monocyte chemo-attractant peptide 2
MD	Doctorate Of Medicine
mg/L	Milligram per liter
MIC	Minimal inhibitory concentration
mRNA	Messenger ribonucleic acid
MW	Molecular weight
NCBI	National Center For Biotechnology Information
NFKB	Nuclear Factor Kappa B
NIH	National Institutes Of Health

Acronym	Definition
Ni-NTA	Nickel nitralo-triacetic acid
NK	Natural Killer
NMR	Nuclear magnetic resonance
NTA	Nitrilotriacetic Acid
OD_{600}	Optical density
OS	Left eye
p38MAPK	p38 mitogen-activated protein kinase
PAGE	Polyacrylamide gel electrophoresis
PAMP	Pathogen associated molecular pattern
PBS	Phosphate buffered saline
PCR	Polymerase chain reaction
proHD-5	Propeptide human defensin 5
PRRs	Pathogen recognition receptor
RBS	Ribosome binding bite
rEK	Recombinant enterokinase
RNA	Ribonucleic acid
RNAP	RNA polymerase
rRNA	ribosomal ribonucleic acid
RT-PCR	Reverse transcription-polymerase chain reaction
SC	Single cut
SDS-PAGE	Sodium dodecyl sulfate - polyacrylamide gel electrophoresis
SDS	Sodium dodecyl sulfate
SLR	Single lens refraction
SNP	Single nucleotide polymorphism
SOC	Super optimum culture media
SSP	Secretory signal peptide
SUMO	Small ubiquitin-related modifier
T4 ligase	T4 ligation enzyme
T7	Recombinant phage with the cloned gene for T7 RNA polymerase
TAP	Tracheal antimicrobial peptide
TBE	Tris-Boric EDTA
T-cell	T cell
TEV	Tobacco Etch Virus
TGF-α	Tumour growth factor alpha
TLR-2	Toll-like receptor 2
TNF-α	Tumour necrosis factor alpha
tRNA	Transport RNA
UK	United Kingdom
USA	United States of America
UTR	Untranslated region
WB	Western blot
X-gal	5-bromo-4-chloro-3-indolyl-beta-D-galacto-pyranosid
X-ray	X-ray

Acknowledgement

I would first like to thank The Almighty Allah, the Most Gracious and the Most Merciful, for allowing me to undertake this study and research project. Special thank goes to Professor Dua HS for accepting me into the PhD programme in the Division of Ophthalmology, University of Nottingham, and to Associate Professor Dr. Andrew Hopkinson for the ideas, suggestions and guidance, and their constant and tireless support and encouragement, they have been providing throughout this study.

I would also like to thank all fellow researchers, colleagues and friends in the Division of Ophthalmology and Visual Sciences, School of Clinical Sciences, University of Nottingham for their help, support and assistance, without which this study would not be possibly accomplished. I am also grateful to Dr. Mohamed Hamed and Dr. Alexander Tarr from the Molecular Biology Lab, Queen's Medical Centre for their kind assistance in the conducting some of the experiments.

Last but not least, my gratitude also goes to my wife Nila Kandi Juita Idris, who has remained by my side throughout the study period. I thank my children Ridhwan, Azreen, Farah, Eizlan, Ezzriq and Insyirah who came to experience the life abroad at the very early stage of their lives, in order to allow me going through the study at the PhD level in Nottingham. I must mention herewith that there were many other people who have contributed in one way or another to this research, whom naming each of them here may not be technically possible. I am very grateful for their understanding, tolerance, support and sacrifice. Thank you very much.

Abstract

Introduction: The emergence of antibiotic resistance has led to the continuing search for discovery of effective antibiotics. Host defence peptides (HDPs) confer defence mechanisms against infection and investigation of their specific roles and interplays are ongoing. Among the HDPs, defensins are a group of effector molecules which plays important roles in humans. Although several stereotypes of human beta defensins (hBDs) such as the hBD1-3 are well studied, other members including the human beta defensin 9 (hBD9), are not entirely known. Understanding the properties of these HDPs will enable us to discover a safe and efficacious, broad-spectrum and resistance-free antibiotic for therapeutic application in the future.

Purpose: The purpose of this study is to clone the *DEFB109* gene, express and purify the hBD9 propeptide, before determining the hBD9 propeptide antimicrobial property using a recombinant system in *Escherichia coli*.

Methods: The second exon of the *DEFB109* was amplified through reverse transcription polymerase chain reaction (RT-PCR) and inserted into selected plasmid vectors. The recombinant plasmid construct was cloned, and transformed into an *E. coli* expression host. The correctly transformed colonies were selected before the plasmid constructs were purified and verified through nucleotide sequencing. Expression and purification of the hBD9 propeptide were carried out and antimicrobial property of the peptide was investigated.

Result: HBD9 fusion protein was successfully expressed and purified. It was shown to have antimicrobial efficacy against *Staphylococcus aureus* and

Pseudomonas aeruginosa. The effect of the free hBD9 propeptide against wider spectrum of organisms needs to be studied in the future.

Executive summary

Chapter 1

The ocular surface (OS) defence mechanism can be divided into anatomical barrier, physiological barrier and immunological barrier which comprise the innate and adaptive immunity. In the anatomical barrier, the bony orbit provides protection to the eyeball including the ocular surface. The upper and lower eyelids protect the eyes from environmental agents such as intense light, heat and rapidly approaching objects, and from infective organisms. When closed, the lid margins form a water-tight barrier and when opened spread the tears across the ocular surface to remove foreign particles including germs. The eyelashes along the eyelid margins enhance the protective mechanism by filtering foreign particles and preventing them from entering the eye.

The physiological barrier in the ocular system includes blinking, Bell's phenomenon, and the tear system containing enzymes such as lysozyme and defence molecules such as globulin and lactoferrin. Blinking and Bell's phenomenon limit the access of pathogens to the ocular surface especially the cornea. The tear system further strengthens the ocular surface defence mechanisms. It hinders infection of the ocular surface which could spread into deeper ocular tissue if not managed appropriately. Further enhancement of the ocular defence is provided by the immunological system in the form of innate and adaptive responses. It forms an important part of ocular surface defence against inflammatory agents including infective organisms. Innate immunity is the first response where a host cellular receptor binds non-specifically with certain ligand of the pathogens (pathogen associated

molecular pattern, PAMPs) leading to a direct killing of the pathogens. In adaptive immunity, upon host encounter with the pathogens, a cascade of events including production of chemokines, and induction and proliferation of white blood cells, is activated which eventually result in the containment of the infection.

Human defence peptides (HDPs) are small cationic amphiphilic molecules. They have between 20 to 50 amino acid residues, nett positive charges between +2 to +9 and around 20 to 50% hydrophobic residues. Defensins are HDPs occurring in plants, insects, invertebrates and vertebrates and demonstrate antimicrobial activity against wide range of pathogens. They are rich in cysteine residues which are typically arranged in the peptide. The most fundamental property of defensins is their antimicrobial activity against gram positive and negative bacteria, fungi, parasites and viruses.

Three families of mammalian defensins have been described, namely, the α-, β- and θ-defensins but only α- and β-defensins have been isolated in humans while θ-defensin has only been described in non-human primates. In humans, α-defensin is mainly found in neutrophils (α-defensins 1-4) and in the Paneth cells of the small intestines (α-defensins 5-6). β-defensins, in contrast to α-defensins, have wider distributions and are mainly found at the epithelial surfaces of tissues such as in intestine, lung, pancreas, kidney, skin and oral cavity.

β-defensin has six conserved cysteine residues linked into three pairs by disulphide bridges. However, in contrast to the α-defensin where the first cysteine is linked with the sixth cysteine, the first cysteine in β-defensin is

linked to the fifth cysteine. The first mammalian β-defensin was isolated from bovine trachea (tracheal antimicrobial peptide) in 1991. The first human β-defensin, hBD1, was initially purified from hemofiltrates in 1995. Expression of *DEFB109* on the OS was first reported by Abedin *et al.* They found that *DEFB109* was down-regulated in OS infection and inflammation and postulated that it may not have any major antimicrobial role as its level was reduced during infections.

The continuous emergence of resistance strains to the existing antibiotics makes the discovery of an efficacious antibiotic which has not only broad spectrum but also resistance-free be given high emphasis. Beta defensins including hBD9 are potential candidates but it may not be straightforward as it seems as they also have other functions such as immunomodulation, anti-apoptosis and anti-cancer. This research was designed and conducted with the intention to further investigate the antimicrobial property of hBD9. As the peptide had never been isolated from any tissue, a genetic engineering method was used to construct the recombinant plasmid DNA. It was later transformed into *E. coli.* Expression of the heterologous protein was followed with purification steps using liquid chromatography methods.

Chapter 2

From the computational methods, there are more than 30 members of hBD that have been identified in humans to date. Most of these genes are located in an 8 Mb region on locus 23.1 of the long arm of chromosome 8, also known as 8p23.1 which contains two clusters. The first cluster contains

DEFB1, *DEFA1* to *-6* and *DEFT1* while the second cluster contains *DEFB4*, *DEFB103* to *-109* and *SPAG11*. Six *DEFB* genes in the second cluster, namely *DEFB4* and *-103* to *-107* were found to be copy number variable but there was no data excluding *DEFB108* and *DEFB109* from the copy number variable region. *In silico* analysis has also identified additional clusters of putative β-defensin genes at 20p13, 20q11.1 and 6p12.

This chapter describes the process of preparing the recombinant plasmid DNA pET21a-*DEFB109* and its transformation into the *E. coli* cloning host. The second exon of *DEFB109* gene encoding the hBD9 propeptide was identified from the NCBI online database and chosen for the cloning work. Primers were designed to amplify the gene from human complementary DNA (cDNA). Forward primer had several motifs including upstream flanking nucleotide residues followed by *Bam*HI recognition site, start codon and several initial nucleotide residues of the *DEFB109* gene. The reverse primers contained several last nucleotide residues of the *DEFB109* gene without the stop codon, *Xho*I restriction site followed by several downstream flanking nucleotides. The primers were synthesised and purchased from Eurofins MWG Operans, Germany.

Conventional PCR was used to successfully amplify the *DEFB109* second exon. Each reaction consisted of 5.0 µl 10X PFU PCR buffer, 2.0 µl 2.5 µM dNTP, 0.25 µl Tween, 1.0 µl PrimerMix, 0.25 µl PFU Ultra II DNA polymerase (Agilent Technologies, London, UK), 1.0 µl DNA template, and PCR water added to a final volume of 25 µl. The reaction cycle used was 95 ^{0}C for 15 minutes for the denaturing step. This was followed by 37 cycles of further denaturing at 95 ^{0}C for 1 min, annealing at 56 ^{0}C for 1 minute and

elongation at 72 °C for 30 seconds. Final elongation step was 72 °C for 10 minutes.

pET21a(+) was chosen as the plasmid vector as it contained the ampicillin resistance, *Bam*HI and *Xho*I restriction sites, HisTag and the stop codon. Both the *DEFB109* PCR product and the pET21a(+) were double digested using the *Bam*HI and *Xho*I restriction enzymes. Upon directional ligation using the T4 DNA ligase system, the *DEFB109* was inserted into the linearised plasmid vector between the *Bam*HI and *Xho*I restriction sites.

The recombinant plasmid DNA pET21a-*DEFB109* was then transformed into the cloning host, *E. coli* NovaBlue cells. 50 µl of the transformed E. coli was cultured onto LB/Amp agar plate and incubated at 37 °C overnight. A single colony was picked and subcultured into LB/Amp broth and incubated at 37 °C and 200 rpm shaking for 3 hours before the purification of the plasmid DNA was performed. The purified recombinant plasmid DNA was verified by sequencing which showed successful cloning of the pET21a-*DEFB109* recombinant DNA.

Although the *DEFB109* gene was successfully cloned into the recombinant plasmid DNA and transformed into the *E. coli* cloning host, it was later realised that there were a few issues with the pET21a plasmid vector. While it allowed insertion of the *DEFB109* gene, it did not have suitable features for expression and purification of a disulphide bond-containing heterologous protein such as hBD9, which included the solubility tag such as Trx tag and proteolytic sites for removal of fusion partner. Therefore, a more suitable plasmid vector with modification of the recombinant strategy was planned while maintaining the conditions for the

cloning reactions such as PCR, restriction digestion, ligation and transformation reaction.

Chapter 3

In addition to hBD9 being fastidious for solubility fusion tag, its expression in *E. coli* is also associated with preferred codon bias. Therefore, while *E. coli* is an easy host to grow, rapidly and at low cost, the recombinant gene needs to be improved to the sequence preferred by the *E. coli*. This chapter describes the conversion of the native to the optimised gene, before both being inserted into the pET32a plasmid vector through various steps of genetic engineering.

In continuation from cloning work described in the earlier chapter, the recombinant strategy was further refined in order to express the soluble fusion protein in high amount. Plasmid vector pET21a(+) was replaced with the pET32(a)+ which has several advantages including Trx solubility tag which support the disulphide bond formation by allowing proper folding of the newly synthesised peptide, and thus increased solubility of the fusion protein. It also has N-terminal HisTag for purification of the fusion protein using immobilised metal affinity chromatography and removal of the fusion partner. The same HisTag can be used to separate the fusion tag from the free hBD9 following proteolysis. Its enterokinase proteolytic site can be utilised to cleave the hBD9 from the fusion partner. The *DEFB109* gene second exon was inserted into the linearised pET32a(+) plasmid vector immediately downstream to the enterokinase cleavage site, between *Nco*I and *Bam*HI restriction sites.

The second exon of the *DEFB109* was also converted into *E. coli* preferred-codon sequence to overcome codon bias and thus increase expression. It was synthesised and ligated to a location similar to the earlier-described location for native *DEFB109* gene, in the linearised pET32a(+). The native and optimised recombinant plasmid DNAs were then transformed into *E. coli* NovaBlue cloning host before being purified, quantified and sequenced for verification. Sequencing result showed that both the native and the optimised pET32a-*DEFB109* plasmid DNAs were present in the cloning host in an in-frame fashion.

The main objective of this chapter was to compare the expression of Trx-hBD9 fusion protein of the native and optimised plasmid DNAs. BL21(DE3)pLysS harbouring the native and the optimised *DEFB109* genes were induced with 0.5 mM IPTG in an incubator shaking at 200 rpm for several incubation periods. SDS-PAGE was run and the gel was analysed for the hBD9 fusion protein. For both the native and optimised genes, the relative expression of fusion protein increased with increasing incubation time. The expression from the optimised gene is marginally higher than from the native gene. The ratio between the optimised and the native hBD9 fusion protein expression was 1.097 ± 0.056 (mean ± standard deviation), across all incubation time points (Table 3.4.1). The optimised gene did not show an advantage over the native gene in terms of the expression of soluble fusion protein induced with 0.5 mM IPTG at 24 ^{o}C across all induction durations.

Peng *et al* conducted a study on the optimised gene expression for hBD2 in BL21(DE3) *E. coli*. They noted that the recombinant fusion protein was more than 50% of total protein expressed and increased by 9-fold

compared to the native gene. Huang *et al* expressed the pET32a-*DEFB103* optimised gene in *E. coli* using 0.5 mM IPTG. They reported fusion protein production of 0.99 g/L and 96 % purity. The soluble target protein was 45% of total soluble protein.

We did not find significant advantage in the fusion protein expression from optimised gene compared to the native gene. This could be due to other factors related to heterologous protein expression in *E. coli*. Although the gene was optimised to that preferred by *E. coli*, the tRNA for the gene was not optimised at the same time. This could hinder improved expression of the optimised gene. However, it is recommended this experiment is carried out several times and the result be verified before the other possibilities are explored.

Chapter 4

Using the pET32a(+)-DEFB109 optimised plasmid DNA, small scale induction experiments were conducted to investigate best conditions for the expression of high amount of soluble hBD9 peptide. Several strains of *E. coli* expression host, IPTG concentration, incubation duration and temperature were tested before in order to determine the suitable expression host and a set of best induction parameters to express high amount of soluble Trx-hBD9 fusion protein. These findings will later be used for the upscale hBD9 expression and purification stage.

Having the hBD9 tagged to Trx solubility fusion partner, the soluble protein was expected to increase but the increment was found to not exceed 50% of the total fusion protein. The insoluble fraction was expressed at

higher concentration compared to soluble fusion protein in BL21A1 and Origami 2 expression hosts, for induction with 0.5 mM IPTG at 24 ^{o}C for 4 hours in incubator shaking at 200 rpm. When the concentrations of soluble fusion protein in induced BL21(DE3)pLysS, BL21(DE3)pLysE and Origami 2 were compared, the highest concentration was found in the BL21(DE3)pLysS.

The influence of IPTG concentration on the soluble fusion protein expression was investigated using 0.3 to 1.2 mM in Origami 2 expression host induction set at 24 ^{o}C and 200 rpm shaking for 3 hours. We found that the highest concentration of soluble fusion protein was given by the sample induced with final concentration of IPTG of 1.0 mM. In another experiment, induction in BL21A1 *E. coli* expression host at 24 ^{o}C and 200 rpm for up to 18 hours incubation also showed increasing soluble fusion protein band intensity when the IPTG concentration was increased from 0.5 to 0.75 and 1.0 mM.

With regard to the induction duration, our experiment in BL21(DE3)pLysS *E. coli* expression host induced with 0.5 mM IPTG at 24 ^{o}C and 200 rpm shaking showed that soluble fusion protein band intensity increased by 1.67, 9.79, 12.25 and 16.38 fold when the duration was extended to 2, 4, 6 and 8 hours, respectively.

The effect of induction temperature on the soluble fusion protein expression was also investigated. Inductions at 28 ^{o}C and 37 ^{o}C were carried out for BL21(DE3)pLysS, -pLysE and Origami 2 *E. coli* expression strains. It was found that expression at 28 ^{o}C produced greater fusion protein band intensity compared to expression at 37 ^{o}C.

Various factors may influence the heterologous expression of Trx-hBD9 fusion protein and each of these factors needs optimisation to achieve highest amount of soluble fusion protein. We found the best condition to achieve this is by performing induction in the BL21(DE3)pLysS *E. coli* strain with 1.0 mM IPTG concentration for 4 hours at 28 ^{o}C at 200 rpm shaking. The 4 hour incubation was preferred after taking time efficiency and availability of orbital shaker incubator in the shared laboratory setting, into consideration.

Chapter 5

The purification involving several steps was conducted. The large scale fermentation of 1L LB/amp media was used for induction in BL21(DE3)pLysS *E. coli* strain harbouring the optimised pET32a-*DEFB109* recombinant plasmid DNA, using 0.5 mM IPTG at 24 ^{o}C and 200 rpm for 4 hours. The expressed soluble Trx-hBD9 fusion protein was purified through several liquid chromatography steps such as the HisTag IMAC, buffer exchange, cation exchange and size exclusion chromatography.

The induced *E. coli* culture was harvested in a high speed centrifuge at 6,000 G and 4 ^{o}C for 20 minutes. The cell pellet was suspended with 10 ml BugBuster cell lysis buffer per gram wet weight of pellet. The bacterial suspension was again centrifuged at 6,000 g and 4 ^{o}C for 20 minutes to separate the insoluble protein (pellet) from the soluble protein (supernatant).

The soluble fraction was subjected to HisTag IMAC using the gravity column and pressure column attached protein purifier (Bio-Rad, Hemel Hempstead, UK), without UV detector, pH sensor and the computerised

analytical software. In the gravity column method, approximately 10% of the loaded amount of fusion protein was lost in the binding follow-through sample. After further loss in the column washing step, the percentage of total eluted fusion protein in 4 fractions was 81.46%. In the pressure column method, SDS-PAGE analyses showed presence of oligomeric fusion protein in the eluted samples. The average percentages of monomeric and dimeric fusion protein were 45.7% and 31.43%, respectively. The rate of protein recovery for this experiment could not be determined due to the unavailability of detection system and analytical software system for the purifier machine.

The HisTag-purified samples of fusion protein subjected to desalting step using the PD10 column. This is to remove the salt and imidazole from the samples before subsequent step of enterokinase cleavage of the hBD9 peptide from the Trx fusion partner. The eluted desalted samples were subjected to SDS-PAGE and the image of the gel was analysed. Bands corresponding to the monomeric and dimeric forms of the fusion protein could be seen in the eluted samples. The protein concentrations in the eluted samples were quantified using the nanodrop spectrophotometer. The average percentage of fusion protein recovery from this step was 77.04% ± 12.81% (mean ± SD).

Cleavage using the recombinant enterokinase enzyme was conducted to separate the hBD9 from its fusion partner. In this step, protein to enzyme ratio, temperature and duration of cleavage were optimised. The cleavage product was subjected to SDS-PAGE for verification of the cleavage result. In the preliminary experiment, 50 µg purified and desalted fusion protein was incubated at 21 ^{o}C (room temperature) with 5 µl of 10X cleavage buffer and 1

iu (1 iu/µl) of rEK to a final volume of 50 µl, for 4 hours. SDS-PAGE and western blot analysis showed there was a band corresponding to approximately 20 kD suggestive of the Trx fusion partner was seen in the SDS-PAGE gel image but there was no band to represent the free target protein was seen. Nevertheless, the western blot analysis showed that there was a single band corresponding to approximately 8 kD suggestive of the free target protein. There was no trace of fusion protein seen on the same western blot membrane.

In addition to low imidazole and salt tolerance, cleavage using rEK was associated with non-specific cleavage. For protein to enzyme ratio of 50:1 and 21 ^{0}C incubation temperature, 16 hour incubation had the highest proportion of appropriately cleaved protein and the lowest miscleaved protein. The non-cleavage rate was 16.4% (2.5 µg). However, allowing cleavage for a longer period was associated with a higher proportion of non-specific cleavage, and thus, reduction in the properly cleaved protein. In conclusion, 2 hour cleavage gives the highest appropriate cleavage rate and lowest miscleavage rate.

Although the rEK cleavage of the fusion protein was shown to be effective, subsequent purification of the free hBD9 peptide was not successful. By using the spin column to bind and remove the rEK enzyme followed by the IEC for retrieval of the free hBD9, the already small amount of the free hBD9 was lost in the bind and wash follow through and could not be detected in eluted samples from SDS PAGE. It was reckoned that the expensive rEK and the low substrate to enzyme ratio were the limiting factors to cleave higher amount of fusion protein. Hence, increasing the efficiency of

cleavage is very important. In addition, the subsequent purification steps must also be sensitive and effective to purify the free hBD9.

Chapter 6

While performing the purification of the free hBD9 following the successful HisTag IMAC and desalting step, preliminary verification of antimicrobial property of the fusion protein was performed. The fusion protein comprised the fusion partner Trx tag and the hBD9 propeptide. It was reported in a study by Wu *et al* that the Trx tag in a control reaction did not have any antimicrobial effect compared to the Trx-BNBD12 fusion protein against gram positive and gram negative bacteria. Therefore, we believed that the antimicrobial effect demonstrated in this work resulted only from the hBD9 and not the Trx tag.

The bacterial load for the antimicrobial experiment was determined using the serial dilution method. Starter cultures of *Pseudomonas aeruginosa* and *Staphylococcus aureus* were allowed to grow to OD_{600} of 0.5. These cultures were diluted approximately 10 times to OD_{600} 0.07 and 0.08 for *Pseudomonas aeruginosa* and *Staphylococcus aureus*, respectively. Serial dilution and culture method revealed that *Pseudomonas aeruginosa* with OD_{600} of 0.07 contained 2.2×10^{14} CFU/ml while *Staphylococcus aureus* with OD_{600} of 0.08 contained 1.36×10^{9} CFU/ml of bacteria.

Based on the CFU count result, approximately 1×10^{6} of each bacterium was incubated with hBD9 fusion protein at a final concentration of 100 µg/ml for 4 hours. 100 µl of reaction were collected at 0, 2 and 4 hour time points, and serially diluted 10-fold for 10 dilutions. 50 µl of each dilution

were then plated onto LB plates for CFU determination. Similar untreated culture was set as a control. At 0 hour time point, both the treated and untreated *Pseudomonas aeruginosa* and *Staphylococcus aureus* had similar CFU counts per ml of culture.

At 2 hour time point, there were reductions seen in the CFU counts of the treated *Pseudomonas aeruginosa* and *Staphylococcus aureus* compared to untreated controls, respectively. Treated *Pseudomonas aeruginosa* showed CFU/ml of 3.6 X 10^7 compared to 2.0 X 10^{10} in untreated control while treated *Staphylococcus aureus* showed CFU/ml of 2.3 X 10^7 compared to 3.6 X 10^{10} in untreated control. At 4 hour time point, bacterial growths were equally confluent in the treated and untreated *Pseudomonas* and *Staphylococcus*, making it impossible to detect any difference in CFU counts. The hBD9 fusion protein concentration of 100 µg/ml was probably too low to have a sustainable effect on the bacterial growth over four hour period of incubation.

It was also shown that there was a certain dose-response relation between the hBD9 fusion protein and the antimicrobial effect. Trx-hBD9 with a concentration of 71 µg/ml inhibited higher load of *Staphylococcus aureus* and *Pseudomonas aeruginosa* than the fusion protein of 38 µg/ml concentration. Nevertheless, the results are only suggestive of possible antimicrobial property of the hBD9. It must be taken with caution and further experiment is required. Only when the free target hBD9 is highly purified and tested repeatedly against microbial agent, can we confirm whether it has an antimicrobial property against specific bacteria or not.

It is recommended that MIC and MBC in which the minimum amount of peptide required to inhibit the growth and to completely kill the bacteria, respectively, be determined using the free hBD9. The spectrum of the susceptible organism can also be determined and compared with the existing data on the antimicrobial efficacy of other beta defensins.

Chapter 1

Literature Review

CHAPTER 1: Literature review

1.1 Introduction

The eye is an organ which allows a person to see by permitting light to reach the sensory retina. The light will be converted into electrical impulses and ultimately transmitted to the responsible visual centre in the occipital lobe of the brain. In order to fulfil this role, the eye is positioned on the head surface with modified lining formed by the conjunctiva and the cornea. This mucosal lining is called the ocular surface (OS) and it is in constant contact with the external environment [1]. As such, it faces a constant threat from invading pathogens, although infection is relatively rare [2]. Therefore, the OS is equipped with built-in protective mechanism against infection, which is conferred largely by the innate immune system [3]. The innate immunity comprises of a relatively simple, but highly efficient, natural immune system to combat microbial challenges. The protein 'effectors' of the innate immune system are believed to be effective endogenous natural antibiotics [4]. The idea of these molecules being efficacious chemotherapeutic agents against infection has been subject to extensive investigation with great promise, though several related issues require attention [5].

The continuous introduction of new generations of more effective antibiotics to the market has been the mainstay to circumvent infection at the OS. However, emergence of resistant strains following widespread use of antibiotics in clinical, veterinary and agricultural industries has made the search for a new effective broad-spectrum antibiotic intensified [6]. The

potential of human defence peptide (HDP) as safe and effective broad-spectrum antibiotic agents continuously receives great attention.

1.1.1 Ocular surface anatomy

The OS contributes to ocular function by allowing light to pass through the tear film and the transparent cornea. It also confers a frontline defence mechanism against environmental insults, which include hostile physical conditions, infection and mechanical injury. The OS comprises the conjunctiva, cornea and limbus (Figure 1.1.1) [7].

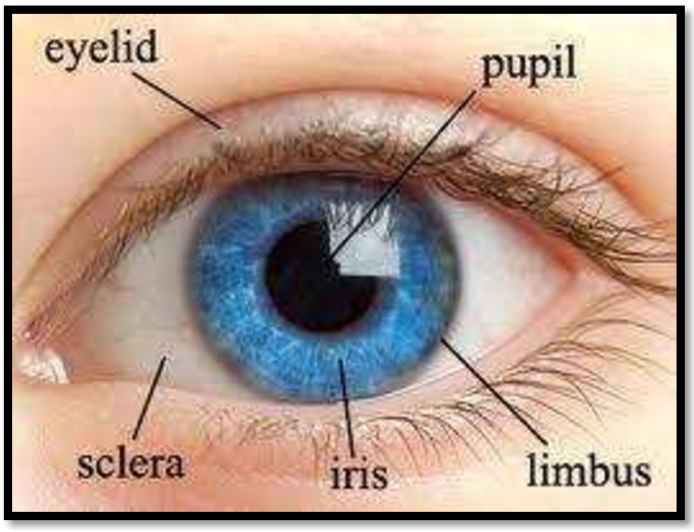

Figure 1.1.1 Photograph of the eye (axial view) showing different structures of the eye. The conjunctiva and the cornea form the mucosal lining of the ocular surface (OS) - *image taken from http://scienceeasylearning.wordpress.com.*

1.1.1.1 Conjunctiva

The conjunctiva is the continuous transparent mucous lining of the inner surface of the eyelids and the anterior eyeball surface, which makes up the majority of the OS (Figure 1.1.2). It originates from the limbus and extends to the eyelid margins.

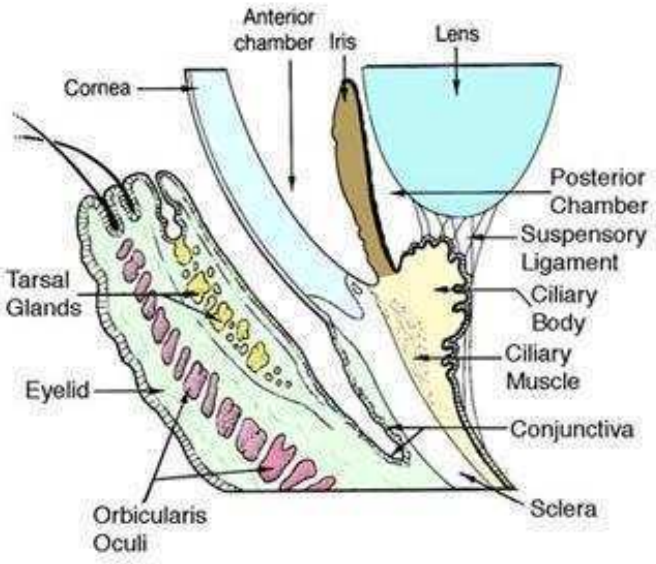

Figure 1.1.2 Diagram of the sagittal view of the eye showing the conjunctival lining which is continuous with the cornea, forming the ocular surface (OS) - *image taken from www.medicalook.com*.

The conjunctiva has two distinct layers:

1.1.1.1 (a) Conjunctival epithelium

Conjunctival epithelium consists of anterior stratified columnar epithelium which is continuous with the corneal epithelium, and is two to seven cell layers thick. It contains numerous unicellular mucous glands (goblet cells) that secrete the inner mucoid layer of the tear film [8].

1.1.1.1 (b) Conjunctival stroma

This is the lamina propria which composed of adenoid and fibrous layers. The lamina propria is composed of connective tissue which contains blood vessels, nerves, and glands. The glands of Krause are accessory lacrimal glands which are located at the superior and inferior fornices where they number approximately 42 and 6 to 8, respectively. These glands

produce the aqueous component of the tear film. The accessory lacrimal glands of Wolfring are another type of accessory lacrimal glands situated near the upper margin of the superior tarsal plate and produce the basal aqueous tear secretion [7].

1.1.1.2 Cornea

The cornea is an almost round, transparent, dome shape part of the OS. It measures 10.6 mm vertically and 11.7 mm horizontally in an average adult and can be divided into five distinct layers. From anterior to posterior, the layers are: (i) the epithelium, (ii), the Bowman's layer, (iii) the stroma, (iv) the Descemet's membrane and, (v) the endothelium (Figure 1.1.3) [8].

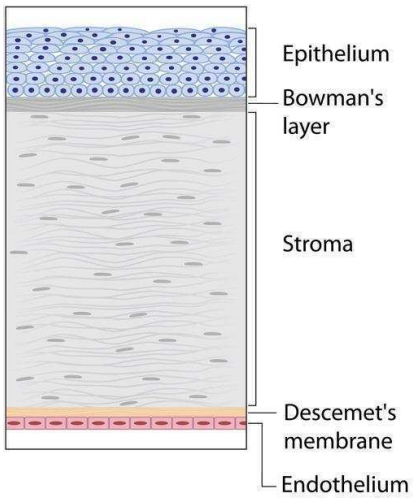

Figure 1.1.3 Diagram of the cross section of the cornea showing the five different layers. The epithelium is the outermost layer while the endothelium is the innermost layer - image taken from http://discoveryeye.org/tag/cornea-2/.

1.1.1.2 (a) The epithelium

Corneal epithelium consists of stratified non-keratinised squamous cells. It has a thickness of 5 to 7 cells and can, in term of cell layers, be divided into basal, suprabasal and superficial wing cell layers. The basal layer rests on epithelial basement membrane which is itself divided into basal lamina lucida and lamina densa. The suprabasal layer is 3 to 4 cells thick while the superficial wing cell layer is 2 to 3 cells thick (Figure 1.1.4). The presence of glycocalyx on the superficial cell layer of the corneal epithelium allows the mucinous layer of the tear film to adhere to the entire corneal surface. The mucinous layer is continuous with the aqueous layer of the tear film. This phenomenon converts the hydrophobic epithelial surface into a hydrophilic surface. Any disruption of the epithelium renders the precorneal tear film unstable [8].

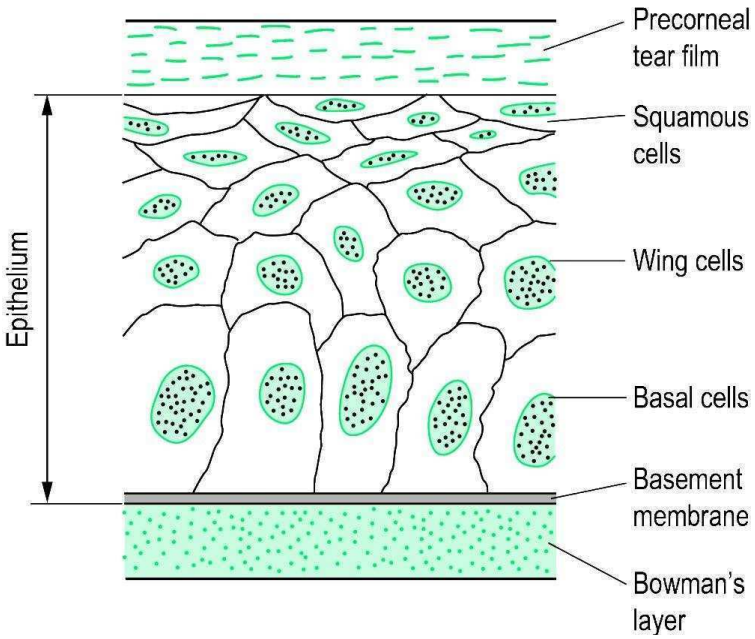

Figure 1.1.4 Diagram of the cross section of the cornea epithelial layer - *image taken from www.medical-dictionary.thefreedictionary.com*.

1.1.1.2 (b) The Bowman's layer

The Bowman's layer lies beneath the corneal epithelial basement membrane and is 8 to 12 µm thick [9]. It consists of strong, fine (20-30 nm), randomly arranged collagen fibrils that end abruptly at the limbus [8, 10]. The anterior surface of this layer lies in contact with the epithelial basement membrane. The posterior boundary merges into the anterior stroma. Injury to Bowman's layer will result in collagen tissue fibrosis leading to scar formation.

1.1.1.2 (c) The stroma

The corneal stroma forms almost 90% of corneal thickness and in an average adult it is 520 µm thick at the centre of the cornea. It consists of about 200 lamellae, each measuring 1.5 to 2.5 µm thick, superimposed on one another, along the corneal plane [8]. Each lamella is composed of

microfibrils made of type 1 collagen, embedded in extracellular matrix called proteoglycan. Microfibrils in the same lamella are systematically arranged parallel to each other at equal distance [11]. However, fibrils in adjacent lamellae are arranged tangentially to each other. The specific fibrils' diameter and their arrangement are largely responsible for the transparency of the cornea [11]. The corneal stroma is avascular and almost completely acellular. These features allow transmission of light through the cornea into the eye. The stroma also acts as a tough layer forming the corneal curvature and providing resistance against invading microorganisms and physical challenges.

In 2013, Dua *et al* reported existence of a novel layer in the pre Descemet's stroma, now termed the Dua's layer [12]. This layer is approximately 10 µm in thickness and composed of type-1 collagen fibrils arranged in transverse, longitudinal, and oblique directions. The presence of this layer explains formation of type 1 big bubble in seen in the deep anterior lamellar keratoplasty despite the removal of the Descemet's membrane.

1.1.1.2 (d) The Descemet's membrane

This layer consists of a strong acellular homogenous basement membrane of the corneal endothelium. The Descemet's membrane is divided into two parts, namely the anterior banded and the posterior non-banded layer. The posterior layer is continuously deposited by the endothelial cells [13], thus making this layer grow throughout life. The average thickness of the entire Descemet's membrane increases from 3 µm in a newborn to 10-12 µm in a young adult and 40 µm in the elderly [14].

1.1.1.2 (e) The endothelium

The endothelium is formed by a single layer of flat polygonal cells. Each cell has high concentration of intracellular organelles indicating a high metabolic activity occurring at this layer. The density of corneal endothelial cells decreases with age [15, 16]. In the newborn it is about 4000 cell/mm^2 but reduces to 1500 cells/mm^2 in the seventh decade of life. A count of less than 700 cells/mm^2 is associated with loss of corneal transparency [17].

1.1.1.3 Limbus

The limbus forms the junction between the transparent cornea and opaque sclera. It is the site of surgical incisions for cataract and glaucoma (Figure 1.1.5). Externally, the epithelial cell border between conjunctiva and cornea possesses multipotential cells important for differentiation of the respective cell types. The internal limbus forms the border between corneal endothelium and anterior trabeculum [18].

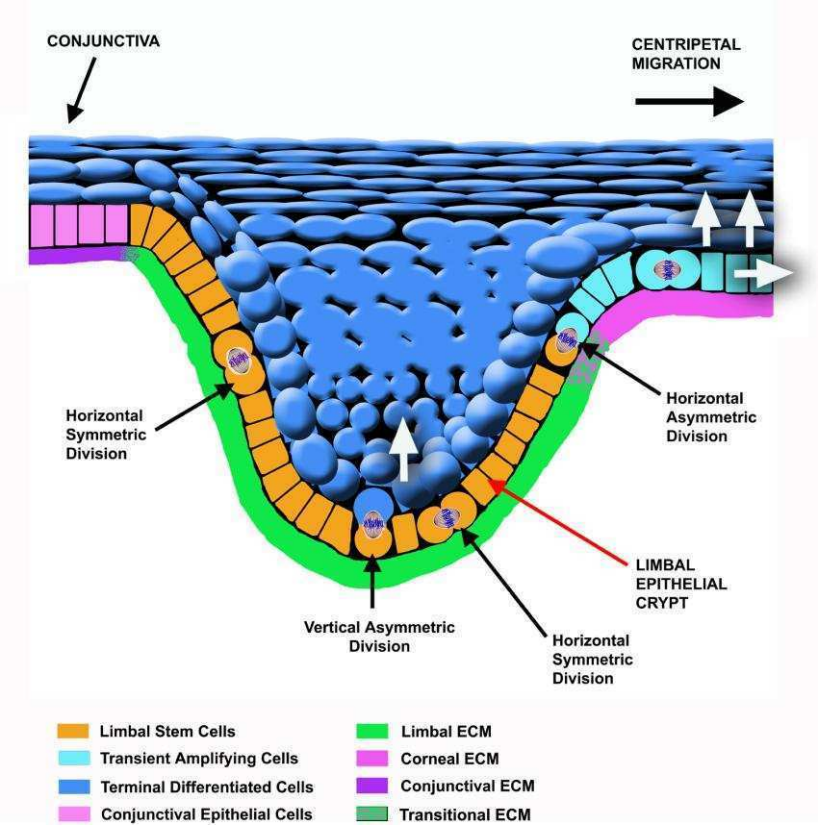

Figure 1.1.5 Diagram of the cross section of the limbus showing migration of limbal stem cell to differentiate into mature corneal epithelium - *image taken from Castro-Munozledo et al [19]*.

1.1.2 Ocular surface defence mechanism

As a frontline barrier, the OS plays an important role to defend the eye from external insult such as physical threats and invading organisms. For this reason, OS is equipped with several protective or defence mechanisms.

1.1.2.1 Anatomical barrier

From the anatomical point of view, several features provide protection for the ocular surface against various threats. First, the eyeball is partially enclosed within the bony orbit. This confers protection and safety to the ocular tissue including the OS from direct mechanical injury [20]. The upper and the lower eyelids act like a pair of curtains to protect the OS from

extreme physical insult such as bright light, heat, and rapidly approaching objects, and from foreign particles including pathogens. They also distribute the tears throughout the OS preventing dryness, cleansing the surface and removing foreign particles. The lid margins, when closed, form a water-tight barrier to keep the pathogens out. The eyelashes, arranged in 2 to 3 rows close to the margin, enhance the protection against entry of foreign particles and pathogens. The firm tarsal plates, made of collagen within the eyelids provide additional strength against mechanical injury to the ocular surface and the eyeball [21].

1.1.2.2 Physiological barrier

The eyeball is located within the bony orbital socket Figure 1.1.6. This phenomenon protects the eyeball and the ocular surface from exposure to external insult.

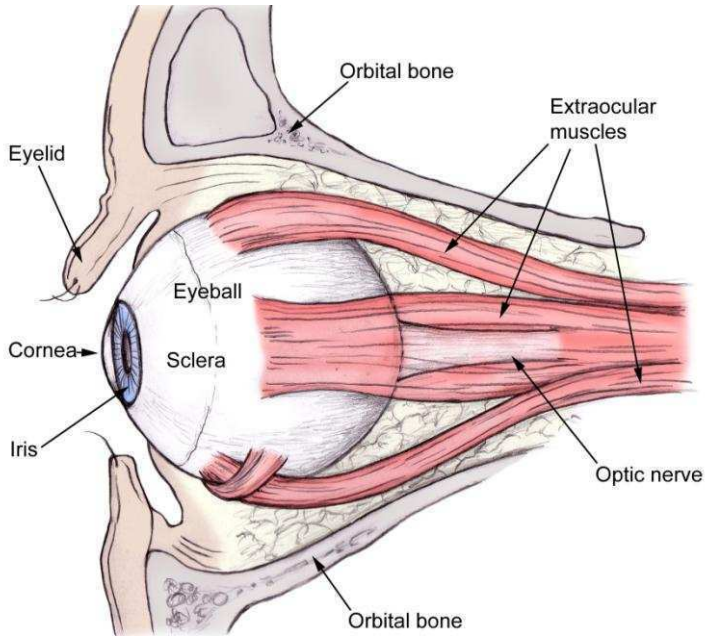

Figure 1.1.6 Diagram showing of the eyeball (sagittal view) in relation to the bony orbital socket - *image taken from www.harvard-wm.org*.

1.1.2.2 (a) Blinking reflex

Blinking reflex can be triggered by various stimuli including touch, menace, bright light and dryness [22]. The eyelid closure efficiently protects the eyes mechanically and prevents potential damage due to the triggering stimuli (Figure 1.1.7).

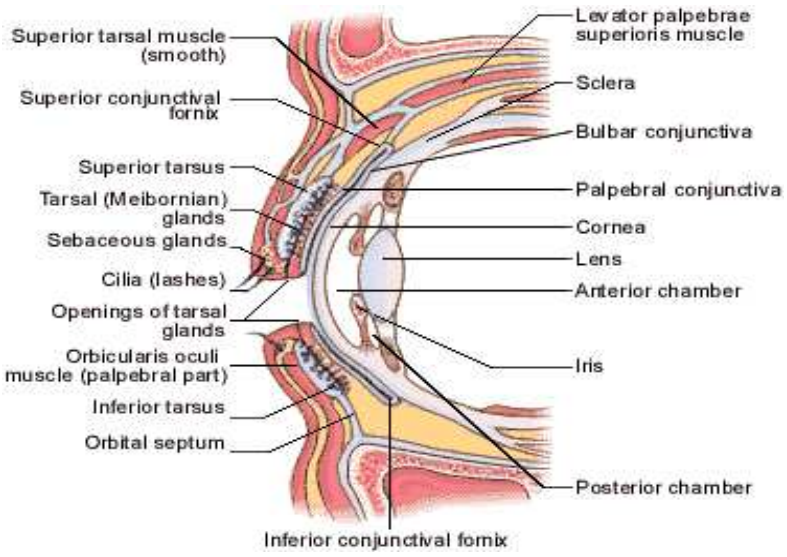

Figure 1.1.7 Diagram of the eyeball (sagittal view) showing the lid functioning to protect the ocular surface and eyeball from external insult - *image taken from www.healthfavo.com*.

1.1.2.2 (b) Tear film

The OS tear film has three components, which are the lipid, the aqueous and the mucin layers (Figure 1.1.8) [23, 24]. The aqueous is secreted by the accessory lacrimal gland of Krause and gland of Wolfring of the lids [25]. The mucin layer is produced by the conjunctival goblet and epithelial cells [26]. It forms a barrier which prevent contact of pathogens with the epithelial cells [27]. The lipid layer is produced by the Meibomian glands in the tarsus [28, 29]. The tears contain immunoglobins, enzymes (eg. lysozyme) and proteins (eg. lactoferrin, lipocalin and β-lysin) [30, 31] which contribute to the OS defence against infective agents. The main function of the pre-corneal tear film is to prevent drying of the OS. In addition to this, the tear also serves to rinse the OS from foreign bodies trapped in the tears. Secretory immunoglobulin (Ig) A binds to bacteria, prevents adherence to corneal epithelia and thus avoids infection. Tear IgG and IgA neutralise some viruses and avert viral invasion [32].

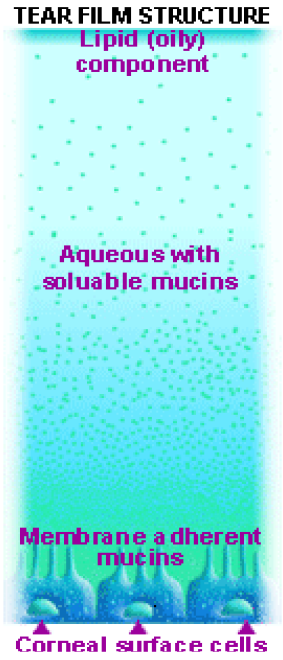

Figure 1.1.8 Diagram showing the different components of the pre-corneal tear film which consists of lipid, aqueous and mucinous layers - *image taken from www.systaine.co.za*.

1.1.2.2 (c) Bell's phenomenon

Bell's phenomenon which is rolling-up of the eyeball during eyelid closure, further displaces the corneal surface away from the lid margin [33]. This will enhance the protection and safety, especially of the cornea.

1.1.2.3 Immune defence system

The immune defence system comprise of two distinct entities that is the innate and the adaptive immunity [34, 35]. The innate immune system is the direct initial host response at the contact point while the adaptive immune system acts as the second line defence [34, 36, 37]. Both entities can involve the cellular and humoral arms of the immune system to accomplish the integrated protective functions, and collectively defend the host against invasion.

1.1.2.3 (a) Innate defence system

Innate immunity is the first line of host defence against pathogens [38, 39]. It is readily present in the host and immediately mobilised when the host is challenged by invading pathogens [5, 40, 41]. A specific ligand in the pathogen outer membrane (pathogen associated molecular pattern, PAMP) is detected by a receptor, the pathogen recognition receptors (PRRs) on the host cell. Binding of both these components triggers a direct killing mechanism of the pathogen [38, 42], mediated by effector molecules of the HDP [37, 43-45].

1.1.2.3 (b) Adaptive defence system

The adaptive immunity is the other form of the immune defence system where pathogens specifically induce a cascade of events leading to defensive response in the host. It takes a relatively longer time to be deployed, especially during first encounter with the pathogens, compared to the innate system. A study done in mice in late 1950s showed that the lymphocyte was the cell type responsible for adaptive immunity [46]. In the said study, mice were heavily irradiated to destroy all the leucocytes including the lymphocytes. They were noted to be unable to mount adaptive immunity against the infective agents. Each type of leucocyte was later introduced after the irradiation and the adaptive immunity was only restored in the affected mice after they had regained their lymphocytes [46].

The adaptive defence mechanism comprises two arms called the humoral and the cell-mediated responses. The cells of the adaptive immune system are the B and T lymphocytes [47]. The B cells, derived from the bone marrow, produce antibodies which form the humoral response. The precursor

T lymphocytes differentiate into cells that either participate in lymphocyte maturation, or kill infected cells. Both humoral and cell-mediated responses are essential to host defence. Among the unique features of the adaptive immune system is the presence of memory. Memory is provided by a small population of B and T lymphocytes which become memory cells and remain for years in the body. At the instance of similar encounter with the cognate antigen, memory cells will be activated and rapidly activate the whole mechanism against the pathogen. The second exposure is usually faster and stronger compared to initial exposure. It is a well-known fact that the innate and adaptive immune systems work in synergy [35]. This integration is carried out by cytokines, and by cell-cell interactions between dendritic cells and lymphocytes in lymph nodes [4].

1.2 The HDPs

HDPs are naturally occurring cationic amphiphilic peptides comprising short sequences of amino acids ranging from around 12 to 50 amino acids in length [48]. They have net positive charges of +2 to +9 due to their lack or small number of acidic residues (glutamate or aspartate) and excess number of cationic residues (arginine or lysine and/or histidine), and around 30–50% hydrophobic residues [49, 50]. The term HDP is preferred to AMPs as it encompasses broader functions of these proteins including neutralisation of endotoxin such as the LPS, and immune-modulation of the innate and adaptive immune system [46, 47, 51, 52].

1.2.1 Classification of HDP

With the ever-expanding knowledge on antimicrobial peptides, a group in the University of Nebraska Medical Center, USA has established the antimicrobial peptide database (APD) in 2003 [53] which was frequently accessed with about 15,000 hits per year [54]. There were also various other databases established and reported but those may be less utilised [55-58]. The database by the researchers in the University of Nebraska Medical Center was updated in 2010 [59]. HDP includes a wide range of proteins, classified according to their structures and different mechanism of actions. They include cationic S100 family proteins [60, 61], peptidoglycan-recognition proteins (PGRPs in vertebrates, PGLYRPs in invertebrates) [62], calcium-dependant lectins (C-type lectins) [63], and iron metabolism proteins such as hepcidin [64].

Based on their molecular structure, size, conformational structure or the predominant amino acid structure, anti-microbial peptides can be classified into the following four classes:

I. The linear α-helical structure without disulphide bond (such as cathelicidin, margainin, cecropins) [65-69].
II. The β-sheet structure characteristically stabilised by disulphide bridges (such as defensins, plectasin or protegrins),
III. Peptides with predominance of one or more amino acid structure,
IV. Loop-structured peptides [66-69].

1.2.1.1 Defensins

Defensins are small cationic peptides [70, 71] occurring in plants [70, 72-74], insects [70, 75, 76], invertebrate [70, 77-79] and vertebrate animals [70, 80] which demonstrate antimicrobial activity against invading organisms. They play important roles as direct effectors of the innate immune system [71, 74, 81], and to a certain extent contribute to the adaptive immune system [82]. They are rich in cysteine residues [83] which are evolutionarily conserved and are typically spaced in the protein. The cysteines are bridged by disulphide bonds into three stereotypical pairs to form three anti-parallel β-strands within the β-sheet structure [84-86]. The canonical six cysteine motif characteristic of the α-defensins is CX-C-X4-C-X9-C-X9-C-C while for β-defensins it is C-X6-C-X4-CX9-C-X6-C-C. Defensins, being members of the antimicrobial peptides group, have been shown to contribute towards host defence against bacteria [87], fungal [88] and viral [50] infections.

To date, three families of mammalian defensins have been described, namely, the α-, β- and θ-defensins [80]. However, only α- and β-defensins have been isolated in humans while θ-defensin has only been described in non-human primates. In humans, α-defensin is mainly found in neutrophils (α-defensins 1-4) [89, 90] and in the Paneth cells of the small intestines (α-defensins 5-6) [91-93]. β-defensins, in contrast to α-defensins, are believed to have wider distributions and mainly found at the epithelial surfaces such as in the intestine and the lung [94, 95]. β-defensin-1 is expressed in the pancreas, kidney and lung epithelia [96]. β-defensin-2 is expressed in the skin and lung epithelia [97]. β-defensin-3, initially described by Harder *et al*, is found to be expressed in the skin, lung, oral cavity and intestine [98].

1.2.1.1 (a) α-Defensins

α-defensin is the first defensin discovered in multicellular organisms, and was first reportedly isolated from the rabbit alveolar macrophages by Selsted *et al* in 1983 [99]. Lehrer *et al* reported on the microbicidal cationic protein 1 and 2 (MCP1 and MCP2) derived from the rabbit lung macrophages which had activity against bacteria such as *Staphylococcus aureus*, *Staphylococcus epidermidis*, *Listeria monocytogenes* and *Klebsiella pneumonia*, at near neutral pH and relatively low ionic level [100].

To date, six α-defensins have been described in human [50]. α-defensin-1 through -4 are expressed mainly in human neutrophils, hence the term human neutrophil peptides (HNPs) for this subgroup. The α-defensin-5 and -6 are mainly found in the Paneth cells at the base of the crypt of Lieberkuhn of the small intestine and are generally regarded as the intestinal defensins [93, 101].

The primary structures of three human neutrophil peptides, namely HNP1-3, were reported by Selsted *et al* in 1985 and found to be comparable to those of the rabbit neutrophil peptides [102]. Wilde *et al* reported on the HNP4 purification and characterisation in 1989 [103].

As a member of the defensin family, α-defensins have six conserved cysteines linked into three pairs by disulphide bonds, giving rise to three anti-parallel disulphide bridges within the β sheet. α-defensins differ from β-defensins in the manner the cysteine residues were linked to form the disulphide strands. In α-defensin, the first cysteine is bonded to the sixth, the second to the fourth and the third bonded to the fifth cysteine. Different peptides within the sub-family have different amino acid sequences.

The crystal structure of the HNP3 was reported by Hill *et al* in 1991, who described it as a six-stranded dimer held together by four hydrogen bonds. These interactions were further enhanced by the hydrophobic interaction between amino acids in each of the two monomers [104]. The structures of human α-defensin-4, -5 and -6 were described by Szyk *et al* in 2007. They used high-resolution X-ray analysis and reported all three defensins share their tertiary structures with the other known α- and β-defensins. They also reported that HNP4 has antimicrobial and chemotactic activity comparable to other HNPs. In addition to that, they revealed both HD5 and -6 did not show chemotactic properties and HD6 did not even show antimicrobial properties [105].

1.2.1.1 (b) β-Defensins

β-defensins, like α-defensin, are small cationic peptides with six cysteine conserves linked into three pairs by disulphide bridges. However, in contrast to the α-defensin where the first cysteine is linked with the sixth cysteine, the first cysteine in β-defensin is linked to the fifth cysteine.

From the historical perspective, the first mammalian β-defensin was isolated from bovine trachea (tracheal antimicrobial peptide) in 1991 [106]. Subsequently, 13 novel β-defensins were isolated from bovine neutrophils [107]. The first human β-defensin, hBD1, was initially purified from hemofiltrates [108] of dialysis patients in 1995 and was later found in the urine as a gram-negative bacteria-killing antibiotic [109]. hBD1 mRNA was isolated from human airway epithelia, demonstrating higher transcripts in the conductive part than in the air exchange region [110].

Unlike the α-defensins, which are most prominently found in neutrophils and in the Paneth cells of the intestine, β-defensins are primarily found in the epithelia and are directed toward protection of the skin and the mucous membrane such as the respiratory tract and the genito-urinary tract.

1.2.1.1 (c) θ-Defensin

The first θ-defensin peptide, Rhesus Theta Defensin-1 (RTD1), was reported by Tang *et al* in 1999 [111]. Like α- and β-defensins, θ-defensin is a small cationic peptide with six conserved cysteines linked together by three disulphide bridges, forming the β-sheet. However, θ-defensins are cyclic peptides [81] and contain two non-peptide elements, each arising from a propeptide with different genetic code [111].

θ-defensin has been isolated from leucocytes and bone marrow in non-human primates, such as the rhesus macaque and olive baboon (*Papio anubis*) [112-114]. Human bone marrow cells express θ-defensin mRNA but lack the corresponding peptide, as the human θ-defensin gene (DEFT) contains a stop codon in the signal sequence that aborts translation [115, 116]. The θ-defensins also have broad spectrum antibacterial and antiviral activity [115]. Retrocyclins are synthetic, humanised θ-defensin peptides, whose sequences are based on those found in human θ-defensin genes. Since there is only a single base change needed in the stop codon to reverse the DEFT gene inactivation in humans, there could in principle be certain populations that have the polymorphism required to express this peptide. It has been shown that their expression can be accomplished in human cervico-vaginal epithelial cells by treatment with an aminoglycoside [117] .

1.2.1.2 Cathelicidin

Cathelicidin was first reported by Zanetti *et al* [118] in 1995, as a peptide containing a stable N-terminal cathelin domain coupled with an antimicrobial C-terminal domain, expressed in mammalian myeloid cells [118-120]. To date, hCAP18/LL-37 remains as the only human cathelicidin ever described. Only hCAP18 gene on chromosome 3 can be translated into a propeptide. hCAP18 (precursor for LL37) is stored, comparable with lactoferrin, in secondary granules in human neutrophils [121] and various other cells including monocytes, natural killer (NK) cells, B cells and mast cells. The epithelia of airways, mouth, tongue, oesophagus, intestines, cervix, vagina, salivary gland, epididymis and testis have been shown to express LL-37 [122, 123]. Furthermore, LL-37 is secreted in human wound, sweat and airway surface fluids [118, 124-127] and is upregulated in response to infection or injury [127, 128]. It has also been detected by mass spectrometry in the tear film [129]. Human hCAP18 is expressed constitutively within neutrophils [120] and testes [130] and is inducibly expressed by keratinocytes [131].

Cathelicidin has broad spectrum activity against bacterial, viral and fungal pathogens. Inflammation or injury seem to be the triggering factors for upregulation of the LL-37/hCAP18 gene, particularly in keratinocytes and leucocytes [132, 133].

1.2.2 Roles of HDP

HDPs have various roles, functions, efficacy and interactions. Ever since the first reported defensin was published [99], many reports on the effect and roles of the defensin molecules have been published. In addition to

the functional properties (mainly antimicrobial) of α-defensins, a few studies have focused on biological activities in terms of the structural properties of these proteins [104, 105, 134, 135].

1.2.2.1 Antimicrobial activity

The most fundamental feature of defensins is their microbicidal activity [50, 136] against gram positive and gram negative bacteria [107, 137], fungi [137], parasites and viruses [138]. The cationic charge of the peptide is an excellent motif to bind with the anionic surface of bacterial cytoplasmic membranes (Figure 1.2.1). They initially straddle between the hydrophilic lipoprotein and the fatty acyl chain of the membrane phospholipids. Once inserted into the membrane, HDPs damage the wall by thinning, forming transient pores and allowing passage of other molecules into the cells, or disrupting the barrier function. Alternatively, HDP may translocate into the cell and destroy the internal organelles (Figure 1.2.1) [65]. In humans, for instance, increased expression of hBD2 protein was found in the plasma of patients with bacterial pneumonia and not in the plasma of those without the infection [139].

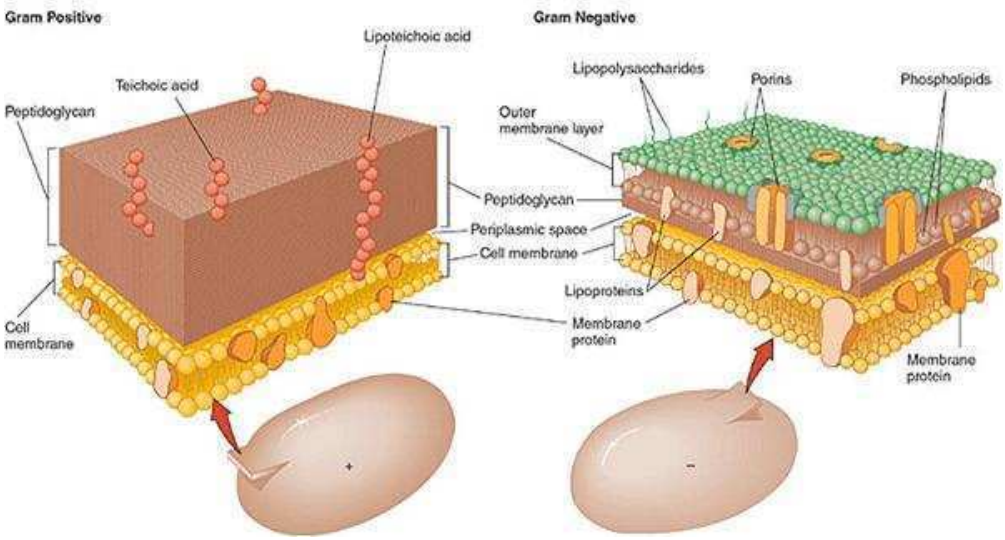

Figure 1.2.1 Diagram showing comparison between the gram positive and gram negative bacterial cell membrane - *image taken from www.water.me.vccs.edu.*

1.2.2.2 Antimicrobial mechanisms of hBDs

The fact that several theories have been proposed for the mechanism of action for the defensins molecules shows that this aspect of the antimicrobial peptide has not been fully understood. However, it is generally accepted that the defensins act on the membrane in a non-specific fashion leading to destabilisation and cell rupture. The possible mechanism of actions underlying this can be categorised into:

a. Pore model: The peptide oligomerises and forms a pore in the cell membrane causing leakage of the cell contents and cell disruption.
b. Carpet model: Several molecules sit on the membrane and initiate necrosis

The anti-microbial property of the β-defensins rests largely on the fact that they increase the permeability of the anionic lipid bilayer membrane of the microbial agents (Figure 1.2.1) leading to subsequent leakage of intracellular content and damage of internal organelles [140]. In 1991, Hill *et*

al reported on the crystal structure of HNP3. They found that HNP3 existed in the dimeric form when crystallised. Based on the HNP3 dimeric crystal, they had suggested its mechanism of bacterial membrane permeabilisation. The dimers, according to them, would form a hydrophobic wedge which is buried into the lipid bilayer and disrupts the interactions and permeabilises the membrane. Other possible mechanisms would have been dimer-pore or general-pore, in which two or more dimers joined together and buried into the lipid bilayer before affecting the pores leading to membrane permeabilisation [104].

1.2.2.2 (a) Pore forming models

The more widely accepted theory indicates that defensins change the bacterial cellular permeability by forming multimeric pores in the lipid bilayer cell membrane. In this simplest description, the defensin molecules bind to the membrane through the cationic and amphipathic structural motifs. Pores are formed across the cytoplasmic membrane of the bacteria and create trans-membrane channels [141]. The formation of these trans-membrane pores causes bacterial membrane depolarisation. Since the bacterial ATP synthesis is dependent on the trans-membrane potential, pore formation interferes with the bacterial metabolism, leading to leakage of internal organelles and causes bacterial cell death.

1.2.2.2 (b) Carpet models

In this model, accumulation of peptides parallel to the surface of the bacterial membrane would disrupt the membrane integrity by extensive

destabilisation [142]. This theory was favoured by Hoover *et al* who found the propensity of defensins such as hBD1 and -2 to oligomerise up to octamers in the case of hBD2 [143, 144]. By forming oligomers, hBDs bind to the membrane through electrostatic charge and disrupt the membrane potential leading to its destabilisation and permeabilisation. Leakage of internal organelles will occur and influx of external fluid will lead to cell lysis.

1.2.2.3 Immunomodulation

Not only do they affect the innate immune system, the β-defensin play roles in the adaptive immune system as well. Defensins promote histamine release and prostaglandin-2 production in mast cells [145, 146]. Human neutrophil defensins were reported to have chemo-attraction towards naive T-cells and immature dendritic cells [52]. Meanwhile beta defensins were claimed to mediate crosstalk between the innate and adaptive immune system by chemo attraction of immature dendritic cells and T-cells [47]. HBD2 was shown to up-regulate the expression of TNF-α and IL-1 in human monocytes following activation by bacterial stimulus [147]. They also play roles in other cellular processes including chemotaxis, angiogenesis, and modulation of adoptive immunological reactions, pro-inflammatory effects, and cancer metastasis.

Defensin expression abnormality was linked with inflammatory bowel disease with increasing frequency. Crohn's disease of the colon was associated with defective hBD2 induction due to low copy number of *DEFB4* in the 8p23.1 gene cluster [148]. This disease was also associated with diminished α-defensin [149]. Because of the roles they serve in the

defensive, regulatory and pathological processes, there has been increasing interest in these proteins over the last decade [150].

1.2.2.4 Wound healing

Although the best described function of HDP is antimicrobial, they are also being developed as potential therapeutic agents in wound healing [151-153]. Expression of cathelicidin and hBD2 and -3 have been observed in epidermal keratinocytes following skin injury [127]. IGF-1 and TGF-α were said to stimulate up-regulation of cathelicidin which then promotes healing by activation of epidermal cells and fibroblasts to form granulation tissue, angiogenesis and chemo-attraction of other cells [154]. HNP1 was shown to increase the expression of pro-collagen mRNA and protein in dermal fibroblast culture [155]. Steinstraesser *et al* showed that in burned human skin, the concentrations of cathelicidin, and hBD1, -2 and -3 increased dramatically [82].

1.2.2.5 Other properties of defensins

Epididymal peptide hBD18 (encoded by *DEFB118* gene) which was formerly known as ESC42 is active against bacteria, androgen-regulated, secreted by the epidydimal lumen, and induces spermatozoa movement by chemotaxis [156]. Another β-defensin in rat, Bin1b, was reportedly claimed to induce progressive sperm motility in immotile immature sperm [157]. Other documented roles of HDP include angiogenesis [158, 159], cancer anti-metastasis [160-162] and coat pigmentation. A canine beta-defensin, *CBD103 (K^B)*, was shown to interact with wild type allele of *Mc1r* gene causing curly black coated Labrador dogs [163].

1.2.3 OS spectrum of HDPs

Like other human tissues in contact with the external environment, human OS has its own repertoire of HDPs. The existence of defensins at the human OS was first reported in 1998 [164-166]. Gottsch *et al* observed that α-defensin mRNA (HNP-1 and -4) and protein (HNP-1,-2 and -3) were detectable in human corneal stroma following transplant rejections and post-infectious keratitis but not in normal cornea [164]. Haynes *et al* [2, 3] observed positive immune-reactivity for HNP1–3 in inflamed conjunctiva and samples of normal tear film. Following this, Zhou *et al* confirmed the presence of HNP1–3 in tear film and showed that HNP-1 and -2 levels in the tears to be in the range of 0.2–1 μg/ml by using liquid chromatography mass spectrometry. The authors believed that infiltrating neutrophils were the source of α-defensins on the OS. β-defensins seems to be absent in human tears [167].

In addition to α-defensin, the cornea and conjunctival epithelial cells express β-defensins too. It has been generally accepted that hBD1 is constitutively expressed [165, 166, 168-171] but there have been differences in opinion with regard to the expression of hBD2 [166, 169, 170, 172]. For instance, McDermott *et al* reported hBD2 was expressed in only two of eight cadaveric corneal epithelia tested [3]. Nevertheless, hBD2 expression is known to be inducible [97]. It was shown that hBD2 expression by SV40-immortalised human corneal epithelial cells was up-regulated by bacterial lipopolysaccharide (LPS) through pathways involving tyrosine kinase and p38 mitogen-activated protein kinase (p38MAPK) and nuclear factor-KB (NF-KB)

[173-175]. Birchler *et al* [176] and Wang *et al* [177] observed that up-regulation of hBD2 expression was mediated by Toll-like receptor 2 (TLR-2).

McDermott *et al* [178] reported that hBD2 was up-regulated in regenerating corneal epithelium in an *in vitro* organ culture model of corneal epithelial wound healing. It was also shown that hBD2 expression by corneal [170] and conjunctival [172] epithelial cells was up-regulated by the pro-inflammatory cytokines interleukin-1 (IL-1) and tumour necrosis factor-α (TNF-α). In the case of corneal epithelial cells, the effects of IL-1 on hBD2 expression were mediated via p38MAP kinase, JNK and NF-KB [170]. McDermott *et al* [3] have reported the expression of hBD3 in corneal and conjunctival epithelial cells. Several studies have indicated that expression of hBD3 is inducible [98, 179, 180] by TNF-α and interferon (IFN)-γ but this could not be reproduced by McDermott *et al* who reported that there was no increase in hBD3 either in corneal [170] or conjunctival [172] epithelial cells following treatment with the said cytokines. RT-PCR has also been used to investigate the expression of hBD4, -5 and -6, but no evidence of their production by corneal or conjunctival epithelial cells was revealed [3].

Kawasaki *et al* [181] made an observation that there was an increment in expression of *DEFB4*, which encodes hBD2, in conjunctival epithelial cells of patients with Sjögren syndrome. These patients had a very severe form of dry eyes resulting from a systemic autoimmune condition. Based on the fact that hBD2 expression can be upregulated by pro-inflammatory cytokines [182] and that such cytokines are increased in dry eyes [183, 184] , it was thought that the increase in hBD-2 expression could be due to the enhanced pro-inflammatory cytokine activity at the OS in this condition [3].

McIntosh *et al* reported that hBD1 to -4, liver expressed antimicrobial peptide (LEAP)-1 and 2 and LL-37 were detected frequently in samples of OS epithelia [185]. Conjunctival and corneal epithelia showed distinct but overlapping profiles of expression. hBD3 and -4 and LEAP1 and -2 were found more frequently in the cornea than in the conjunctiva [185]. Expression of hBD3 was more commonly found in corneal and conjunctival specimens with infections [185]. In slight contradiction to this finding, Huang *et al* did not find hBD4 expressed in their samples of corneal and conjunctival cells [2].

Narayanan *et al* reported that hBD1 and -3 were expressed constitutively in conjunctival epithelium of normal eyes while hBD2 was only expressed in conjunctival epithelium of dry eyes. They suggested that the baseline protection on the OS was provided by hBD1 and -3 while hBD2 enhanced this protection in cases of dry eyes [172].

Garreis *et al* [186] showed that hBD1, -2, -3 and -4 are constitutively expressed in conjunctival epithelial cells and also partly in cornea. The conjunctiva, cornea, lacrimal apparatus and human tears contain significant amounts of hBD2 and-3, the highest concentration found in the cornea [186].

In general, current data shows that the epithelia of the human OS constitutively express hBD1 and hBD3, whereas hBD2 expression can be upregulated with appropriate stimuli, such as infection and inflammatory cytokines. Further evidence on hBD4 expression is required. HNP1 through -3 are normally present in the tear film, and, during inflammation, they may be released in the cornea by infiltrating inflammatory cells.

1.2.4 Human Beta Defensin 9 (hBD9)

Expression of *DEFB109* on the OS was first reported by Abedin *et al* in 2008 [187]. They found that *DEFB109* was down-regulated in OS infection and inflammation and postulated that it may not have any major antimicrobial role as its level was reduced during infections. They also postulated it may have a role in the wound healing [187]. On a similar note, Premratanachai *et al* [188] reported on the constitutive expression of *DEFB109* and its down-regulation in gingival keratinocytes following stimulation with *Candida albicans* [188]. The findings of these studies are in agreement with the study of Islam *et al* [189] who found that cathelicidin and hBD1 were down-regulated during invasion of the intestine by *Shigella* bacteria. This finding supported the opinion that infections might be associated with reduced expression of *DEFB109*. Whether this is the effect or cause of the infection is still not fully understood. An explanation offered was this could be the immune escape mechanism in which cell defence is down-regulated to allow commensalisation by certain bacteria [189].

1.3 Therapeutic application of HDP

1.3.1 HDP in clinical settings

Despite rigorous effort to design an efficacious HDP-based therapeutic agent, clinical success has been rather limited [190, 191]. Only a few peptides have shown promising results as potential single drug therapy in preclinical studies [192, 193]. A pharmaceutical company in the USA had been developing a broad-spectrum antimicrobial agent to be used against bacteria, fungi and viruses [194]. In another study, Plectasin, a recently

discovered fungal defensin from *Pseudoplectania nigrella*, was found to be effective against gram positive *Streptococcus pneumoniae* in mouse models of peritonitis and pneumonia [195].

A few other studies have reported progress in clinical settings. In a study conducted among children with meningococcal sepsis, rBPI21 (Neuprex, a HDP synthesised by polymorphonuclear lymphocytes) was offered as a form of treatment [196]. Although the investigators reported an increase in morbidity, there has been an improvement in functional outcome but not in mortality rate [197]. Other HDPs that have advanced to at least phase 3 clinical efficacy trials include Pexiganan (frog magainin derivative; for impetigo and diabetic foot ulcers), Iseganan (porcine protegrin derivatives for oral mucositis) and Omiganan (cattle indolicidin variant) for catheter-related infection [65].

1.3.2 Development of HDP as topical ophthalmic agent

Topical delivery of therapeutic agents either in the form of eyedrops or ointment constitute a form of drug administration for OS infection. The drug can act directly on the offending threats, without the unnecessary systemic propagation and thus preventing systemic side effects. The peptide molecules will directly affect the growth of the pathogens without having the issues of absorption and enzymatic digestion in the alimentary system. The advantages of having the HDP as a topical antibiotic includes broad-spectrum of organism sensitivity and minimal risk for resistance development, if any. On the other hand, the main disadvantages of topically administered peptide include OS toxicity and potential drug interaction with tear content apart from the high cost for research and development. It has

been shown that HDPs are labile in an environment with high salt, divalent cation and serum protein concentrations. In addition to these, the natural peptides were also prone to damage by proteases. For instance, chymotrypsin-like enzymes may damage the peptides rich in basic amino acids, which is the hallmark of the HDPs [65].

There are several reports published on the effect of topical antimicrobial peptides to treat OS infections. Nos-Barbera *et al* [198] showed rabbits infected with intrastromal injection of *Pseudomonas aeruginosa,* and later treated with synthetic peptides containing partial sequence of cecropin A (an insect peptide) and melittin (from bee venom) had reduced inflammatory signs and less bacterial-related damage than placebo-treated controls. Mannis *et al* tested the effect of a synthetic peptide named COL-1 in a rabbit model of *Pseudomonas aeruginosa* keratitis [199]. Although the peptide showed potent antimicrobial activity in *in vitro* study, no clinical benefit was observed in the *in vivo* situation. Furthermore, the rabbits treated with peptide demonstrated similar inflammation compared to controls and these could be due to the reduction in peptide activity in the OS tear environment.

Components of the tear film were shown to alter the activity of HDPs. Many HDPs have activity sensitive to the high salt concentration of the surrounding environment, making them less or ineffective on the OS [200, 201]. On a positive note, different HDPs may act additively or synergistically so much so that it may not take a high concentration of individual hBD to exert the antimicrobial effect [202, 203]. This may also be an alternative strategy to circumvent the HDP toxicity. Although there is a relatively high concentration of salt in tears and the hBDs are mostly salt-sensitive, the

interaction between tears and the microbial peptide has not been fully investigated. Nevertheless, the efficacy of microbial peptide in an animal model of keratitis and its relation to the ocular surface environment is an important issue to be resolved in the quest to develop antimicrobial peptide into an effective topical antibiotic.

1.3.3 Future perspective of a HDP drug

Apart from the categorical role of antimicrobial peptides, hBD1-3 have also been shown to play roles as chemokines for dendritic cells and as such may contribute to adaptive immunity too [204]. hBD may have roles in the treatment of cancer. It was previously shown that modification of amino acids in human cathelicidin induces cell death of carcinoma but not normal cells [162]. In addition to this, the migration of rate of hBD1-3 transfected squamous cells carcinoma was significantly lower than that of the control cells. Transfection with hBDs may directly inhibit tumour cell growth and may have a possible role as a therapeutic strategy for tumours [205]. With these reported effects of defensins, the future is set for them to be explored as a form of therapeutic agents in the future, if not soon.

Chapter 2

DEFB109 cloning

CHAPTER 2: Cloning of *DEFB109*

2.1 Introduction

Prior to the completion and submission of the human genome by the Human Genome Project Research Institute (HGPRI) in April 2003 [206], representation of *DEFB109* as a pseudogene has probably diverted interest in examining the hBD9 peptide as antimicrobial agent. However, the completion of the human genome project and the discovery of the *DEFB109* gene sequence without the premature stop codon have renewed the interest in this peptide.

The invention of restriction enzymes revolutionised the recombinant technique of genetic engineering as the gold standard for expression of protein using the plasmid construct transformed into expression hosts. However, certain codon bias requires attention as the host may not express foreign or heterologous protein as effectively as it does for native protein.

Several ways may offer solutions for this issue. One of the options is simultaneously co-producing the transfer RNA (tRNA) for the peptide/amino acids. Baca *et al* co-transformed a plasmid carrying the gene encoding the tRNA of rare codons in *E. coli*. This had increased the levels of overexpressed protein [207]. Lee *et al* demonstrated that by co-expressing the tRNA of the RNA codon, heterologous protein expression increased by several fold in the expression host *Streptococcus gordonii* [208].

The alternative method is to convert the human gene into a sequence with host preferred codons. By adopting this strategy, a higher amount of correctly folded protein may be expressed. The preferred codon for some

amino acids is unique for the expression host species. In this study, the host cloning and expression hosts were *E. coli* K12. This bacterium was chosen based on the reasons of easy and rapid growth and the widely studied genetics of the bacteria.

2.1.1 Defensin genetics

The evolutionary relationship between defensins in vertebrates and those in invertebrates is not clearly defined to date. Nevertheless, it is most clearly defined within the vertebrate kingdom. Phylogenetic studies have revealed that a primordial β-defensin gene is the common ancestor for all defensins in all vertebrates [78, 209-211]. The β-defensins have evolved in the vertebrates before the divergence of mammals from the birds. It gave rise to the α-defensins in glires and primates after they had diverged from other mammalian species [211, 212]. The θ-defensins then originated in primates after they had separated from other mammalian species [115, 211]. From here, the θ-defensin gene in humans underwent polymorphisms and became a pseudogene after they had separated from the other primates. They also revealed that chicken genome encodes a total of 13 different β-defensins, with no other class of defensins found which all mapped to a dense cluster on a locus on the short arm of chromosome 3, abbreviated as 3q3.5-7 [213].

Most defensin genes in humans are located in an 8 Mb region on the locus 23.1 of the long arm of the chromosome 8, which also known as 8p23.1 [214-216]. Within this locus, there are two clusters. The first cluster contains *DEFB1*, *DEFA1-6* and *DEFT1*. The second cluster contains *DEFB4*, *DEFB103-109* and *SPAG11* [211, 217, 218]. A similar pattern of clustering was also observed in other species [219-221]. Most β-defensin genes have

two exons; the first exon encodes the SSP and propiece and the second exon encodes for the mature peptide. All α-defensins arising from the myeloid cells have 3 exons and the first exon encodes the untranslated region (UTR) [80]. The propiece in α-defensin is larger than that in the β-defensin. The intron sizes of β-defensins vary widely between 1 and 10 kbp, in contrast to the shorter introns in α- and θ-defensins [211].

In addition to this, subsequent *in silico* analysis has also identified additional clusters of putative β-defensin genes at 20p13, 20q11.1 and 6p12 [222]. Schutte *et al* in 2002 performed a computational search using a hidden Markov model (HMM) combined with BLAST on the draft of the human genome [222]. By doing so, they discovered 28 new human β-defensin genes distributed into five syntenic clusters on three different chromosomes. Two clusters were on chromosome 8p23.1, one cluster on chromosome 6p12.3 and two clusters on chromosome 20p13 and 20q11.21. The two clusters on chromosome 8p23.1 are separated by about 4 Mbp [212]. The 6p12.3 cluster contained five defensin genes, namely the *DEFB110* to *-114*. The cluster on chromosome 20q11.1 contained 10 defensin genes, namely the *DEFB15* to *-24* [210, 223], while cluster 20p13 contained *DEFB25* to *-29* [222, 224].

A similar search strategy was performed, and reported in 2003 by Kao *et al* [225]. They identified six new *DEFB* genes, all having similar six conserved cysteines, namely the *DEFB106*, *-108*, *-109*, *-118*, *-129* and *-131*. The gene cluster assignment for these new genes was in agreement to that found by Schutte. Tissue expression for these genes was different in that

DEFB108 and *-129* were only expressed in the testis, but *DEFB109* was shown to be ubiquitous in all tested tissues [225].

Semple *et al* reported on the *DEFB* genes which included *DEFB105, -106, -107* and *-108* and claimed that the *DEFB109* was a pseudogene due to the presence of a stop codon in the first exon [226]. They found that *DEFB105-108* were predominantly expressed in the male reproductive tract leading to the suggestion that the male reproductive tract was equipped with a complex innate defence mechanism.

Patil *et al* in 2005 reported on 39 human *DEFB* genes including four novel human β-defensin genes which were the *DEFB133, -134, -135* and *-136* [212]. *DEFB130* and *-131* which were not assigned earlier [222, 225] have been assigned to 8p23.1. *DEFB133* has been assigned to cluster 6p12.3. When compared to chimpanzee, they discovered all the orthologues of *DEFB*, except those for *DEFB110* and *DEFB128.*

Six *DEFB* genes located at the 8p23.1 locus, namely *DEFB4*, *DEFB103*, *-104*, *-105*, *-106* and *-107* were found to be in the copy number variable region. There was no data excluding *DEFB108* and *DEFB109* from the copy number variable but *DEFB1* was not within this copy number variable region [227].

2.1.2 *DEFB109*

DEFB109 itself consists of two exons. The first exon spans 66 nucleotides and serves as the secretion signal peptide (SSP) [80, 228]. The second exon gives rise to the production of pro-peptide [80]. Following the translation of the peptide, the SSP is cleaved. Unlike in α-defensin where the

cleavage enzyme has been identified to be matrilysin in mouse and trypsin in human, the cleavage enzyme for β-defensin has not been discovered [229].

DEFB109 was first reported by Schutte in 2002 [222]. Kao *et al* and Semple *et al* further described the defensin gene duplication in 8p22-23 locus and argued that the *DEFB109* gene was a pseudogene. This was due to the presence of a stop codon at base pair 40 in its first exon [226]. Hence, they postulated that the mature peptide could not be translated. Nevertheless, the final draft of the human genome reference sequence has indicated that *DEFB109* is a true translatable gene which is located in different locations which were chromosomes 8, 13, 20 and 4.

Gene duplication studies have shown that the defensin gene cluster in locus 8p23.1 experienced duplication [230]. Wehmeyer *et al* claimed that *DEFB109* was functional based on their observations that *DEFB* genes were polymorphic and that *DEFB109* exon 2 was expressed in gingival keratinocytes. They found that the polymorphism detected in *DEFB109* exon 1 represented a missense SNP at the stop codon that alters TAA (stop codon) to TCA (serine).

Abedin *et al* have shown that the *DEFB109* was constitutively expressed at the mRNA level in the ocular surface epithelia [187]. They interestingly showed that the *DEFB109* mRNA expression was however down-regulated in cases of infection and inflamed eyes. Hence, they suggested the possibility of other roles than as an antimicrobial for hBD9. Mohammed *et al* [231] have shown that hBD9 was detected in the conjunctival and corneal epithelia by immunochemistry methods. Otri *et al* [232] showed that *DEFB109* mRNA expression following exposure to

Acanthamoeba castellanii was up-regulated at 9 hour time point with variable down-regulation at earlier stage. Based on the finding of these reports, it is strongly believed that *DEFB109* is coded in multiple locations and although a pseudogene was found, there are other true genes in the human genome. It is likely that the gene is duplicated and a copy has undergone single nucleotide polymorphism (SNP) leading to a stop codon present early in the SSP, making that particular copy a pseudogene.

This part of the study was based on the *DEFB109* second exon coding for the hBD9 propeptide. The first exon coding for the SSP was not involved as it was generally believed that the SSP would have been cleaved following translation and therefore did not contribute to the function of the hBD9. As such, the primers for the second exon of *DEFB109* were designed. The cloning strategy was decided upon and optimisation was carried out. The primers were designed to include several motifs to flank the gene for the preparation of the gene insert. This gene insert was to be ligated into the multiple cloning sites (MCS) of the selected plasmid vector.

2.2 Objectives

The objectives of this chapter were:

a. To amplify the *DEFB109* second exon encoding the hBD9 propeptide via conventional PCR.
b. To prepare the linearised plasmid vector with hanging ends for the directional ligation with the *DEFB109* gene to form the recombinant DNA construct.

c. To propagate the recombinant DNA construct in *E. coli* cloning host followed by verification by DNA sequencing.

2.3 Methods

2.3.1 *DEFB109* gene identification

The National Centre for Biotechnology Information (NCBI) nucleotide database, which includes sequences from several sources including GenBank and RefSeq, was searched for *DEFB109* gene sequence. '*DEFB109*' was used as the initial query term and when submitted resulted in several item. Item described for Homo sapiens beta 109 mRNA with complete cDNA sequence (cds) with GenBank access code DQ12013.1 was chosen and submitted to sequence analysis tool, NCBI BlastN software. This step further resulted in several complete sequences from which the second exon of the DEFB109 was identified, and used for cloning work.

2.3.2 Sample collection

Amniotic membranes (AM) from ten different individual samples were harvested using a protocol which was published previously [233]. In brief, amniotic membranes were removed from transport media and washed in phosphate buffered saline (PBS) for 10 minutes, repeated 3 times. The membrane was later placed in a petri dish with the epithelial side up and covered with 5 µl thermolysin (125 µg/µl) and incubated for 10 minutes. Membranes were later transferred to PBS and shaken vigorously to remove epithelial cells from the membrane. Treated membranes were then transferred to fibroblast culture medium (FCM) and agitated for 4 hours

before being transferred to individual Bijoux tubes containing 5 ml FCM and frozen at -20 ^{o}C. PBS from which the membrane was removed, was centrifuged at 6000 x g for 10 minutes. The cells were pooled and stored at -20 ^{o}C till required for mRNA extraction.

2.3.3 Total RNA extraction and cDNA synthesis

The cells were lysed with 700 µl guanidine thiocyanate (RLT) buffer with 10 µl 14.3 M β-mercaptoethanol (β-ME) added per 1 ml of RLT buffer. The cell lysate was homogenised with Qiashredder spin column (Qiagen, Manchester, UK) by loading 700 µl of the lysate into the column, which was placed in a 2 ml collection tube and spun for 2 minutes at full speed in a microcentrifuge. Total RNA was purified from the AM epithelial cells by using the RNAEasy Total RNA kit (Qiagen, Manchester, UK) according to the manufacturer's manual.

The cDNA was reverse-transcribed from total RNA using the Quantitech Reverse Trancriptase Kit (Qiagen, Manchester, UK) as per manufacturer's instruction manual. Up to 1 µg of the purified RNA sample was incubated with 2 µl gDNA wipeout buffer 7X in a final volume of 14 µl for 2 minutes at 42 ^{o}C before transfer to ice. 4 µl Quantiscript RT buffer 5X, 1 µl RT primer mix and 1 µl reverse trancriptase enzyme were added to the entire 14 µl gDNA-eliminated reaction. The mixture was incubated at 42 ^{o}C for 30 minutes followed by 95 ^{o}C for 3 minutes. The completed reverse transcription reaction was stored in -20 ^{o}C till required for RT PCR.

2.3.4 Nanodrop RNA quantification

This procedure was done at the Post-genomic Lab, in the Department of Pathology, Queen's Medical Centre, University of Nottingham, Nottingham. Specimens were kept in ice during transfer. The machine was first cleaned, initialised for RNA40 before being blanked with RNAse-free water. 1 µl of specimen was loaded for measurement. Results were labelled, saved and printed for record keeping purposes.

2.3.5 Primer design

After determining the *DEFB109* gene sequence, forward and reverse primers were designed to amplify the second exon of *DEFB109*, which would be translated into the hBD9 pro-peptide. Several considerations were taken into account when designing the primers. First, the start codon was incorporated into the forward primers, upstream by several oligonucleotide residues of *DEFB109*. Second, to allow the incorporation of a HisTag at the carboxyl terminal of the translated protein, the intrinsic stop codon at the end of the gene was eliminated from the reverse primer. Inclusion of endonuclease restriction sites, one each for the forward and reverse primer, was required to allow the gene product to carry compatible ends for ligation. Lastly, a few nucleotide residues were added upstream of the restriction sites on the forward primer and downstream of the reverse primer, for effective digestion by the endonuclease enzymes.

The designed sequences of the primers were then analysed by using the online primer analysis software (http://www.premierbiosoft.com/NetPrimer/AnalyzePrimer.jsp) for the possibility of hairpins or dimer formation. The primers were then tested by

performing *in silico* PCR using the UCSC genome software (http://genome.ucsc.edu/), to verify the resultant PCR product.

2.3.6 PCR

The conventional PCR was performed using the Hybaid Express thermocycler (Hybaid, Middlesex, UK). Each reaction consisted of 5.0 µl 10X PFU PCR buffer, 2.0 µl 2.5 µM dNTP, 0.25 µl Tween, 1.0 µl PrimerMix, 0.25 µl PFU Ultra II DNA polymerase (Agilent Technologies, London, UK), 1.0 µl DNA template, and PCR water added to a final volume of 25 µl. The reaction cycle used was 95 ^{o}C for 15 minutes for the denaturing step. This was followed by 37 cycles of further denaturing at 95 ^{o}C for 1 min, annealing at 58 ^{o}C for 1 minute and elongation at 72 ^{o}C for 30 seconds. Final elongation step was 72 ^{o}C for 10 minutes.

After performing PCR using the initial PCR conditions, gradient PCR was performed to optimise the result. The same PCR mixture was used but the PCR cycle was modified. We used different annealing temperatures between 54 ^{o}C and 64 ^{o}C. The annealing temperature which gave the optimal result, as shown by agarose gel electrophoresis, was then selected as the annealing temperature in subsequent PCR.

2.3.7 Agarose gel electrophoresis

To prepare agarose 2% (w/v) gel, 2 g of agarose powder (Sigma Aldrich, Gillingham, UK) was added to 100 ml 1x Tris-Borate EDTA (TBE) (Fisher Scientific, Loughborough, UK) buffer in a 250 ml flask. The solution was heated until the powder had fully dissolved and then allowed to cool to room temperature. 0.4 µg/ml ethidium bromide (EtBr) (Sigma Aldrich,

Gillingham, UK) was added to the solution and mixed by gently swirling the flask. The solution was then poured into the casting tray with well comb in place. The gel was allowed to set before the comb was removed. The casting tray with the gel content was transferred into the electrophoresis tank. 10 µl of DNA samples were mixed with 2 µl of 6X gel loading dye (Thermo Scientific, Loughborough, UK) and loaded into the wells. The voltage supply was set at 90 V for 90 minutes. The gel was viewed under ultraviolet viewer immediately after completion of the electrophoresis. Photographs of the gel were captured using Nikon digital single lens reflex (SLR) camera.

2.3.8 Gel purification

Gel purification was done using the gel purification kit (Macherey Nagel, Thermo Scientific, Loughborough, UK) according to the manufacturer's recommendation. The DNA bands from the agarose gel were carefully excised, weighed and placed in the micro-centrifuge tubes. 300 µl of buffer NT1 was added for every 100 µg of the excised gel. 4 µl of silica matrix was added for every µg of the DNA. The mixtures were then incubated at 50 ^{o}C for 10 minutes and vortexed every 2-3 minutes until all the gel has dissolved. The sample was then centrifuged at 10,000 g for 30 seconds. The supernatant was subsequently discarded. 500 µl of buffer NT2 were added to the pellet and vortexed briefly before being centrifuged at 10,000g for 30 seconds. The supernatant was discarded and the pellet underwent two cycles of washing with wash buffer, and centrifuging at 10,000 g for 30 seconds before the supernatant was discarded. The silica pellet was then dried at room temperature for 10 minutes before being eluted in 25 µl of elute buffer, resuspended by vortexing and centrifuged at 10,000g for 30 seconds.

The DNA-containing supernatant was then transferred to a clean tube. The DNA sample was later subjected to quantification steps by using a nanodrop spectrophotometer.

2.3.9 Restriction digestion

The circular pET21a(+) (Novagen, Merck Millipore, Watford, UK) was double digested using *Bam*HI and *Xho*I restriction enzymes to form a linearised plasmid vector with overhanging ends for a directional ligation step. By selecting *Xho*I as the downstream restriction enzyme, the HisTag will be positioned immediately after the hBD9 propeptide in the fusion protein.

The restriction digestion was performed using two different enzymes digesting at different sites. This was planned with the intention to create two sticky ends on the plasmid vector and corresponding ends on the gene insert. Having achieved this, correct directional insertion of the gene into the plasmid, or the recombination, could take place during ligation. It also ruled out self-ligation of the linearised plasmid or misdirected ligation of the gene insert.

The reaction prepared consisted of 0.3 µl (100 mg/ml) bovine serum albumin (BSA), restriction buffer 10X (3 µl), 1 µl each of *Bam*HI and *Xho*I enzymes (New England Biolabs, Herts, UK) and 1 µl (1 µg/µl) of the pET21a(+) plasmid DNA with PCR water added to a final reaction volume of 25 µl. The reaction mixture was incubated at 37 ^{o}C for an hour in the Hybaid Express (Hybaid, Middlesex, UK) thermocycler.

The reaction was later optimised to achieve the best result. For the subsequent restriction of the plasmid DNA, 0.3 µl (100 mg/ml) BSA (Sigma Aldrich, Gillingham, UK), 3 µl 10X restriction buffer, 2 µl (20,000 units/ml)

each of *Bam*HI and *Xho*I enzymes (New England Biolabs, Herts, UK) and 2 µl (1 µg/µl) of the plasmid DNA with water added to a final reaction volume of 40 µl. The restriction mixture was incubated at 37 ^{o}C for two hours in the thermocycler (Hybaid Express, Middlesex, UK). Negative controls consisting of the same reaction but omitting either the plasmid DNA or the restriction enzymes were run simultaneously. Restriction digestion was followed with agarose gel electrophoresis. All of the reactions were loaded into the well with 2 µl of 6X gel loading dye (Thermo Scientific, Loughborough, UK). Agarose gel 2% (w/v) electrophoresis was run at 90 V for 90 minutes to visualise the product and presence of cut plasmid at 5 kbp and a faint band of 220 bp to indicate that the double restriction digest was successful.

2.3.10 Ligation

Following double restriction digestion of the plasmid vector and the gene insert, ligation was conducted to obtain the recombinant plasmid DNA. The ligation reaction consisted of 1 µl (400,000 units/ml) T4 DNA ligase (New England Biolabs, Herts, UK), 2 µl ligation buffer (New England Biolabs, Herts, UK), 1 µl gene insert at 25 ng/µl concentration and 3, 5 or 10 µl double digested plasmid vector at 30 µg/µl concentration. Double-distilled water was added to achieve final reaction volume of 20 µl. The amount of plasmid used was varied to obtain different insert to plasmid molecular ratios. The ligation reactions were incubated at 16 ^{o}C for 16 hours followed by 65 ^{o}C for 10 minutes to deactivate the ligase enzyme, in the Hybaid Express (Hybaid, Middlesex, UK). Negative controls without either the T4 DNA ligase or insert were run simultaneously (Table 2.3.1).

Table 2.3.1 Table summarising the typical ligation reactions and controls for the construction of the recombinant plasmid DNA. DC, double cut; SC, single cut; /, included; X, omitted.

	L1	L2	L3	L4	L5	L6	L7	L8
H_2O, add to 20 µl	/	/	/	/	/	/	/	/
T4 DNA ligase buffer, 2 µl	/	/	/	/	/	/	/	/
T4 DNA ligase, 1 µl	X	X	/	/	/	/	/	X
Gene Insert, 2 µl	X	X	X	X	/	/	/	x
Plasmid DNA	DC, 2 µl	Uncut, fresh plasmid 1 µl	DC	SC	DC	DC	DC	SC
Remark	Transformation negative control	Transformation positive control	Double restriction control	Ligation positive control	2:1	4:1	6:1	Ligation negative control

2.3.11 Transformation into cloning host

The ligation mixture was later transformed into competent cloning cells of NovaBlue *E. coli* (Novagen, Merck Millipore, Watford, UK), which has high transformation efficiency and ability to retain the plasmid construct stable in the long term. In brief, 2 µl of the ligation mixture was gently mixed with 50 µl NovaBlue *E. coli* (Novagen, Merck Millipore, Watford, UK) and incubated on ice for 5 minutes. The mixture was then transferred into a water bath set at 42 ^{o}C for 45 seconds before placed in the ice again for another two minutes. 200 µl of super optimum culture (SOC) medium was added and the mixture was incubated in shaker incubator at 37 ^{o}C 230 revolution per minute (rpm) for an hour. Meanwhile, the culture plates were set to 37 ^{o}C; Luria Bertani (LB) agar plates were laid with 100 µl of 20 mg/ml X-gal and 20 µl 0.1 M isopropyl-thio-galactoside (IPTG) using a sterile plastic spreader. This was

followed by inoculation of 50 µl of the 'revived' transformed *E. coli* onto the newly prepared LB/X-gal/ IPTG agar and incubated overnight at 37 ^{o}C. The culture plates were examined on the following morning for growth of the colonies.

2.3.12 Verification of transformed gene

A single colony from the transformation culture plate was inoculated into 15 ml of fresh LB broth containing ampicillin. The culture broths were incubated in the shaker incubator at 37 ^{o}C, at 200 rpm overnight. The cells were harvested via centrifugation in the swing-bucket centrifuge (Hettich, Newport Pagnell, UK) at 6000 x g for 10 minutes at 4 ^{o}C. The cell pellet was subjected to plasmid DNA purification using the Qiagen miniprep spin column (Qiagen, Manchester, UK). The purified plasmid DNA was then quantified using nanodrop spectrophotometer before being sent for direct sequencing at Eurofins MWG Operon, Ebersberg, Germany.

2.3.13 Transformation into expression hosts

The verified and correctly oriented recombinant plasmid DNA was transformed into the expression host which was purchased from Invitrogen, Paisley, UK. For the transformation, 50 µl aliquots of *E. coli* competent cells BL21 Star (DE3) pLysS, BL21 (DE3) pLysE, TOP10F' and BL21-A1 (Invitrogen, Paisley, UK) from the -80 ^{o}C storage freezer were thawed in ice. 2 µl of the recombinant plasmid DNA were added and mixed by gentle pipetting. The mixture was incubated on ice for exactly 30 minutes followed by heat shock at 42 ^{o}C for 30 seconds in the water bath. The reactions were transferred onto ice again for another two minutes. 250 µl of preheated super

optimum broth with catabolic repressor, SOC media, were added to the mixtures before incubation in the shaker incubator at 37 ^{o}C, 230 rpm for 1 hour. After an hour of incubation, 50 µl of the transformation reaction was cultured on the LB/Ampicillin agar plates and incubated at 37 ^{o}C overnight. The culture plates were inspected on the following day for colonies. Blue colonies contained intact plasmid vector while the white colonies contained the recombinant plasmid DNA. For a positive control, the same transformation steps were applied by using the pUC19 plasmid in replacement of the hBD9 plasmid construct.

2.3.14 Colony PCR

Colony PCR was performed exactly like the conventional PCR described above but the DNA template used was the bacterial colonies. The colony to be tested was touched with the pipette tip and transferred to the PCR reaction mixture. The PCR cycles used were similar to the conventional PCR.

2.4 Results

2.4.1 Identifying *DEFB109* for cloning

The search for *DEFB109* gene sequence from the NCBI nucleotide database, as described in the method section, returned 7 hits that included *DEFB109* complete cDNA, *DEFB109*P1 and *DEFB109*P1B. Search for *DEFB109* in the gene database resulted in 3 hits, namely, *DEFB109* (NR_000008.100), *DEFB109*P1 (NR_024044.2) and *DEFB109*P1B (NR_003668.2). When blasted against the human genome, it resulted in 5

different contigs in 3 human chromosomes (NT_0775531.4, NT_0237336.17 and NT_167187.1 in chromosome 8, NT_0097140 in chromosome 12 and NT_006316.16 in chromosome 4). To confirm the correct sequence to act as a template for *DEFB109* cloning, *DEFB109* sequences from five different contigs in the human genome were collated and CLUSTAL-compared. This identified that the *DEFB109* version at 7.8 Mb in chromosome 8 was the functional version. This version of the *DEFB109* was therefore used for the purpose of primer designing.

Table 2.4.1 Primers designed for the amplification of the DEFB109 second exon encoding for the hBD9 propeptide.

Primer	Sequence
Forward primer	GTC GC GGA TCC A ATG GGT TTG GGT CCT
Reverse primer	GTG GTG CTC GAG TTT CAA GTT AGG

The sequence of amplified PCR product would be:

Figure 2.4.1 Sequence of the PCR product showing the insertion of the *DEFB109* gene flanked by the N-terminal *Bam*HI recognition site, stop codon and C-terminal *Xho*I recognition site, with the intrinsic stop codon removed and being in-frame with the C-terminal HisTag sequence when ligated into pET21a(+).

2.4.2 *DEFB109* gene amplification using PCR

Forward and reverse primers were successfully designed which incorporated the necessary motifs for the planned recombination strategy. The preliminary PCR experiments were not successful due to suboptimal annealing temperatures. This was later overcome through PCR optimisation using a gradient PCR. The annealing temperature was increased from 56 ^{o}C to 58 ^{o}C and the gene of interest was successfully amplified, producing a band corresponding to the 220 bp gene product (Figure 2.4.2). A stock of the gene product was prepared and stored at -20 ^{o}C for subsequent purification and cloning.

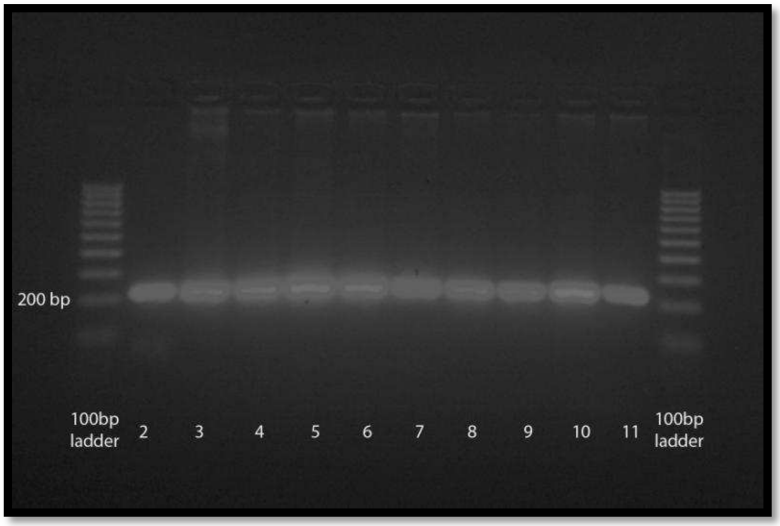

Figure 2.4.2: Photograph of agarose gel showing presence of bands corresponding to 220 bp in lane 2-11, indicating the *DEFB109* gene has been successfully amplified.

2.4.3 Plasmid selection

The pET21a(+) plasmid system was chosen because it has multiple restriction sites in the multiple cloning sites (MCS) for different restriction enzymes. We used these restriction sites for cutting the plasmid and creating a sticky or overhanging end. This would ensure the correct directional ligation of the gene insert into the plasmid to form the recombinant plasmid DNA. The gene was inserted between the *Bam*HI and *Xho*I restriction sites and the ligated plasmid would have lost its restriction site for *Eco*RI. *Eco*RI could then be used to verify if the plasmid is intact or had been digested and ligated.

pET21a(+) has a sequence conferring resistance to ampicillin. This would confer ampicillin-resistance to the transformed bacteria and render the untransformed bacteria non-viable upon exposure to ampicillin.

When the MCS was digested by the restriction digestion enzymes, the host lost its ability to produce galactosidase. Without the galactosidase, X-gal could not be metabolised thus causing the colony to be white in colour. In

cases where the restriction and ligation have not taken place, and the host bacterium was transformed with the intact plasmid, galactosidase was produced and the X-gal was metabolized to form 5-bromo-4-chloro-indolyl which is spontaneously oxidized to the bright blue insoluble pigment 5,5'-dibromo-4,4'-dichloro-indigo, and thus stained the colony blue.

For the purpose of purification, the C-terminal HisTag which is located just after the *Xho*I endonuclease restriction site will be utilised in the process of IMAC protein purification. The short HisTag is considered small and may not necessarily be removed as it hardly interferes with target protein function.

2.4.4 Restriction digestion of pET21a(+)

In this experiment the plasmid used was a recombinant pET21a(+) vector which contained a 220 bp *DEFB109* gene insert between the *Bam*HI and *Xho*I restriction sites, from a previous study of our group. This plasmid was chosen as it would be easier to trace the free gene fragment in a successful experiment rather than to trace a smaller 50 bp gene should the empty pET21a(+) be used. Presence of free gene represented by a band located between the 200 and 300 bp ladder fragments would indicate the success of the double restriction digestion.

A double restriction digest of the plasmid DNA using the previously mentioned recipe and conditions was performed and is shown in Figure 2.4.3. In the lanes with double digested plasmid, there is a smaller band corresponding to the 280 bp fragment detected. These bands represent the free gene insert between the *Bam*HI and *Xho*I restriction sites. The larger part of the double digested plasmid has migrated further compared to the single digested plasmid. As expected, because the difference in size

between the two was small (difference of 280 bp), difference in migration was also minimal.

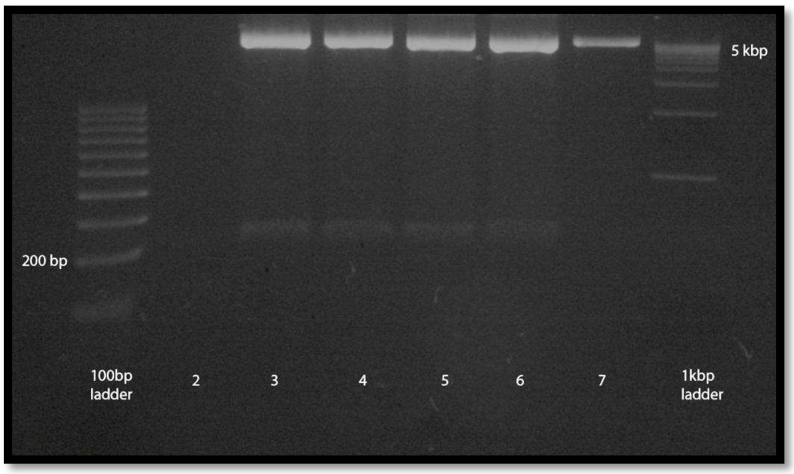

Figure 2.4.3: Photograph of agarose gel showing double restricted plasmid band corresponding to 5 kbp fragment bands with presence of smaller free fragment of 250 bp, in lanes 3, 4, 5 and 6. Lane 2 is negative control and lane 7 is single restriction digestion.

A repeat of the experiment was conducted using the recombinant plasmid DNA and the empty pET21a(+). This was conducted to show that, the same digestion that worked with the recombinant plasmid would also work with the empty plasmid DNA. The result of this experiment is shown inFigure 2.4.4. The lane allocation in the gel electrophoresis is summarised in Table 2.4.2.

Table 2.4.2 Table summarising the lane allocation for agarose gel in Figure 2.4.4.

Lane no.	Description
Lane 1	1 kbp ladder
Lane 2	Uncut recombinant plasmid
Lane 3	*Bam*HI-HF recombinant plasmid
Lane 4	*Xho*I recombinant plasmid
Lane 5	Double cut recombinant plasmid
Lane 6	Uncut pET21a plasmid
Lane 7	*Bam*HI cut pET21a plasmid
Lane 8	*Xho*I cut pET21a plasmid
Lane 9	Double cut pET21a plasmid
Lane 10	Double cut pET21 a plasmid new miniprep
Lane 11	Double cut recombinant plasmid new miniprep
Lane 12	100 bp ladder

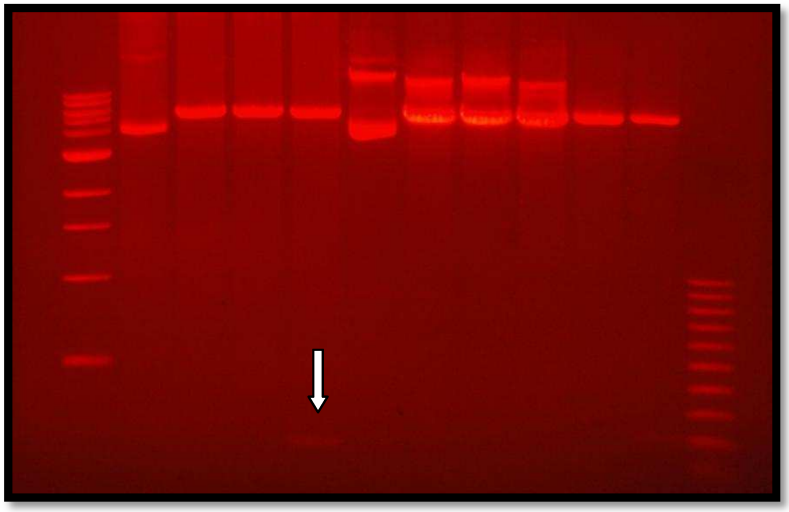

Figure 2.4.4 Photograph of the gel showing the double restriction digestion of the recombinant plasmid DNA and the pET21a(+) vector. L, lane; bp, base pair.

Following the successful double restriction digestion of the plasmid DNA, the bands in the gel were excised and subjected to gel purification using a spin column kit (Qiagen, Manchester, UK).

2.4.5 Restriction digestion of *DEFB109* gene insert

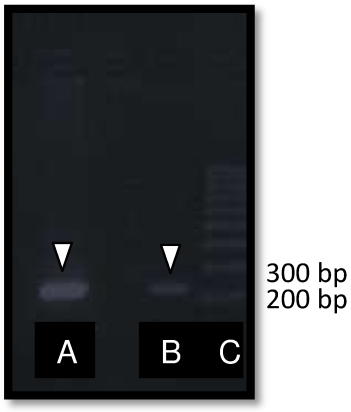

Figure 2.4.5 Photograph of the restriction digestion of the *DEFB109* gene insert showing the undigested gene (A) are at the same position with double digested gene (B) corresponding to 220 bp because the latter is shorter by a few bp compared to the former. (C) molecular weight ladder.

2.4.6 Ligation

The ligation reactions were set to have different insert to plasmid molecular ratios. This was performed to increase the probability of successful reaction. The results of the reactions could only be only concluded when the transformation and culturing were completed. All the set ligation reactions were transformed accordingly and the culture plates were examined for colonies.

Table 2.4.3 Summary of the reactions and the controls set up in the T4 ligation process to construct the recombinant plasmid DNA. DS, double cut; SC, single cut; /, included; X, omitted.

	L1	L2	L3	L4	L5	L6	L7	L8
H_2O, add to 20 µl	/	/	/	/	/	/	/	/
T4 DNA ligase buffer, 2 µl	/	/	/	/	/	/	/	/
T4 DNA ligase, 1 µl	X	X	/	/	/	/	/	X
Insert 20 ng/ul x 2 µl	X	X	X	X	/	/	/	x
Plasmid, 58 ng/ul	DC, 4.23 µl	Uncut, fresh plasmid (267 ng/ul), 1 µl	DC, 4.23 µl	SC, 4 µl	DC, 8.46 µl	DC, 4.23 µl	DC, 2.82 µl	SC, 4 µl
Remark	Transformation negative control	Transformation positive control	Double restriction control	Ligation positive control	2:1	4:1	6:1	Ligation negative control

2.4.7 Transformation and culturing

Transformations were successful and were indicated by positive culture of a single white colony on LB/Amp culture plates from reaction L7 after overnight incubation at 37 ^{o}C. The single colony was subcultured into 3 ml of fresh LB/Amp broth and incubated in the orbital shaker at 37 ^{o}C, 230 rpm for 3 hours to reach the OD_{600} 0.5 in triplicate. The subcultures were then plated onto LB/Amp agar plates in duplicate and incubated at 37 ^{o}C overnight. On the following day, the plates were examined for growth or organisms in colonies (Figure 2.4.6).

Figure 2.4.6: Culture plates following inoculation of transformants onto fresh Luria Bertani (LB) with ampicillin (LB/Amp) culture plates. Presence of white colonies indicates the ligation and transformation have been successful.

2.4.8 Colony PCR

Colony PCR was performed and showed that the gene of interest was successfully amplified as evident by the agarose gel showing bands corresponding to 220 bp (Figure 2.4.7).

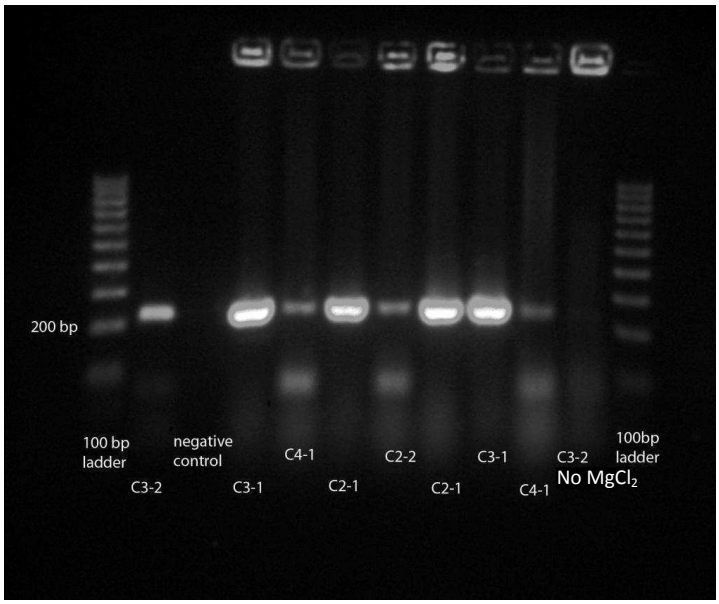

Figure 2.4.7: Photograph of agarose gel showing bands corresponding to the size of *DEFB109* gene. Lane label: C indicates TOP10F bacterial host, followed by culture and colony number. Negative control consisted of PCR reaction without the bacterial sample.

2.5 Discussion

There has been no reported study on expression of hBD9 pro-peptide and its functional characteristics. Although there have been a few reports on recombinant production of other human β-defensins, to the best of our knowledge, this is the first attempt to clone *DEFB109* gene and express the hBD9 protein using the *E. coli* expression system. As mentioned earlier, as a member of the β-defensin family, hBD9 was assumed to have the hallmark antimicrobial effect, albeit this has yet to be proven scientifically.

Amplification of the gene by conventional PCR needed optimisation as primer dimers formed in the beginning without gene product. Gradient PCR was performed and had shown that increasing the annealing temperature from 56 ^{o}C to 58 ^{o}C resulted in successful *DEFB109* gene amplification.

Difficulties had also been encountered with the double restriction digestion procedure. Although the stock plasmid DNA was double-restricted, the enzymatic activity was not 100%. Therefore, there was still a portion of the plasmid which was not double-restricted. In the agarose gel, the uncut plasmid was not distinctively separated from the cut plasmid. When excising the restricted band for gel purification, the unrestricted plasmid must have been included. This was later transformed into the bacterial host. Therefore, during transformation and culture, a positive result was observed but sequencing did not verify this.

At the earlier stage of our experiment we recognised failure to add 5 to 6 nucleotide residues to flank the restriction enzymes recognition sites in the forward and reverse primers. As a consequence, although the endonuclease restriction sites were present, the enzymes could not recognise the sites and effectively digest the gene. The sticky ends could not be produced to make the insert compatible with the restricted plasmid. Therefore, ligation was not successful as was expected.

It was also subsequently found out that the forward primer did not have to carry a start codon (ATG). This was because the translation of the recombinant plasmid DNA did not start at that particular start codon. In fact, the translation will start at the ribosomal binding site (RBS) [234], upstream to the MCS of the plasmid pET21a(+). The presence of the start codon in the forward primer would have only added an extra methionine amino acid at the N-terminal of the pro-peptide.

The removal of the stop codon at the reverse primer was necessary. This motif in an in-frame sequence would have terminated the translation at

the site of the stop codon. No further translation beyond the stop codon would take place and the HisTag would be missing from the fusion protein.

The pET21a(+) fusion partnership was not advantageous for the high expression of the soluble hBD9 protein. pET21a(+) plasmid vector has T7-Tag which only facilitates the detection of the fusion protein. Unlike the Trx tag or MBP, the T7 fusion tag did not give the advantage to enhance the production of the disulphide bond in the target protein for proper folding.

The proteolytic strategy was not included in the construction of the recombinant plasmid DNA. pET21a(+) had no proteolytic cleavage site which can finally be utilised to separate the fusion tag from the target protein. The frequently used proteolytic enzymes include the rEK, thrombin factor Xa and TEV. As such, different pET vector other than pET21a(+) is required for this purpose.

The design of the plasmid pET21a(+) also would require removal of a single base pair beyond the *Bam*HI, in order to make the C-terminal HisTag sequence in-frame and allow successful translation of the HisTag in the fusion protein. Failure to adhere to this requirement would disrupt the reading frame making it incompatible for the translation of the HisTag.

Although the cloned pET21a(+)-hBD9 recombinant plasmid DNA was not suitable for the expression of the hBD9 fusion protein, the cloning conditions have been successful as evident in the colony PCR (Figure 2.4.7), and could be applied in the construction of future plasmid construct. The recombinant plasmid DNA can also be the *DEFB109* DNA template in future works. A plasmid vector which supports the formation of disulphide bond and

incorporates the proteolytic system in it, such as pET32a(+), would be preferred.

Chapter 3

DEFB109 gene optimisation

CHAPTER 3: *DEFB109* gene optimisation

3.1 Introduction

The human genome uses four nucleotide bases, namely the purines adenine (A) and guanidine (G), and pyrimidines thymine (T) and cytosine (C). A sequence of nucleotide triplet termed a codon encodes for a specific amino acid. Since there are four nucleotides and can therefore be 64 possible codons to code for only twenty amino acids, one or more codon may be linked with each amino acid. For example, both codons CAC and CAG encode histidine and they are called synonymous codons. Methionine and tryptophan are the only two amino acids that are encoded by a single codon, ATG and TGG, respectively.

In a given species, certain codons are used more often than other synonymous codons for a specific amino acid. These codons are referred to as the preferred codons. A species such as *E. coli* has a different set of preferred codons compared to other species, such as humans. Because of this preference, heterologous protein expression in an expression host such as *E. coli* can be hampered [235].

3.1.1 tRNA optimisation

tRNA for a rare codon is produced less frequently compared to the preferred codon tRNA. As such, the translation of the amino acid would be affected. A strategy to increase production of the heterologous protein from the rare codon usage would be to co-express the tRNA for the said rare codon.

Rosano *et al* reported the effect of using codon bias-adjusted *Escherichia coli* strain for the expression of recombinant proteins [235]. This strain of *E. coli* (BL21(DE3)-CodonPlus-pRIL) contained extra copies of tRNA genes which are transcribed into extra tRNA that recognise the codons not preferred by the *E. coli*. By doing this, the efficiency of expression of a heterologous gene in *E. coli* would increase. The level of expression and solubility of the recombinant proteins were analysed by SDS-PAGE and western blot. Their result showed that solubility in the codon bias adjusted strain was reduced compared to the normal unadjusted strain. The host *E. coli* growth was also found to be hampered across all the induction temperatures tested. They concluded that expression of these proteins was detrimental to the solubility state of the protein. This could be related to the increased translation rate leading to protein misfolding and aggregation.

3.1.2 Gene optimisation

Instead of using the native human codons, the gene for the protein can be transformed into that preferred by the expression host. This can be done using various methods of gene synthesis. Chen *et al* reported 9-fold increase in the expression of heterologous protein in *E. coli* when using the optimised gene compared to unoptimised native gene [236].

3.1.3 *DEFB109* gene optimisation

The preferred codon for various organisms has been submitted to an online database. This included that for *E. coli* and one such database is run by Kazusa DNA Research Institute, Japan (http://www.kazusa.or.jp). The

following is the preferred codon table for *E. coli* K12 which was retrieved from http://www.kazusa.or.jp/codon/cgi-bin/showcodon.

Table 3.1.1 showing the frequency of codon usage for each amino acid by *Escherichia coli* K12.

fields: [triplet] [amino acid] [fraction] [frequency: per thousand] ([number])			
UUU F 0.57 19.7 (101)	UCU S 0.11 5.7 (29)	UAU Y 0.53 16.8 (86)	UGU C 0.42 5.9 (30)
UUC F 0.43 15.0 (77)	UCC S 0.11 5.5 (28)	UAC Y 0.47 14.6 (75)	UGC C 0.58 8.0 (41)
UUA L 0.15 15.2 (78)	UCA S 0.15 7.8 (40)	UAA * 0.64 1.8 (9)	UGA * 0.36 1.0 (5)
UUG L 0.12 11.9 (61)	UCG S 0.16 8.0 (41)	UAG * 0.00 0.0 (0)	UGG W 1.00 10.7 (55)
CUU L 0.12 11.9 (61)	CCU P 0.17 8.4 (43)	CAU H 0.55 15.8 (81)	CGU R 0.36 21.1 (108)
CUC L 0.10 10.5 (54)	CCC P 0.13 6.4 (33)	CAC H 0.45 13.1 (67)	CGC R 0.44 26.0 (133)
CUA L 0.05 5.3 (27)	CCA P 0.14 6.6 (34)	CAA Q 0.30 12.1 (62)	CGA R 0.07 4.3 (22)
CUG L 0.46 46.9 (240)	CCG P 0.55 26.7 (137)	CAG Q 0.70 27.7 (142)	CGG R 0.07 4.1 (21)
AUU I 0.58 30.5 (156)	ACU T 0.16 8.0 (41)	AAU N 0.47 21.9 (112)	AGU S 0.14 7.2 (37)
AUC I 0.35 18.2 (93)	ACC T 0.47 22.8 (117)	AAC N 0.53 24.4 (125)	AGC S 0.33 16.6 (85)
AUA I 0.07 3.7 (19)	ACA T 0.13 6.4 (33)	AAA K 0.73 33.2 (170)	AGA R 0.02 1.4 (7)
AUG M 1.00 24.8 (127)	ACG T 0.24 11.5 (59)	AAG K 0.27 12.1 (62)	AGG R 0.03 1.6 (8)
GUU V 0.25 16.8 (86)	GCU A 0.11 10.7 (55)	GAU D 0.65 37.9 (194)	GGU G 0.29 21.3 (109)
GUC V 0.18 11.7 (60)	GCC A 0.31 31.6 (162)	GAC D 0.35 20.5 (105)	GGC G 0.46 33.4 (171)
GUA V 0.17 11.5 (59)	GCA A 0.21 21.1 (108)	GAA E 0.70 43.7 (224)	GGA G 0.13 9.2 (47)
GUG V 0.40 26.4 (135)	GCG A 0.38 38.5 (197)	GAG E 0.30 18.4 (94)	GGG G 0.12 8.6 (44)
Coding GC 52.35% 1st letter GC 60.82% 2nd letter GC 40.61% 3rd letter GC 55.62% Genetic code 1: Standard			

The following is the codon weight chart (Optimizer) summarising the *E. coli* codon usage. It shows how frequently each codon is used by *E. coli* K12.

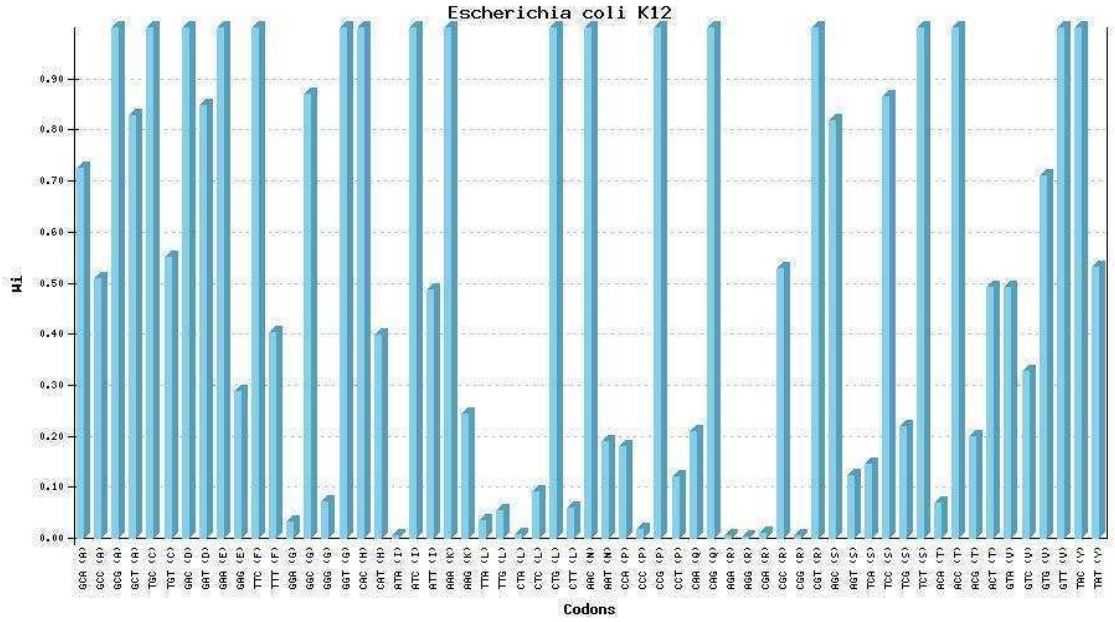

Figure 3.1.1 Codon weight chart (Optimizer) summarising the *E. coli* codon usage. It shows how frequently each codon is used by *E. coli* K12.

The sequence of the native human *DEFB109* gene is shown in Figure 3.1.2 with the corresponding peptide sequence in alignment. This nucleotide sequence of the second exon will translate into hBD9 propeptide which has 65 amino acids. Of these, there were five arginines and seven lysines. The arginine in native *DEF109* was coded using codons AGG (1), CGA (1) and AGA (3) which are rarely used in *E. coli* K12 strains. These codons were reported to be associated with poor protein synthesis [237, 238]. None of the arginine residues were coded using *E. coli* preferred codons, which are CGG or CGT.

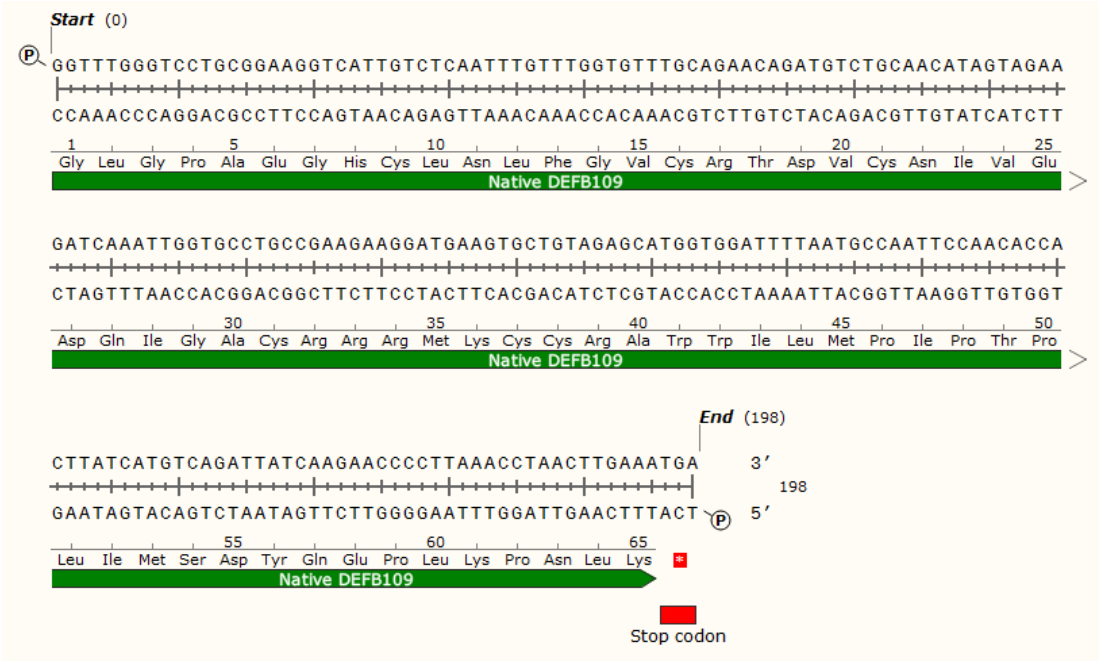

Figure 3.1.2 Sequence of the native *DEFB109* and the corresponding hBD9 peptide sequence.

In order to overcome the effect of preferred codon bias in the expression host, the above DNA sequence was optimised to the preferred codon usage of *E. coli* K12. The gene was submitted to the Genius optimisation software by Eurofins MWG Operans and the optimised gene was synthesised for usage in this study. The optimised gene sequence is shown in Figure 3.1.3.

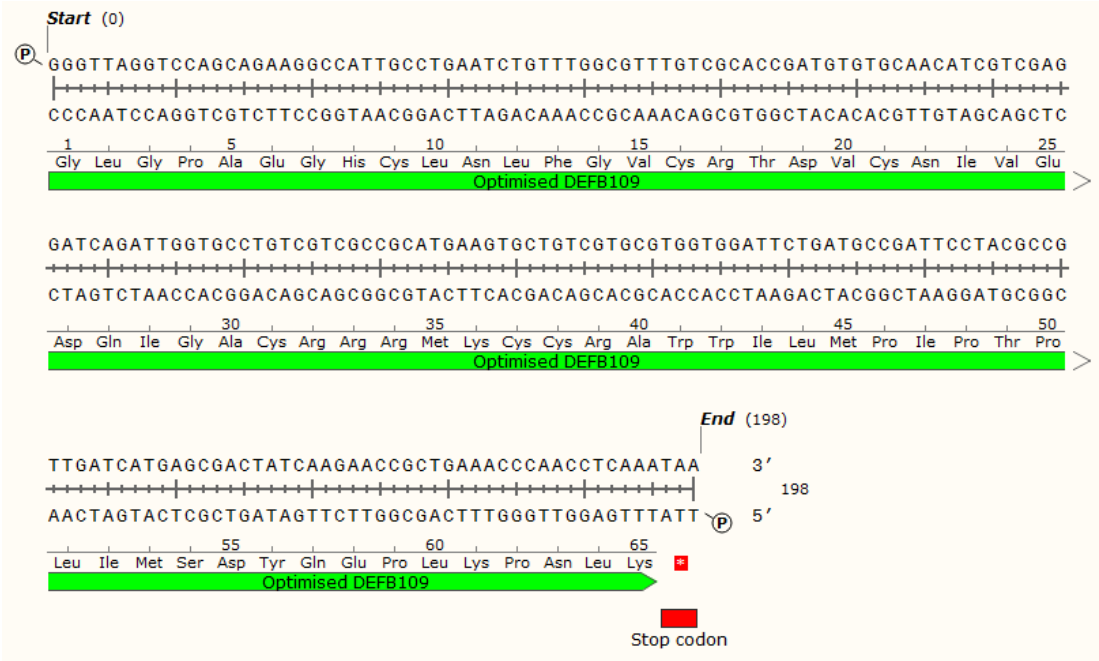

Figure 3.1.3 Nucleotide sequence for the K12 *E. coli* preferred codon optimised *DEFB109* and the corresponding hBD9 peptide sequence.

The codons usage in the native gene (query) was compared with codons usage in the optimised sequence and is summarised in Table 3.1.2. The optimised gene synthesised and used in this study was also submitted to the gene optimizer software for comparison and double-checking (http://genomes.urv.es/OPTIMIZER) [239]. According to the second software, the optimised gene showed improvement from the native gene and could have slightly been further optimised to increase the probability of successful expression.

Table 3.1.2 Table comparing the amino acid synonymous codons in native and optimised *DEFB109* gene.

Codons	Native	Optimized	Codons	Native	Optimized
GCA (A)	1	0	GCC (A)	1	0
TGC (C)	4	6	TGT (C)	2	0
GAA (E)	3	3	GAG (E)	0	0
GGA (G)	0	0	GGC (G)	0	0
CAC (H)	0	1	CAT (H)	1	0
ATT (I)	3	0	AAA (K)	2	3
TTG (L)	3	0	CTA (L)	0	0
CTT (L)	2	0	ATG (M)	3	3
CCA (P)	3	0	CCC (P)	1	0
CAA (Q)	2	0	CAG (Q)	0	2
CGA (R)	1	0	CGC (R)	0	0
AGC (S)	0	0	AGT (S)	0	0
TCG (S)	0	0	TCT (S)	0	1
ACG (T)	0	0	ACT (T)	0	0
GTG (V)	0	0	GTT (V)	1	3
TAT (Y)	1	0	TAA (.)	0	0
GCG (A)	1	3	GCT (A)	0	0
GAC (D)	0	3	GAT (D)	3	0
TTC (F)	0	1	TTT (F)	1	0
GGG (G)	0	0	GGT (G)	5	5
ATA (I)	1	0	ATC (I)	1	5
AAG (K)	1	0	TTA (L)	1	0
CTC (L)	1	0	CTG (L)	0	7
AAC (N)	2	3	AAT (N)	1	0
CCG (P)	0	6	CCT (P)	2	0
AGA (R)	3	0	AGG (R)	1	0
CGG (R)	0	0	CGT (R)	0	5
TCA (S)	1	0	TCC (S)	0	0
ACA (T)	2	0	ACC (T)	0	2
GTA (V)	1	0	GTC (V)	1	0
TGG (W)	2	2	TAC (Y)	0	1
TGA (.)	0	0	TAG (.)	0	0

3.2 Objectives

a. To optimise the *DEFB109* native gene into the K12 *E. coli* preferred codon sequence.

b. To incorporate the native and optimised pET32a(+)-*DEFB109* plasmid constructs into the K12 *E. coli* expression hosts.

c. To compare the Trx-hBD9 fusion protein expression in *E. coli* harbouring the optimised gene with that from *E. coli* harbouring the un-optimised native *DEFB109* gene.

3.3 Methods

3.3.1 Digestion of the pET32a(+) plasmid vector

The circular pET32a(+) (Novagen, Merck Millipore, Watford, UK,) was double digested using *Nco*I and *Bam*HI restriction enzymes to prepare the linearised plasmid vector with overhanging ends for the downstream ligation step. By selecting *Nco*I as the upstream restriction enzymes, the target peptide will be positioned immediately after the enterokinase cleavage site in the fusion protein. For the restriction digestion of the pET32a(+), the optimised reaction conditions for pET21a(+) (2.3.9, page 91) was applied and found to be effective.

3.3.2 Digestion of the gene inserts

The native *DEFB109* gene insert was amplified using PCR, using the conditions described in previous chapter, from the pET21a(+)-*DEFB109* recombinant plasmid with incorporations of *Nco*I and *Bam*HI restriction site sequences in the forward and reverse primers, respectively. The optimised

DEFB109 gene with upstream *Nco*I and downstream *Bam*HI restriction site sequences were purchased from Eurofins MWG Operon, Ebersberg, Germany. These gene inserts were then subjected to double restriction digestion using the *Nco*I and *Bam*HI enzymes, at the conditions described in previous chapters, to render them compatible for directional ligation using T4 DNA ligase.

3.3.3 Ligation

The native and optimised *DEFB109* gene inserts were ligated into the linearised pET32a(+) plasmid vector using the directional ligation with T4 DNA ligase as described in previous chapter (2.3.10, page 92). In brief, the double digested *DEFB109* gene insert was incubated with the digested plasmid DNA at variable insert to plasmid molecular weight ratios in 20 µl final reactions containing 1 µl (400,000 units/ml) T4 DNA ligase enzyme, 5 µl ligation buffer at 4 ^{o}C for 16 hours followed by inactivation at 65 ^{o}C for 10 minutes.

3.3.4 Transformation into cloning host

The ligation product was transformed into NovaBlue *E. coli* (Novagen, Merck Millipore, Watford, UK), using the rapid heat shock chemical transformation system. In brief, the transformation mixture was added to the 50 µl NovaBlue cells and mix gently by pipetting. The mixture was incubated on ice for 5 minutes before shocked at 42 ^{o}C for 1 min and returned to ice for another 2 min. 200 µl of warm SOC media was then added to the *E. coli* and the cells were incubated in the shaker incubator at 37 ^{o}C 230 rpm for half an hour.

The transformed NovaBlue *E. coli* hosts were later subjected to the colony selection culture using the LB/Amp/Xgal agar. Untransformed NovaBlue cells will not grow, as they do not have the plasmid construct carrying the resistance against ampicillin. Transformed *E. coli* with recombinant plasmid DNA will form a white colony while the transformed colony with intact plasmid vector will turn blue. A white colony was desired as it represented *E. coli* containing recombinant plasmid DNA.

3.3.5 Plasmid purification and sequencing

The cloning host was cultured in 10 ml of LB/Amp broth and plasmid purification using the Qiagen Miniprep Kit according to the manufacturer's recommended protocol was performed. The eluted recombinant plasmid DNA was quantified using the nanodrop spectrophotometry and verified by sequencing at Eurofins MWG Operon, Ebersberg, Germany.

3.3.6 Transformation into expression host

The sequence-verified pET32a(+)-hBD9 plasmid construct was transformed into the BL21(DE3) pLysS *E. coli* expression host by using the heat shock chemical transformation based on the protocol described in the previous chapter (2.3.13, page 94).

3.3.7 Induction of expression host

The overnight starter culture of the expression host was diluted into fresh LB/Amp to produce OD_{600} of approximately 0.01. This fresh culture was further grown for another 3 hours to OD_{600} of approximately 0.5 before

induction using 0.5 mM IPTG at induction temperature of 24 ^{o}C for 4 hours in an orbital incubator shaking at 200 rpm.

3.4 Results

3.4.1 Gene verification

The gene verification by sequencing using the T7 promoter primer was performed and results obtained from the Eurofins MWG Operon, Ebersberg, Germany were as the following:

Sequence confirmation for the native gene recombinant DNA:

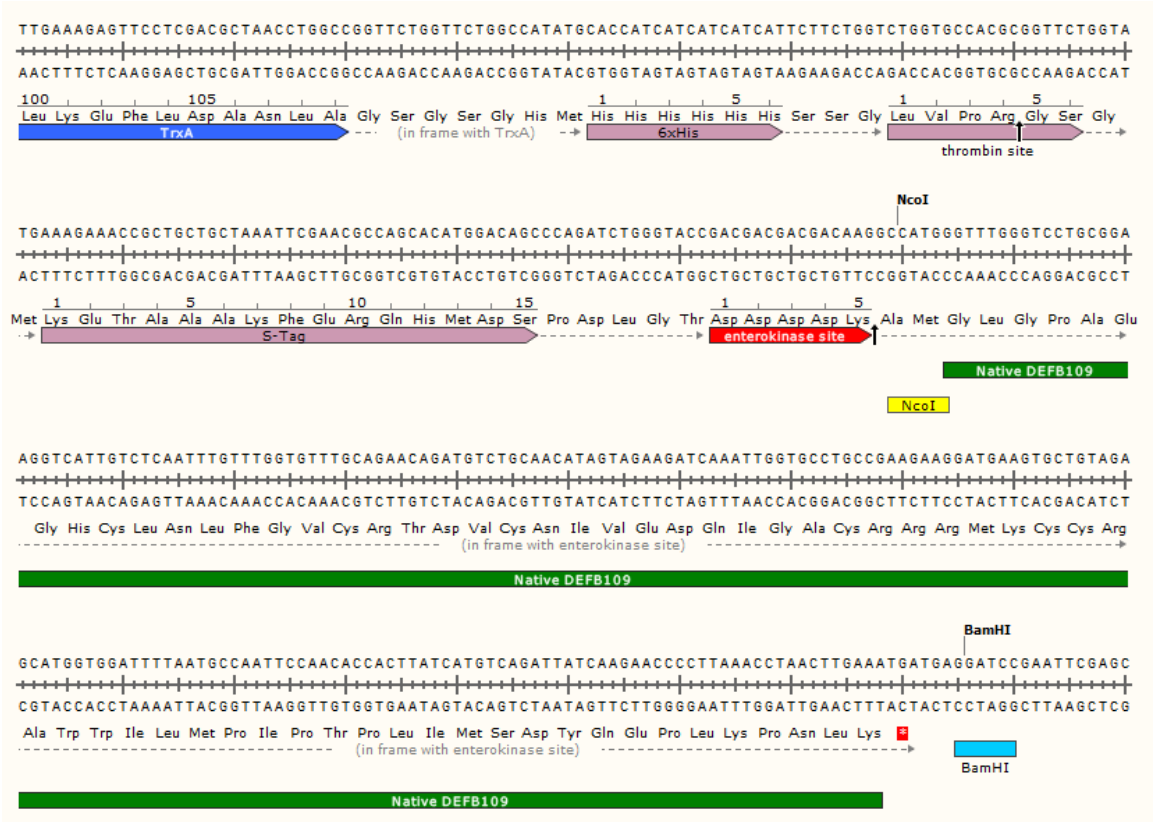

Figure 3.4.1 Sequence of the purified recombinant plasmid DNA showing the Trx fusion partner, N-terminal HisTag, rEK recognition site, *Nco*I restriction site, in-frame native *DEFB109* gene, double stop codon and *Bam*HI restriction site.

Sequence confirmation for the optimised gene recombinant DNA:

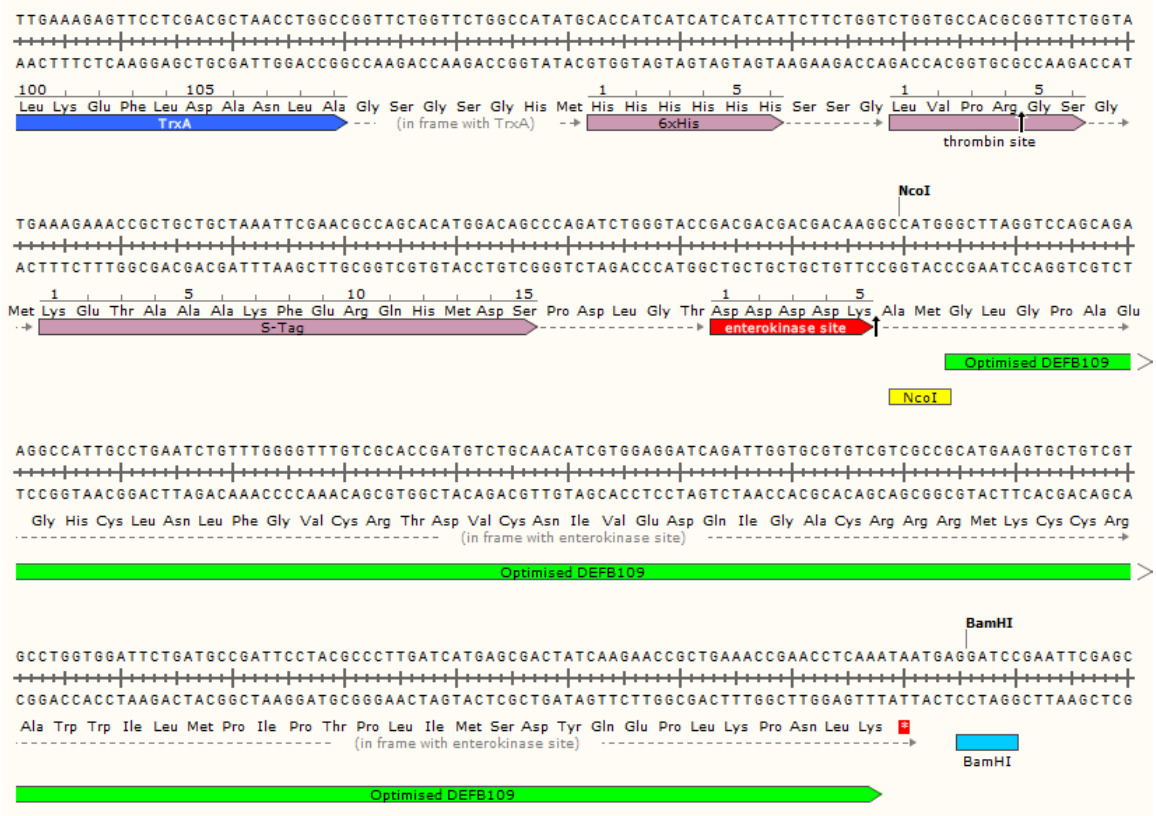

Figure 3.4.2 Sequence of the purified recombinant plasmid DNA showing the Trx fusion partner, N-terminal HisTag, rEK recognition site, *Nco*I restriction site, in-frame optimised *DEFB109* gene, double stop codon and *Bam*HI restriction site.

It was found from the above gene sequences (Figure 3.4.1 and Figure 3.4.2) that both the native and the optimised *DEFB109* genes were accurately ligated into the pET32a(+) plasmid DNA in in-frame fashion. The recombinant plasmid contained the start codon following the ribosomal binding site, Trx tag, N-terminal HisTag, rEK cleavage site, *Nco*I and *Bam*HI restriction sites and the double stop codon to ensure efficient truncation of the translated recombinant protein, located after the *DEFB109* gene. When aligned, the native and the optimised gene are identical at 75% of the nucleotide residues (Figure 3.4.3). This this was due to the changes from

rare codon to preferred codon to overcome the issue of codon bias in the *E. coli* host and allow a higher amount of protein to be expressed [240].

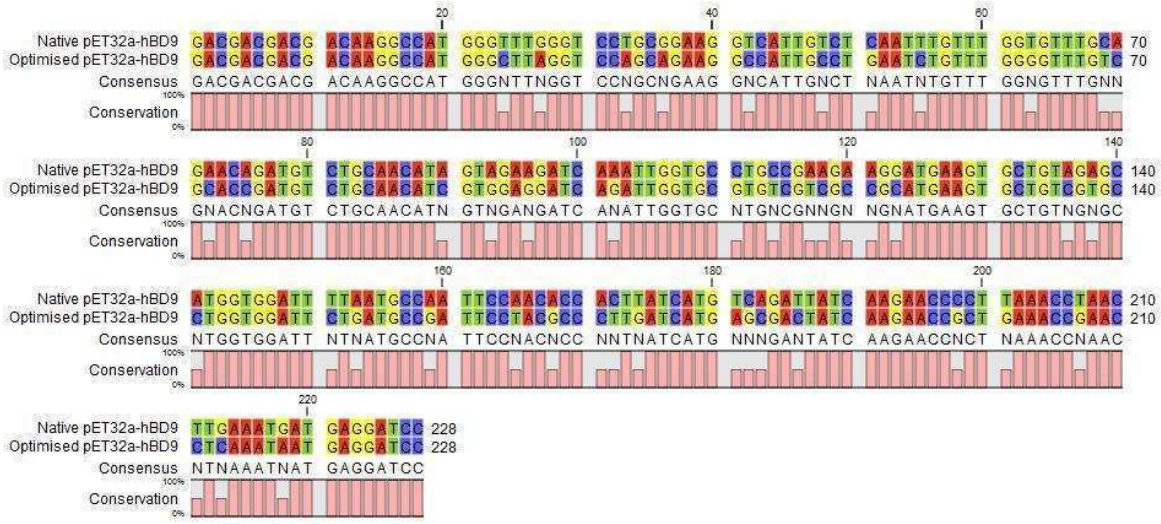

Figure 3.4.3 Photograph of sequence alignment showing the difference between the native and optimised *DEFB109* recombinant plasmid DNA.

3.4.2 Transformation into cloning host

The ligation reaction was mixed with 50 µl competent NovaBlue *E. coli* cells and mixed gently by pipetting. The cells were kept on the ice for 5 minutes before being heat shocked at 42 ^{o}C for 45 seconds in the water bath. They were later transferred back into ice for another 2 minutes. 200 µl of warm SOC media were added and the cells were incubated in the shaker incubator at 37 ^{o}C 200 rpm for an hour. The revived cells were inoculated onto the LB/Amp culture plates and incubated overnight at 37 ^{o}C.

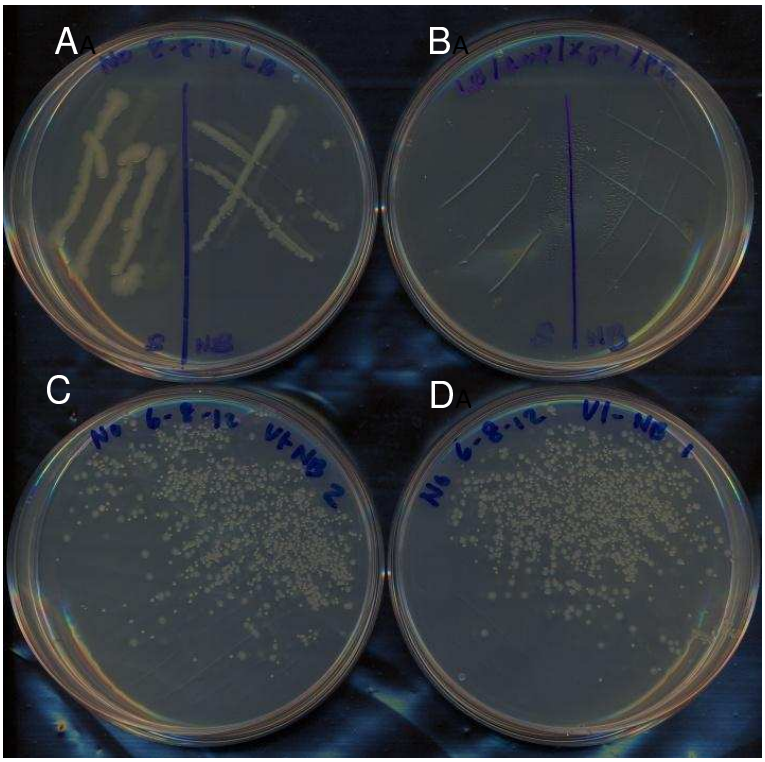

Figure 3.4.4 Photograph of the LB/Amp culture plates showing numerous colonies grown for the transformed Novablue cells (C, D). The culture of BL21(DE3)pLysS and Novablue on LB agar and LB/Amp/Xgal was also prepared as positive (A) and negative (B) culture controls.

3.4.3 Transformation into various expression hosts

Following the successful cloning of the recombinant plasmid DNA into cloning host, purification was performed and gene verification was performed via gene sequencing (Eurofins MWG Operon, Ebersberg, Germany). The purified plasmid DNA was then transformed into several expression hosts.

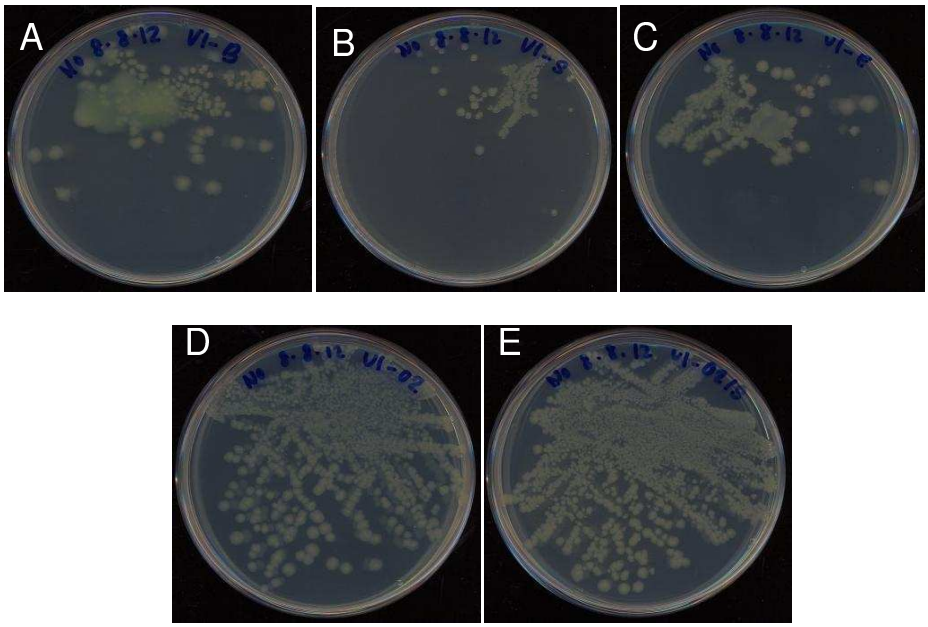

Figure 3.4.5 The culture of optimised *DEFB109* plasmid construct into the BL21-A1 (A), BL21(DE3)pLysS (B), BL21(DE3)pLysE (C), Origami2 (D) and Origami2pLysS (E) *E. coli* strains

3.4.4 Induction of the optimised *DEFB109*

The transformed BL21-A1 was induced with 1.0 mM IPTG at 24 ^{o}C for 6 hours. This was followed by fractionation, SDS-PAGE and western blotting.

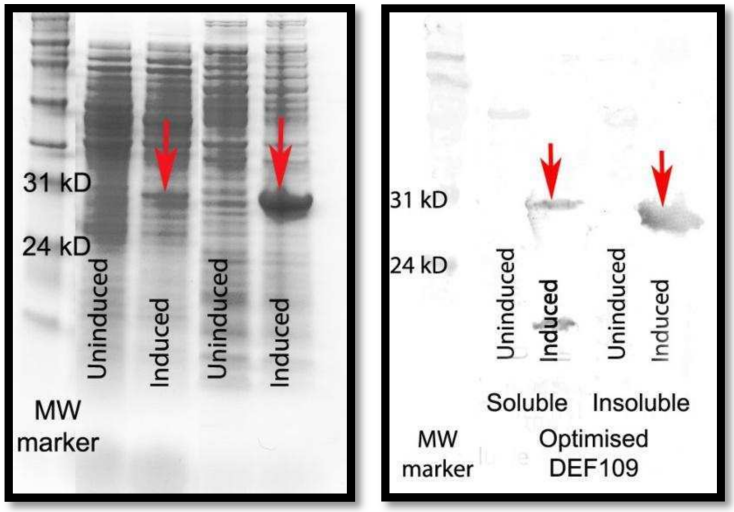

Figure 3.4.6 Photographs of the SDS-PAGE (left) and Western Blot (WB, right) of the hBD9 fusion protein in BL21-A1 *E. coli* expression host showing bands representing the soluble and insoluble fractions.

3.4.5 Expression of optimised *DEFB109* in various hosts

The expression hosts, namely the BL21(DE3)pLysS and the pLysE, transformed with optimised *DEFB109*, were induced with 1.0 mM IPTG at 24 ^{o}C for 6 hours, and the soluble and insoluble fractions were run in SDS-PAGE and WB. The results of the electrophoresis were as follows:

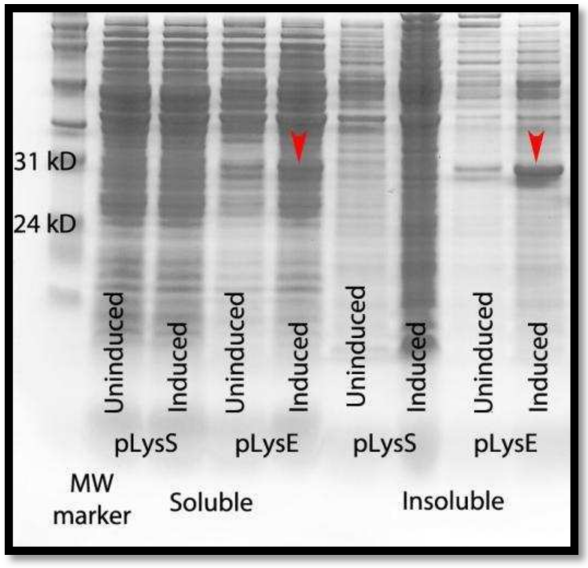

Figure 3.4.7 Photographs of the SDS-PAGE of fusion protein from BL21(DE3)pLysS and pLysE fractions. The bands were seen in the soluble and insoluble pLysE but not successfully shown in pLysS host. Although the samples loaded were normalised for volume, there seems to be overloading of the samples in all lanes.

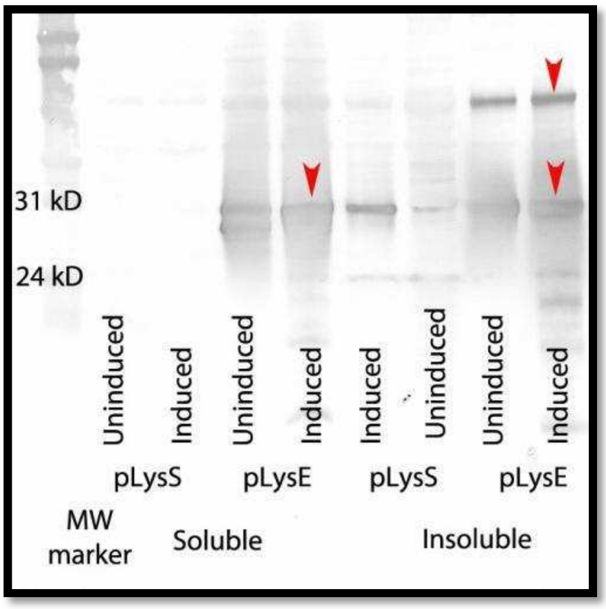

Figure 3.4.8 WB showing the bands (lower arrows) representing hBD9 fusion protein in BL21(DE3)pLysS and pLysE hosts. Oligomeric bands (top arrow) were also detected in the insoluble pLysE sample.

From the SDS-PAGE (Figure 3.4.7), bands corresponding to the hBD9 fusion protein were detected in the insoluble fraction from pLysS and in the soluble and insoluble fractions from the pLysE strain. In addition to this, the western blot showed corresponding bands representing the hBD9 in the soluble pLysS fraction and both the soluble and insoluble pLysE fractions (Figure 3.4.8). In the insoluble pLysE samples, in addition to the monomeric fusion protein, there were also oligomeric forms detected.

3.4.6 Comparative expression of native and optimised genes

The expressions of the fusion protein from the native and optimised genes were performed at two different induction temperatures.

3.4.6.1 Induction at 24 ^{o}C

BL21(DE3)pLysS harbouring the native and the optimised *DEFB109* genes were induced with 0.5 mM IPTG in an incubator shaking at 200 rpm for several incubation periods. SDS-PAGE was run and the gel was analysed for the hBD9 fusion protein (Figure 3.4.9).

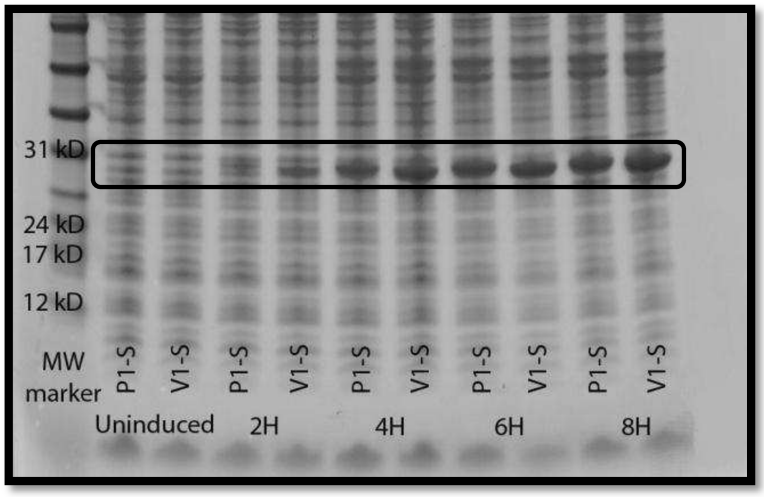

Figure 3.4.9 Photograph of the SDS-PAGE gel showing the soluble hBD9 fusion protein band from the induced soluble BL21(DE3)pLysS *E. coli* harbouring the native and optimised gene at different time points. MW, molecular weight; P1-S, native gene in pLysS E *coli*, V1-S, optimised gene in pLysS *E. coli*.

For both the native and optimised genes, the relative expression of fusion protein increased with increasing incubation time. The expression from the optimised gene is marginally higher than from the native gene. The ratio between the optimised and the native hBD9 fusion protein expression was 1.097 ± 0.056 (mean ± standard deviation), across all incubation time points (Table 3.4.1). The optimised gene did not show an advantage over the native gene in terms of the expression of soluble fusion protein induced with 0.5 mM IPTG at 24 ^{o}C across all induction durations.

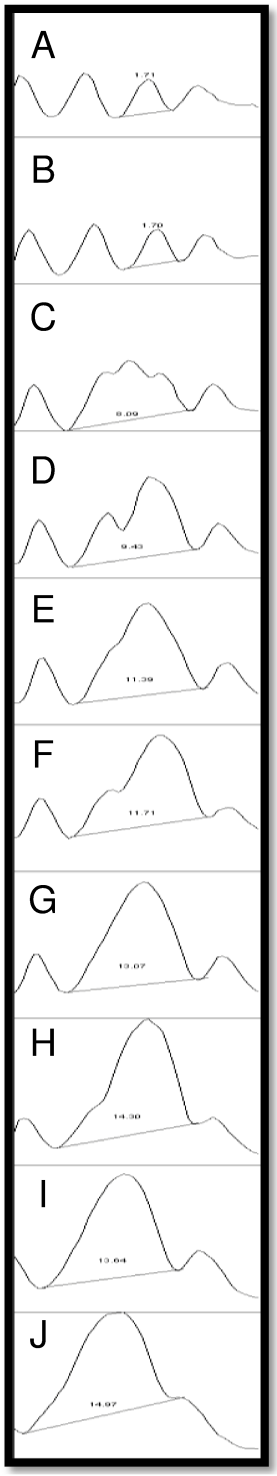

Figure 3.4.10 Image J plots of the hBD9 fusion protein bands in the SDS-PAGE in Figure 3.4.9. Native gene uninduced (A), 2 hour (C), 4 hour (E), 6 hour (G), 8 hour (I); optimised gene uninduced (B), 2 hour (D), 4 hour (F), 6 hour (H), 8 hour (J).

Table 3.4.1 Table summarising the hBD9 fusion protein expression relative to the uninduced sample in native and optimised genes, and the optimised to native expression ratio for various time points.

Incubation time	Relative band intensity		Optimised:native
	Native	Optimised	
Uninduced	1	1	1
2 hour	4.74	5.53	1.17
4 hour	6.68	6.87	1.03
6 hour	7.67	8.39	1.09
8 hour	7.99	8.78	1.10

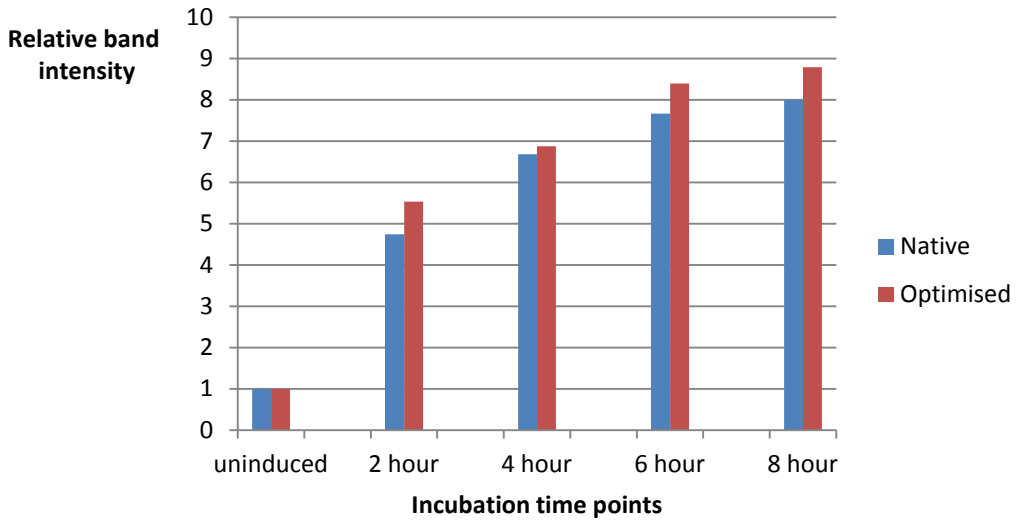

Figure 3.4.11 Bar graph showing the hBD9 fusion protein expression relative to the uninduced samples in the native and optimised genes.

3.4.6.2 Induction at 20 °C

The *E. coli* hosts harbouring the native or the optimised gene were induced with 0.5 mM IPTG with for 4 hours with shaking at 200 rpm. The soluble and insoluble fractions were then subjected to SDS-PAGE and western blotting. The gel and membrane were scanned and shown in Figure 3.4.12 (soluble fraction) and Figure 3.4.13 (insoluble fraction). In the soluble

fraction, there was a slight increase of fusion protein in the optimised gene compared to unoptimised gene in pLysS strain. Optimised pLysE strain did not show an obvious increase in soluble fusion protein compared to native pLysE, nor did the BL21-A1 strain.

In the insoluble fraction, optimised BL21-A1 and pLysS showed higher production of fusion protein compared to the native gene. There was no band seen in the pLysE lanes.

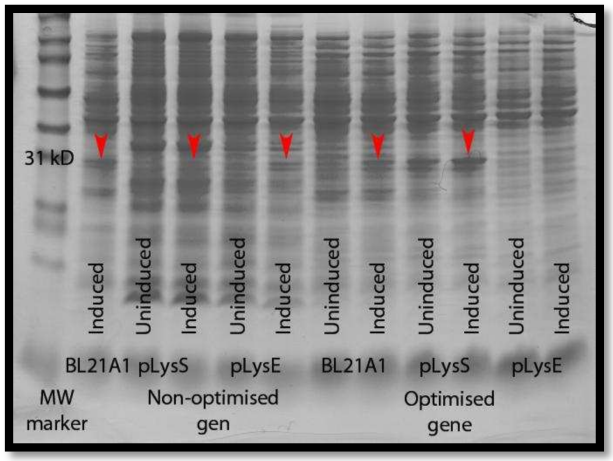

Figure 3.4.12 Photograph of SDS-PAGE showing soluble hBD9 fusion protein band (arrow head) in native and optimised DEFB109 gene in various expression hosts.

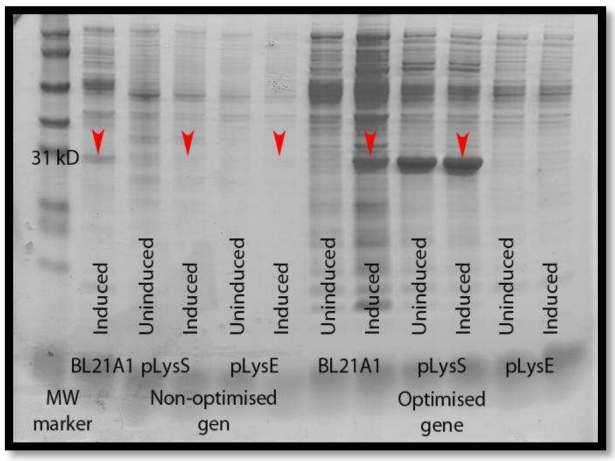

Figure 3.4.13 Photograph of SDS-PAGE showing insoluble hBD9 fusion protein band (arrow head) in native and optimised DEFB109 gene in various expression hosts.

From the western blot analysis, the insoluble fraction exceeded the amount of soluble fraction in all expression host strains. In the soluble fraction (Figure 3.4.14), in agreement with the SDS-PAGE, the optimised pLysS has visibly higher fusion protein compared to the native strain. Optimised pLysS also showed higher amount of oligomeric bands. Optimised gene in BL21-A1 did not show a distinct advantage over the native gene.

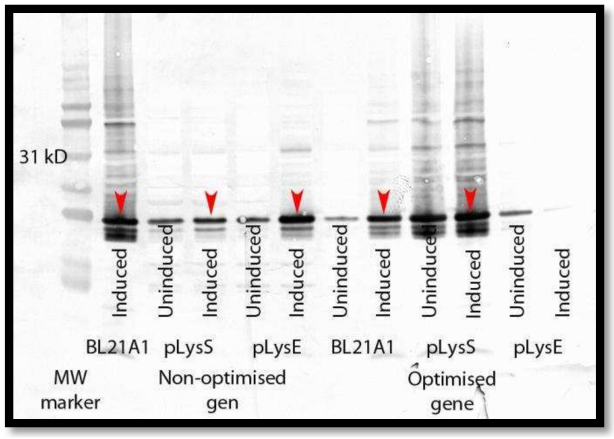

Figure 3.4.14 Photograph of WB membrane showing soluble hBD9 fusion protein band (arrow head) from native and optimised *DEFB109* genes in various expression hosts.

For the insoluble fraction, western blot analysis (Figure 3.4.15) showed that the optimised genes in both the BL21-A1 and pLysS had higher fusion protein band intensity compared to the native gene strains. There seemed to be unexpected finding for induction in pLysE optimised gene (soluble and insoluble), probably due to mislabelling (induced and uninduced) of samples.

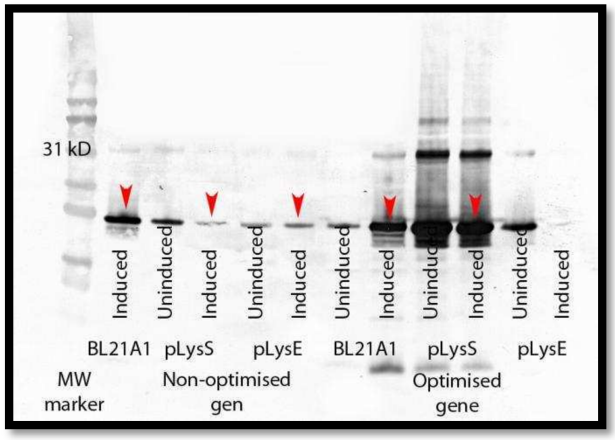

Figure 3.4.15 Photograph of WB showing insoluble hBD9 fusion protein band (arrow head) from native and optimised DEFB109 genes in various expression hosts.

3.5 Discussion

Different organisms may have preference towards certain set of codons for the amino acids. In line with this, they also have abundant tRNAs for preferred codons. This rule also applied to *E. coli* which is the most frequently used expression system for the overexpression of heterologous protein [241]. This was largely attributable to its well-known gene characteristics as well as easy, rapid and economically efficient growth of this organism. However, due to the said bias towards its own set of preferred codons, high throughput expression of the heterologous protein in *E. coli* could be jeopardised [235]. Therefore, a clear strategy for overexpressing non-native or heterologous protein in such *E. coli* is needed which includes optimisation of the native gene codons.

In this chapter, it was shown that the native and optimised *DEFB109* gene was successfully ligated into the linearised pET32a(+) as shown in the gene sequencing data. The recombinant DNA constructs were successfully transformed into the NovaBlue (Novagen, Merck Millipore, Watford, UK) cloning host. The sequencing test for the gene also showed that it was in-frame with the start codon (ATG) of the *Nco*I recognition site. Translation of these DNA constructs would have produced the desired native and optimised Trx-hBD9 fusion proteins.

Studies have reported that an optimised gene has resulted in better expression of β-defensin fusion protein in the *E. coli* [242-244]. It was the objective of this study to reproduce this claim. At induction conditions set for 0.5 mM IPTG concentration, at 20 ^{o}C for 4 hours in a shaker set at 200 rpm, the BL21(DE3)pLysS expressed higher proportions of soluble fusion protein

compared to pLysE and Origami 2. Not only did the protein form aggregates, expression in pLysE and Origami 2 produced significant amounts of oligomeric fusion protein. As such, the pLysS *E. coli* was chosen as the expression host for subsequent expression experiments.

When comparing the expression in the native gene to that of the optimised gene, with the given induction conditions, there was only slight increment in the amount fusion protein expressed. This was in contrast to the finding reported by Peng *et al* who did a study on the optimised gene expression for hBD2 in BL21(DE3) *E. coli*. They noted that the optimised recombinant hBD2 fusion protein was more than 50% of total protein expressed and increased by 9-fold compared to the native gene [244]. Huang *et al* expressed the pET32a-*DEFB103* optimised gene in *E. coli* using 0.5 mM IPTG. They reported fusion protein production of 0.99 g/L and 96% purity. The soluble target protein was 45% of total soluble protein [245].

Whether this seemingly non-advantageous optimised gene finding rests on the optimisation itself or on the host is an interesting question. To resolve this, it is thought that we can optimise the gene for a different hosts such as other bacteria, yeast, filamentous fungi or prokaryotic algae [246], and look at the expression in that host. Should the expression remain similar to the native gene, the likelihood is that the gene and/or expressed protein are fastidious, beyond the issue of codon bias of the expression host.

Findings reported by Rosano *et al* are also relevant. They used the method of preferred codon tRNA co-expression in recombinant production of several plant proteins in *E. coli* host. When the preferred tRNA involved more

than 5 % of the amino acids, the solubility was adversely affected and so was the growth rate of the expression host [235].

Chapter 4

hBD9 expression

CHAPTER 4: hBD9 expression

4.1 Introduction

Apart from the modification of the human gene into the *E. coli* preferred codon synonymous protein, there were several other expression factors that require optimisation. The factors can affect the amount expressed and the solubility of the protein. The total amount of the expressed protein is important but a higher proportion of soluble protein is most important. Solubility is important as the protein in the aggregate or insoluble inclusion body form does not demonstrate the physiological property.

The solubility of a protein overexpressed in *E. coli* depends on several factors which include the sequence dependent and sequence independent factors. Thermostability increases solubility while *in vivo* half-life inversely affects the solubility. The amino acid (Asn, Thr, Tyr) composition and tripeptide frequency of the protein were also found to influence solubility. These factors were shown to be correlated to the propensity of a protein to be soluble when overexpressed in *E. coli* [247].

The expression of heterologous protein in *E. coli* is not without challenge. Depending on the type of the desired protein, it has always been the aim to produce correctly folded soluble protein in adequate amount for downstream characterisation experiments. This chapter describes the optimisation of the expression in terms of the expression hosts, IPTG concentration, induction duration and induction temperature. This exercise will lead to the determination of improved parameters for the expression of the hBD9 pro-peptide.

4.1.1 Expression host *E. coli*

A few organisms are capable of becoming expression hosts in heterologous recombinant protein expression. This includes *E. coli*, yeast and mammalian cells. The mammalian cells may contain oncogenic or viral DNA. BL21(DE3) *E. coli* strain is probably the commonest expression host utilised in the recombinant peptide expression. Apart from being easily and rapidly growing, it is also economical and robust.

The considerations in choosing the most appropriate *E. coli* include the toxicity of the target protein, membrane protease gene mutation, thioredoxin reductase mutation and induction regulation.

BL21-A1 *E. coli* have the T7 promoter incorporated into the Ara-B gene. This results in tighter control of the plasmid gene and prevents leakage/background expression of the protein before the start of induction. In the production of a toxic peptide, this will allow the host cells to grow adequately to a certain number before being induced and start the production of the peptide itself.

The pLysE plasmid expresses the T7 lysozyme at higher levels than the pLysS plasmid, conferring a greater level of control over the T7 polymerase. This is usually only required when the recombinant protein to be expressed may be toxic to the host. The pLysE plasmid also renders the cell resistant to chloramphenicol (CmR) and contains the p15A origin. The p15A origin allows pLysE to be compatible with plasmids containing the ColE1 or pMB1 origin.

4.1.2 Expression host selection

E. coli was chosen as the expression host because of the ease and rapid growth, cheap and non-fastidious media it grows in and because of its well-understood genetics. Nevertheless, they have several disadvantages which include protein misfolding and non-sense mutation. Within the K12 *E. coli* family, there are various strains produced. Each of them has the purpose of improving expression of different types of recombinant protein. As such, complete understanding and careful selection of expression host strains would be necessary in order to obtain the best possible expression of recombinant hBD9 protein.

4.1.2.1 BL21-A1

The BL21-A1 (Invitrogen, Paisley, UK) *Escherichia coli* strain offers the tightest regulation of expression for production of toxic proteins using the T7 promoter. This strain was constructed by inserting a chromosomal copy of the T7 RNA polymerase gene (*T7 RNAP*) under the control of the arabinose-inducible *araBAD* (arabinose) operon [248]. The *pBAD* promoter for *araBAD* operon tightly regulates expression of the T7 RNAP, and hence expression of the peptide of interest in T7-mediated plasmid systems. In the presence of arabinose, transcription from P_{BAD} promoter is turned on while in the absence of arabinose, the transcription is almost negligible. The basal expression can be further reduced by addition of glucose which reduces the cAMP thus preventing the expression of the *pBAD* promoter. Upon induction, the *pBAD* promoter exhibits strong expression of the RNA polymerase. The resultant RNA polymerase will in turn activate the plasmid DNA T7 promoter resulting

in high-level protein production. In addition, expression levels can be adjusted, or reduced, to improve protein folding and solubility [249].

4.1.2.2 BL21(DE3) pLysS

BL21(DE3) strains are the most widely used hosts for protein expression from pET recombinant plasmid DNA. They have the advantages of being deficient in both *lon* and *OmpT* genes encoding for membrane proteases. This allows the recombinant protein to be expressed without the risk of proteolytic action from the host defence mechanism.

DE3 indicates that the host is a lysogen of λDE3, and therefore carries a chromosomal copy of the T7 RNA polymerase gene under the control of the lacUV5 promoter. Such strains are suitable for production of protein from target genes cloned in pET vectors, by induction with IPTG.

pLysS strains express T7 lysozyme, which further suppresses basal expression of T7 RNA polymerase prior to induction, thus controlling the pET recombinants plasmid gene encoding the target proteins that may affect host growth and viability. However, the disadvantage of this tight control is the overall reduction in the total recombinant protein expression.

4.1.2.3 BL21(DE3) pLysE

BL21(DE3)pLysE *E. coli* are used with T7 promoter-based expression vectors. Like BL21(DE3) pLysS *E. coli*, BL21(DE3) pLysE carry the λDE3 lysogene and contain pLysE plasmid, which constitutively expresses T7 lysozyme. The pLysE plasmid in BL21(DE3) pLysE expresses higher levels of T7 lysozyme than in BL21(DE3) pLysS. This would result in more

suppression effect on the basal production of the target protein which is necessary when the recombinant protein to be expressed is toxic.

4.1.2.4 Origami 2 (DE3)

Origami 2 host strains are E *coli* K-12 families that have mutations in both the thioredoxin reductase (trxB) and glutathione reductase (gor) genes, which significantly enhance disulfide bond formation in the E. *coli* cytoplasm. The Origami 2 strains are kanamycin sensitive; like the original Origami strains, the *gor* mutation is still selected for by tetracycline. In order to reduce the possibility of inter-molecular disulfide bond formation, strains containing mutations in *trxB* and *gor* are recommended merely for the production of proteins that require disulfide bond formation for accurate folding. DE3 indicates that the host carries a chromosomal copy of the T7 RNA polymerase gene under control of the lacUV5 promoter. As such, it is suitable for use for target genes cloned in pET vectors by induction with IPTG.

4.1.3 Recombinant plasmid DNA

Plasmid DNA is a small circular, double stranded DNA molecule different from the cell's chromosomal DNA which naturally exists in bacterial cells. Plasmid serves as a vehicle to introduce foreign DNA into bacteria. The replication of the plasmid DNA is independent of the host chromosome. Therefore when the cells replicate, the daughter cells will also contain the plasmids. Choosing a correct type of the plasmid vector is crucial. This depends on the strategy employed in the overexpression of the target protein. The main components of the vector would be an antibiotic resistance

gene, solubility enhancer partner, affinity tag, protease recognition and restriction digestion sites.

The plasmid copy number variability is also influential in the overexpression of the target protein. A high copy number plasmid should not be used in cases where expressed protein is toxic or has a higher propensity for inclusion body if high amount of protein is produced. In these cases, low copy number plasmid is preferred to allow high amount of soluble protein to be expressed [241]. Low copy number plasmids included pWSK29, pWSK30, pWSK129 and pWSK130 carry the replicon called pSC101 and produce approximately six to eight plasmid copies per cell [250]. Various plasmid vectors had been researched in the past for the production of various defensins. Such plasmid carriers include pQE-30, pET32a, pBV220, pET28a and pGEX-4T-2 and pMAL-p2 [236].

4.1.3.1 Fusion partner

Commonly used fusion partners with particular purpose of increasing recombinant protein expression include maltose binding protein (MBP), thioredoxin (Trx) and N-utilising A (NusA). MBP is a 40 kD peptide to assist in the expression and purification of recombinant protein in the *E. coli*. It can also increase the heterologous proteins solubility and allow detection by immunoassay methods. The expressed fusion protein can be purified using the one-step chromatography with immobilised amylase and eluted by 10 mM maltose. It is also tolerant to high pH (7 - 8.5) and salt content too but not to denaturing agents.

Trx tag is mainly indicated for the prevention of inclusion body and therefore increasing the solubility of the fusion protein. However, the cellular

cytoplasmic environment is not conducive the expression of heterologous proteins with disulphide bonds such as β-defensins. By having Trx tag in the fusion partner, the intracytoplasmic expression will be enhanced and the solubility of the fusion partner can be increased [251].

NusA may act as solubility enhancer and is particularly used for protein known or likely to form inclusion bodies. The disadvantage of these tags is that they could not be used as affinity tag. Therefore, affinity tags such as HisTag are necessary and can be included as a polylinker peptide in the fusion protein [252].

4.1.3.2 Antibiotic resistance

By having a gene for antibiotic resistance, the plasmid confers a system whereby a transformed colony can be selected. Only the colony of bacteria containing the plasmid with resistance will grow in the media with the antibiotic. The commonly used antibiotic selection systems included ampicillin, kanamycin and tetracycline.

4.1.3.3 Affinity tag

The commonly used affinity tags include the HisTag which has a small (six residues) cluster of histidine residues and manipulates the immobilised metal in the affinity chromatography for purification. HisTag will bind to metal ion ligands such as Ni^{2+}, Co^{2+}, Cu^{2+} or Zn^{2+}, which are immobilised by chelators such as NTA. Elution is by using pH alteration of the buffer or by introducing free imidazole. However, high concentration of imidazole in the buffer is associated with certain disadvantages including incompatibility with NMR and crystallisation studies and protein aggregation [252].

4.1.3.4 Proteolysis recognition site

The fusion partner of various types needs to be separated from the target protein. This can be achieved by having a specific cleavage site in the vector, and manipulated during the cloning of the gene. The cleavage site will be used by certain proteases to split the fusion protein from the target protein. Some of the commonly used proteases, their recognition sequence and cleavage points are listed in Table 4.1.1.

Table 4.1.1 A list of commonly used proteases and their recognition sites and the points of cleavage (indicated by /). X can be any amino acid.

Proteases	Recognition site
Enterokinase	X-Asp-Asp-Asp-Asp-Lys/Not Pro-X
Factor Xa	X-Leu-Glu(or Asp)-Gly-Arg/X
HREVC proteases	X-Leu-Glu-Val-Leu-Phe-Gln/Gly-Pro-X
TEV	X-Glu-Asn-Leu-Tyr-Phe-Gln/Gly-X
Thrombin	X-P4-P3-Pro-Arg or Lys/P1-P2-X

4.1.4 IPTG concentration

Isopropyl thio-galactoside (IPTG) is a galactose analogue which has the capability to activate the lysogene in the *E. coli* chromosome to produce T7 RNA polymerase enzyme. IPTG will bind to the T7 promoter and initiate the transcription of the gene for T7 RNA polymerase enzyme (T7 RNAP). T7 RNA polymerase enzyme will then transcribe from the T7 promoter in the recombinant plasmid DNA and thus expression of the heterologous protein in the expression host *E. coli*.

It is generally believed to be best to induce the cells slowly to allow time for the correct folding of the recombinant protein and increase solubility.

IPTG concentrations in the range of 0.5 mM to 1.0 mM were usually applied [236, 253].

4.1.5 Induction temperature

It is well known that temperature affects recombinant protein expression and the solubility of the protein expressed. The expression host grows faster at 37 ^{o}C but this can be too fast for the correct protein folding and the expression of recombinant protein may be affected by formation of aggregated inclusion bodies. The previously reported successful induction temperature ranges from 20 ^{o}C to 34 ^{o}C.

Xu *et al* used various cultivation temperatures and found cultivation temperature of 34 ^{o}C was the best for expression of hBD4. This temperature resulted in a higher concentration of fusion protein as well as higher percentage of soluble fusion protein [253]. Cultivation temperature of 37 ^{o}C was associated with the least fusion protein concentration and percentage of soluble protein [253]. Meanwhile, Xu *et al* found that 28 ^{o}C was the best temperature for optimised hBD2 production in MBL medium [253].

4.1.6 Induction duration

The expression hosts grow in an exponential fashion. At the beginning of the induction, the growth is usually at the mid logarithmic phase with OD_{600} of approximately 0.5. From this point, the host will grow rapidly to reach the exponential plateau stage of the growth. This could take several hours. It is therefore not necessary to prolong an induction longer than the time to reach the plateau as it will not increase the amount of the protein dramatically. It will also encourage the protein to form the oligomers.

Peng *et al* incubated their expression host for eight hours at 28 ^{o}C [236]. They achieved productivity of up to 1.3 g of soluble Trx-hBD2 fusion protein for every litre of induced culture, and at the end of the process gained overall recovery of 29.2% of the recombinant protein.

4.2 Objectives

a. To determine the expression host for best expression of soluble fusion protein.
b. To determine the IPTG concentration for the best expression of soluble fusion protein.
c. To determine the induction temperature for the best expression of soluble fusion protein.
d. To determine the induction duration for best expression of soluble fusion protein.

4.3 Methods

4.3.1 Preparing the culture

A single colony of transformed *E. coli* expression host was picked and cultured into 5 mls of Luria Bertani (LB) culture medium mixed with ampicillin at a final concentration of 50 µg/ml. The culture medium was incubated in the shaker incubator at 37 ^{o}C with shaking at 230 rpm overnight. On the following morning, the overnight culture was subcultured into fresh LB medium with 50 µg/ml ampicillin, at 1% (v/v) and allowed to grow further to achieve mid log phase of growth with OD_{600} of 0.5, which usually takes approximately between two to three hours. 10 ml of the starter culture is then transferred to

the polyethylene tube for induction and uninduced control. The polyethylene tubes were weighed for purpose of determining wet weight of the cell pellet. Apart from not having IPTG added to it, the control samples were treated similarly to the induced samples.

4.3.2 Induction

The induction was started with introduction of IPTG of appropriate concentration into the tubes containing the *E. coli* expression host harbouring the recombinant plasmid DNA. The cells were incubated at different incubation settings to investigate the effect of various factors. The cultures were shaken at 230 rpm in the shaker incubator (New Brunswick, Fisher Scientific, Loughborough, UK).

4.3.3 Harvesting the induced *E. coli*

At the end of the induction, the cells were harvested by centrifuging them at 6000 X g for 10 minutes at 4^{o}C. Once completed, the supernatant was carefully decanted. The pellet was resuspended and washed with phosphate buffered saline (PBS) before being centrifuged again. The pelleted cells were weighed to obtain the wet weight of the cell. These data were then recorded.

4.3.4 Lysis of the cells

The cells were lysed using BugBuster (Novagen, Merck Millipore, Watford, UK) at 5 ml/gram wet weight. The suspension was incubated on a roller at room temperature for 20 minutes with intermittent vortexing. Total protein was sampled and stored at -20 ^{o}C before the suspension was

centrifuged at 6,000 x g with temperature of 4 ^{o}C for 20 minutes to separate the soluble from the insoluble protein. After centrifugation, the supernatant containing the soluble fusion protein was carefully decanted into a cleaned tube, labelled accordingly and stored until needed. The pellet was weighed to represent the insoluble protein mass.

4.3.5 Fractionation

The cell lysate was fractionated into soluble and insoluble fractions by centrifugation at 6,000 x g for 20 minutes at 4 ^{o}C (Hettich, Newport Pagnell, UK). Before centrifugation, 20 µl of the lysate was set aside for SDS-PAGE, representing the total protein.

4.3.6 SDS-PAGE

Before loading, the samples were normalised based on the calculated amount of total protein with buffer to obtain approximately equal concentration so that the same loading volume can be used for all samples. The samples were then mixed with gel loading buffer and heated at 95 ^{o}C for 5 minutes. 5 µl of mixture was loaded in each well of the 1 mm thick 10% NuPAGE BisTris precast gel (Thermo Scientific, Loughborough, UK) before the electrophoresis was run at 45 mV for 40 minutes in MES SDS running buffer (50 mM MES, 50 mM Tris base, 1% SDS, 1 mM EDTA, pH7.3).

4.3.7 Gel staining

The protein bands separated in the gel were fixed by heating the gel for 1 minute in the microwave oven, alternating with washing for 1 minute using the double-distilled water. This cycle was repeated for 3 times before the

water was replaced with Coomasie blue SafeStain® dye (Sigma Aldrich, Gillingham, UK). The gel was left on the rocker (Stuart, Stone, UK) for three hours. The gel was then washed with double-distilled water for another three hours on the same rocker before being scanned for record keeping.

4.3.8 Quantifying the protein band in the gel

The softcopy images of the gel were directly analysed using the Image J software for quantification of the band intensity [236]. The colour images were first converted into 8-bit black and white before the lanes were defined and the graphs corresponding to the bands were plotted. The graphs were converted into closed peaks and the areas representing the band intensities were generated by the software. Comparison of the areas was then performed and analysis was carried out.

4.4 Results

4.4.1 hBD9 fusion protein solubility in BL21-A1

In this experiment, the expression of hBD9 protein from optimised recombinant plasmid DNA pET32a(+)-*DEFB109* in BL21-A1 was examined. The cells were grown to OD_{600} 0.5 before induction with 0.5 mM IPTG and 20% (w/v) arabinose A at 24 ^{o}C for 4 hours. The cells were harvested, lysed and fractionated before the proteins were separated using SDS PAGE. The induction reaction worked well as shown by the prominent bands (20.4 kD) of induction control J (Novagen, Merck Millipore, Watford, UK), which was the empty pET32a(+) in the BL21(DE3) *E. coli* expression host, in the soluble induced lanes. There were faint bands corresponding to the fusion protein. There seemed to be no difference in the induced and uninduced samples. The soluble fraction showed even fainter bands compared to the total and the insoluble fractions (Figure 4.4.1).

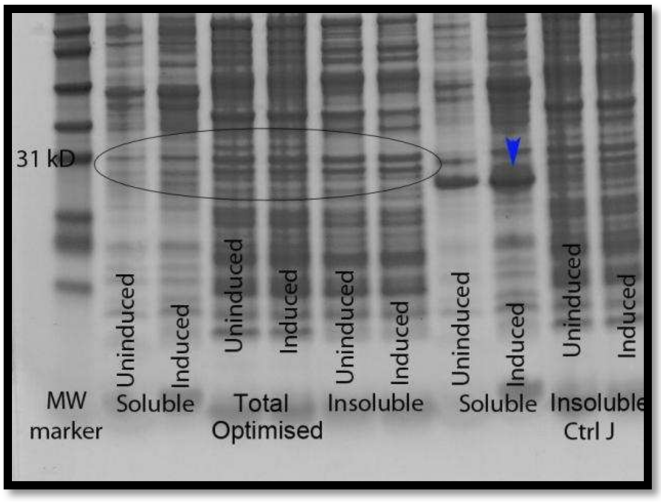

Figure 4.4.1 Photograph of the SDS-PAGE gel showing the Trx-hBD9 fusion protein induction in BL21-A1 *E. coli*. There were more prominent bands in induced lanes of the soluble fraction compared to the uninduced lane. The control protein J was expressed more in the induced lane (arrow head) than in the uninduced soluble lanes.

4.4.2 hBD9 fusion protein solubility in Origami 2

In this experiment, the expression of Trx-hBD9 fusion protein from optimised recombinant plasmid DNA pET32a(+)-*DEFB109* in Origami 2 was examined. The cells were grown to an OD_{600} of 0.5 before induction with 0.5 mM IPTG. Induction was carried out at 24 ^{o}C for 4 hours. The cells were harvested, lysed and fractionated before the proteins were separated using SDS-PAGE. The induction worked well as shown by the prominent bands (20.4 kD) of induction control J in the soluble induced lanes. There were marked bands seen for the total and insoluble fraction, more so in the induced lanes (Figure 4.4.2). For the soluble fraction, a slight increase in band intensity representing the induced samples was seen.

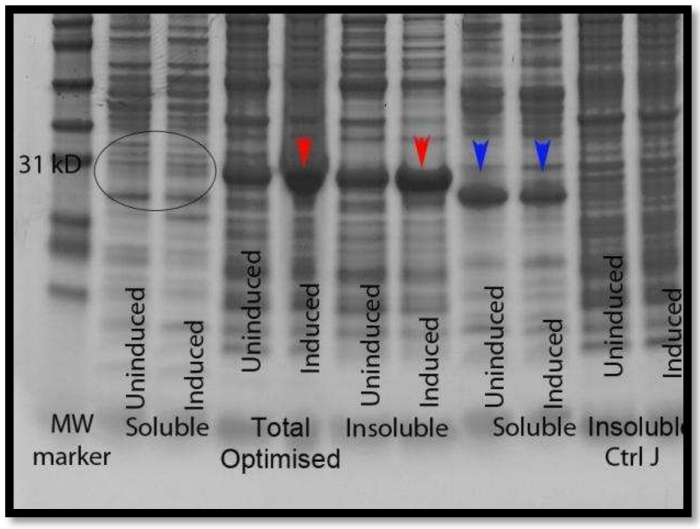

Figure 4.4.2 Photograph of the SDS-PAGE gel showing marked band corresponding to the hBD9 fusion protein in the total and insoluble fractions (red arrow heads) of the Origami 2 host. However, there were only faint bands in the soluble component detected (circle). The induction control J (blue arrow heads) was also expressed in this experiment.

4.4.3 hBD9 fusion protein expression in various hosts

Various hosts which included BL21(DE3)pLysS and pLysE, and Origami 2 *Escherichia coli* were investigated for the expression of the soluble and insoluble fractions. Induction was performed using IPTG 0.5 mM for 4 hours at 24 ^{o}C. The pLysS protein was entirely solubilised, leaving no insoluble fraction at all. The pLysE and Origami 2 *E. coli* lysates were fractionated into soluble and insoluble protein before being subjected to SDS-PAGE (Figure 4.4.3).

The induced *E. coli* strains produced higher amounts of the fusion protein compared to the uninduced strains. In the pLysE and Origami2 strains, the insoluble hBD9 fusion protein was higher compared to the soluble protein. Although the loaded induced soluble samples were not optimal, there were hardly any traces of a band corresponding to the fusion protein detected in the induced soluble samples of these strains.

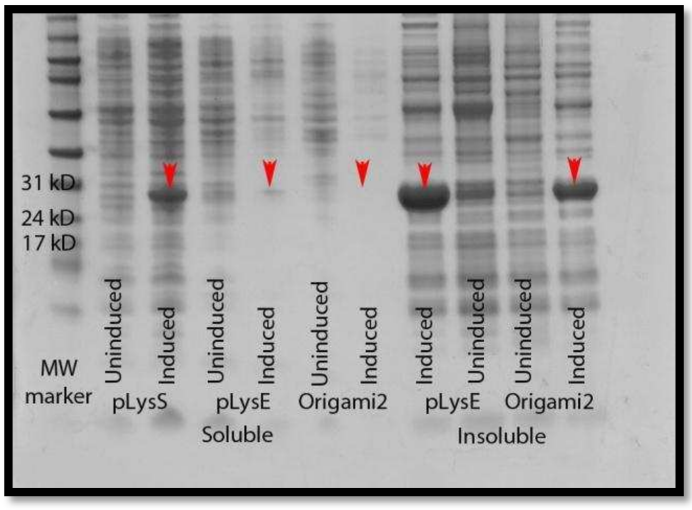

Figure 4.4.3 Photograph of the SDS-PAGE gel showing hBD9 fusion protein expression in various expression hosts. Induction was using 0.5 mM IPTG at 24 ^{o}C for 4 hours. The samples were normalised for volume used.

Image J was used to compare the bands' intensity in the gel (Figure 4.4.4). The BL21(DE3)pLysS soluble fusion protein increased by 19-fold in the induced compared to the non-induced soluble samples. The soluble samples of the pLysE and Origami 2 were not analysable by image J. In the insoluble fractions, the band intensities in the induced pLysE and the Origami 2 were 7.5 and 7.8 folds more than the uninduced samples, respectively.

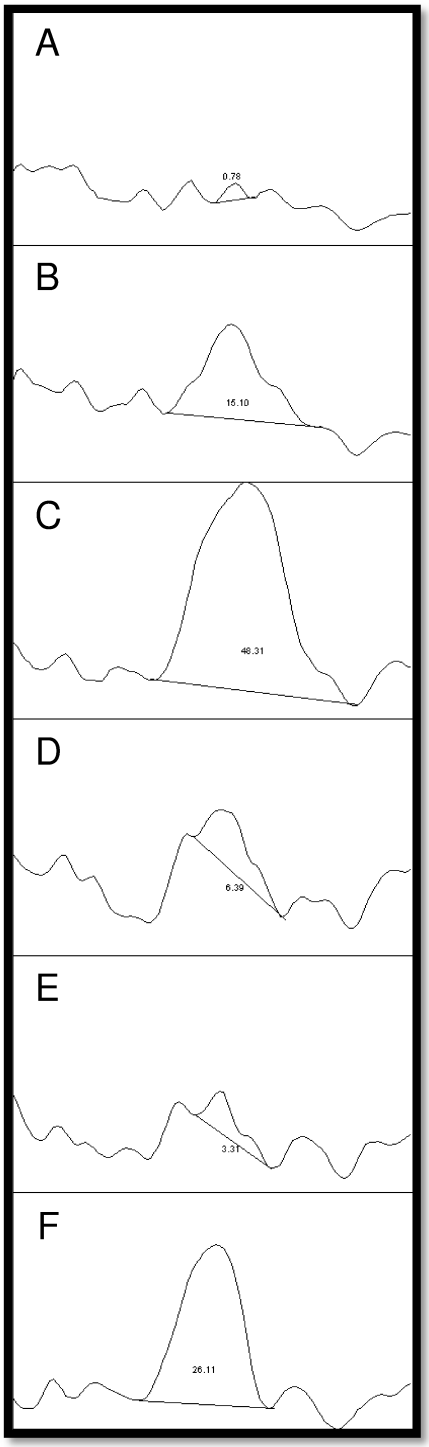

Figure 4.4.4 Image J plot showing the areas corresponding to the bands for uninduced (A) and induced (B) BL21(DE3)pLysS, insoluble induced (C) and uninduced (D) pLysE, insoluble uninduced (E) and induced (F) Origami 2 expression hosts.

4.4.4 Optimisation of the IPTG concentration

4.4.4.1 Influence of IPTG concentration at a given condition

Induction was carried out in Origami 2 *E. coli* expression host for 3 hours duration at 24 ^{o}C and 200 rpm shaking, using IPTG concentrations from 0.3 mM to 1.2 mM. SDS-PAGE was performed and the gel was stained for analysis (Figure 4.4.5). There seemed to be no marked changes in the band intensities from the photograph. Image J was used to plot graphs (Figure 4.4.6) for objective comparison of the band intensities. Analysis showed an initial downward trend of band intensities from 0.3 mM to 0.7 mM IPTG concentration before increasing to a peak at 1.0 mM IPTG concentration (Figure 4.4.7).

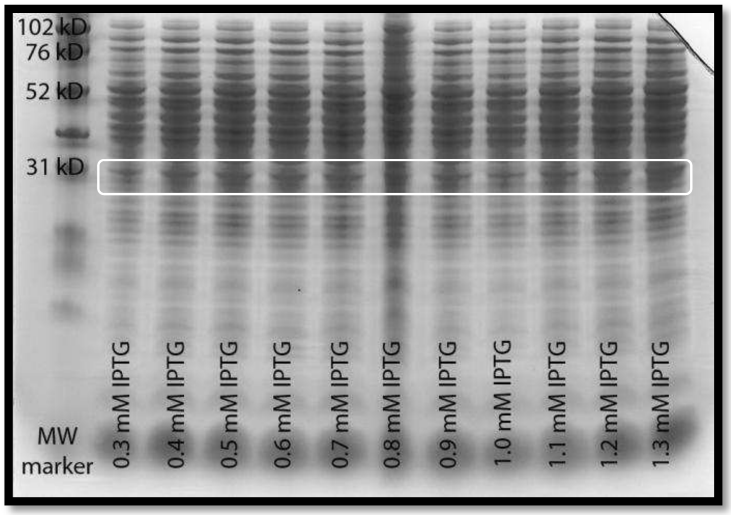

Figure 4.4.5 Photograph of the SDS-PAGE for soluble hBD9 fusion protein in Origami 2 induced at 28 °C for 3 hours across different IPTG concentrations. It seemed that that there were no glaring changes in the band intensity across all IPTG concentrations tested.

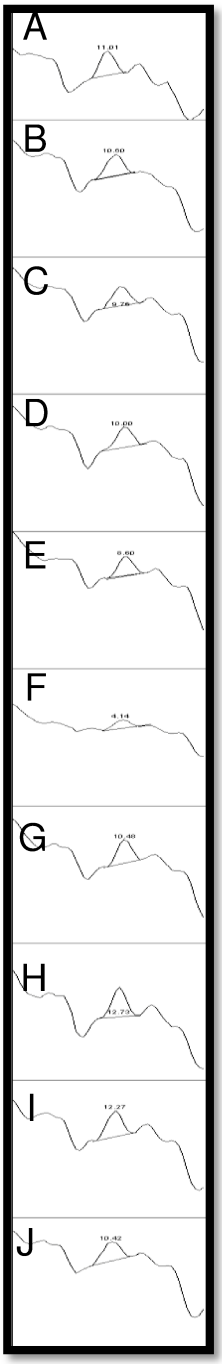

Figure 4.4.6 Image J plots showing the band intensity for the lanes in SDS-PAGE in Figure 4.4.5.

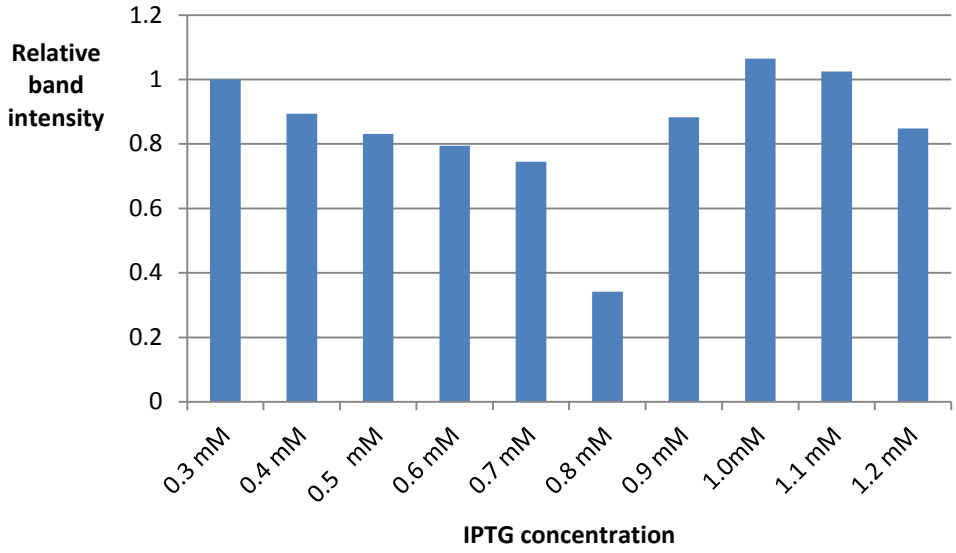

Figure 4.4.7 Bar graph showing the relative intensity of the hBD9 fusion protein bands from Figure 4.4.6.

4.4.4.2 Influence of IPTG concentration at different durations

The influence of different IPTG concentrations on the expression of Trx-hBD9 fusion protein expression was examined. In the induction of BL21-A1 *E. coli* at 24 ^{o}C and 200 rpm shaking, there seemed to be an increment in the band intensity as the concentration was increased from 0.5 mM to 0.75 mM and 1.0 mM (

Figure 4.4.8). For 3 hours incubation, 0.75 mM IPTG gave the highest band intensity while for 6 hour incubation the 1.0 mM gave the highest band intensity (Figure 4.4.9 and Figure 4.4.10).

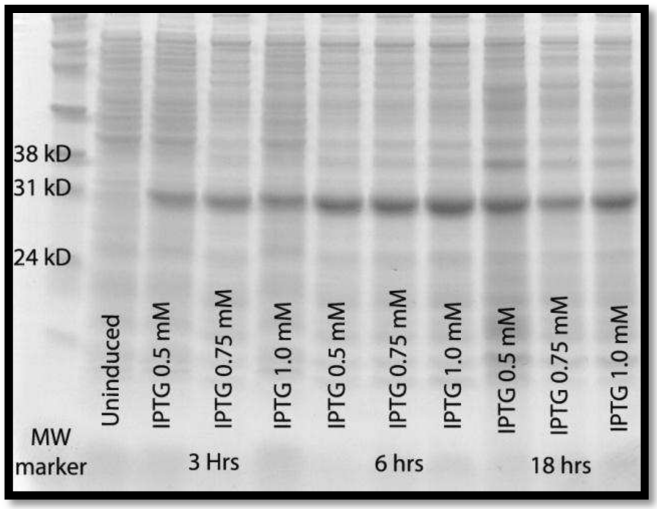

Figure 4.4.8 Photograph for SDS-PAGE showing the insoluble fusion protein expression in the BL21-A1 *E. coli* following induction with various IPTG concentrations for different durations.

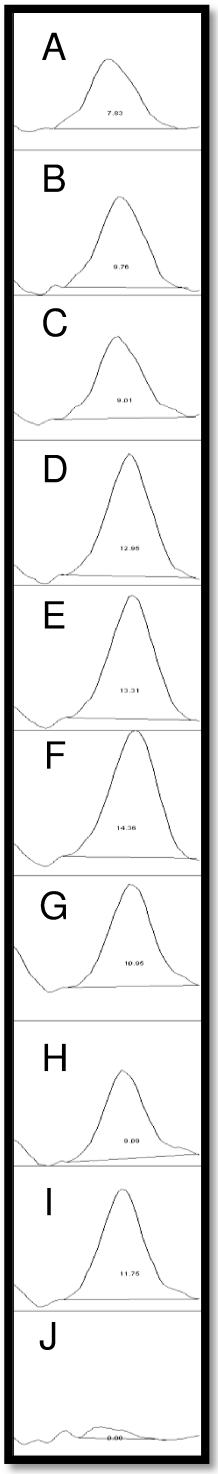

Figure 4.4.9 Image J plot of the band intensitiy from the SDS-PAGE in showing the difference for the 3 hour, 6 hour and 18 hour incubations in BL21(DE3)pLysS *E. coli* at different IPTG concentrations.

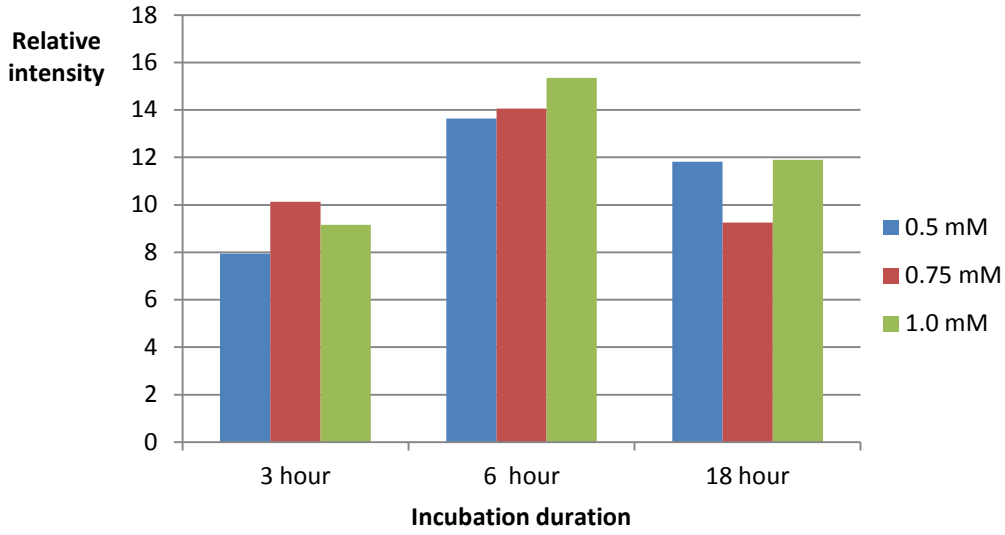

Figure 4.4.10 Bar graph showing the relative band intensity for the fusion induced with 0.5 mM, 0.75 mM and 1.0 mM IPTG for 3, 6 and 18 hour incubations.

4.4.5 Optimisation of the induction duration

To determine the best induction duration, induction was carried out in BL21(DE3)pLysS expression host using 0.5 mM IPTG at 24 ^{0}C for 2 to 8 hours. The uninduced samples were also set at the same conditions. The proteins were fractionated and the soluble fractions were subjected to SDS-PAGE. There was hardly any background expression noted in the uninduced samples probably attributable to the tight control by lysozyme in the pLysS strains. In contrast, the induced samples showed bands representing the hBD9 fusion protein (Figure 4.4.11).

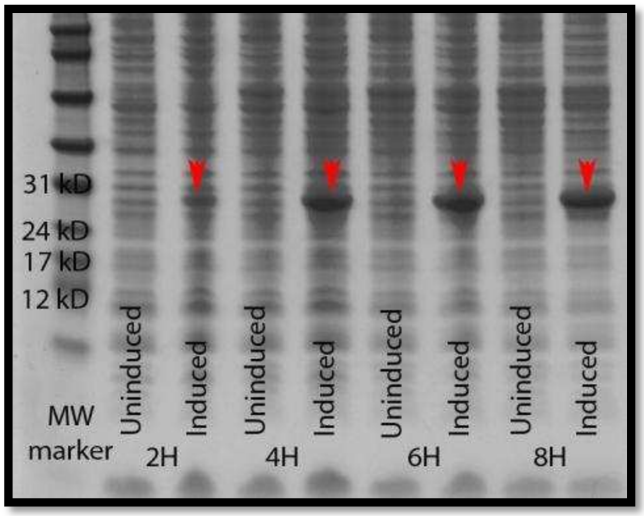

Figure 4.4.11 Photograph of SDS-PAGE showing enhanced hBD9 soluble fusion protein bands at different induction durations, in induced compared to uninduced samples of various incubation durations.

By using the Image J software, band intensity analysis showed that the expression levels were 1.67, 9.79, 12.25 and 16.38 fold higher than the control in the 2, 4, 6 and 8 hour incubations, respectively (Figure 4.4.11).

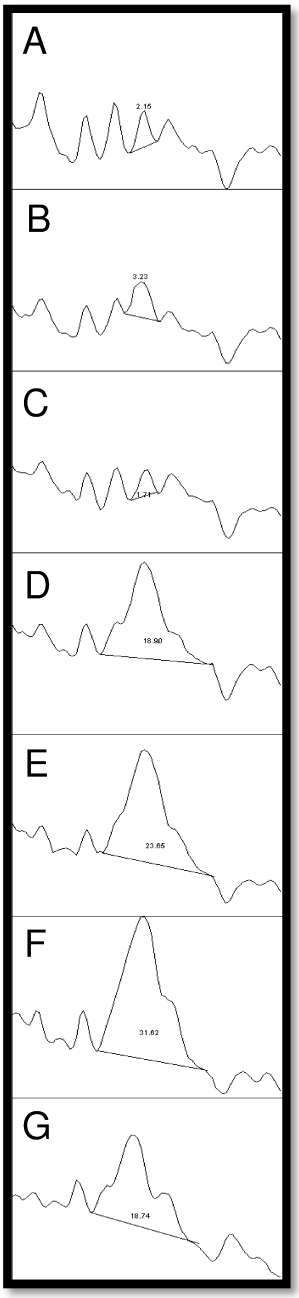

Figure 4.4.12 Image J plot for SDS-PAGE showing the peaks representing the band intensity with the increment in the duration of induction. Uninduced, 2 hour (A); induced, 2 hour (B); uninduced, 4 hour (C); induced 4 hour (D); uninduced 6 hour (E), induced 6 hour (F); uninduced, 8 hour (G) and induce, 8 hour (H).

4.4.6 Optimisation of incubation duration using western blot

In the incubation duration optimisation, further analysis was carried out to compare the hBD9 expression in BL21(DE3)pLysS strain using 0.5 mM at 24 ^{o}C after 2 hour and 4 hour incubations. Although the SDS-PAGE showed

a very similar pattern, the western blot analysis showed an observable difference in the expressions of the induced and uninduced 2 hour and 4 hours samples (Figure 4.4.13).

When analysed by using Image J software, there was no difference found in the fusion protein band intensity between the induced and uninduced control either at 2 hour or 4 hour incubations from the SDS-PAGE image (Figure 4.4.14). When similar analysis was performed on the western blot image, there were marked band intensity differences between the induced and uninduced samples both for 2 and 4 hour incubations. The 4 hour incubation sample showed higher band intensity compared to 2 hour sample. The ratios between induced and uninduced samples at 2 and 4 hours were 2.71 and 3.68, respectively. The ratio of band intensity in the induced 4 hour sample to that of the induced 2 hour sample was 1.35 (Figure 4.4.15).

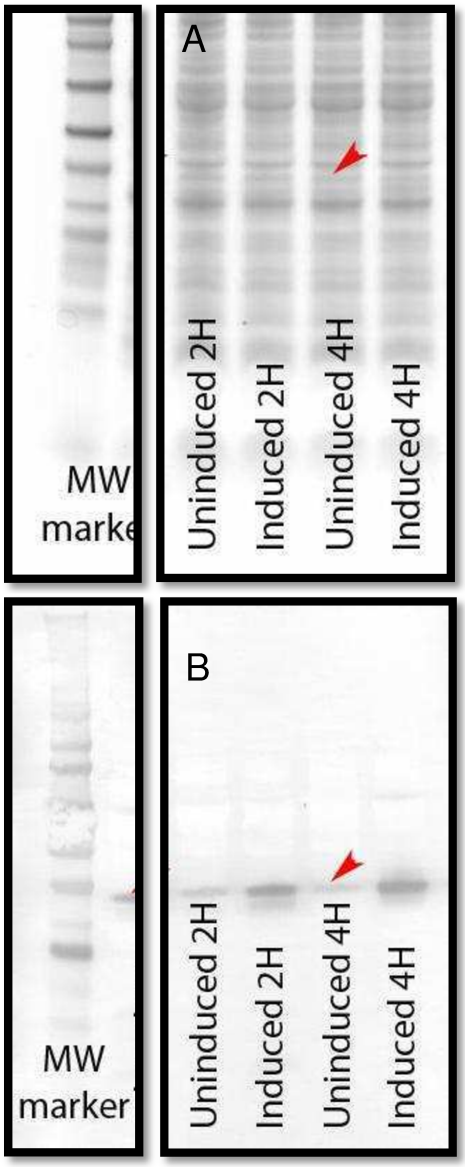

Figure 4.4.13 SDS-PAGE (A) and western blot, WB (B) of the induction at 2 and 4 hours incubation 24 ^{o}C, showing increased expression of the fusion protein.

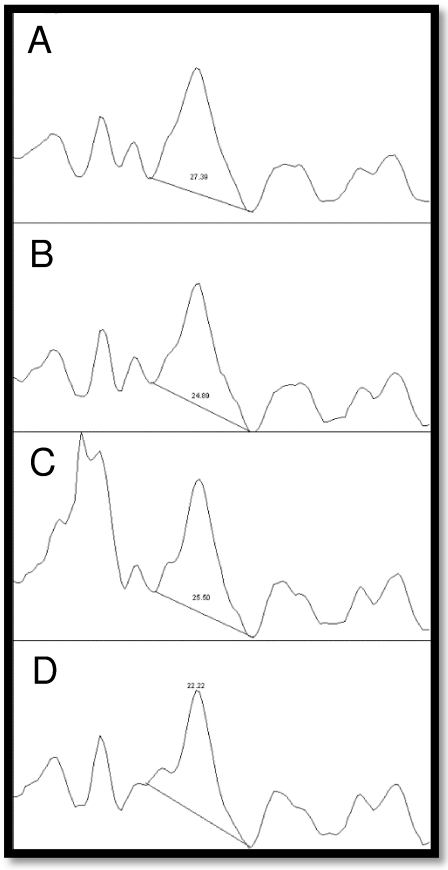

Figure 4.4.14 Image J plot for SDS-PAGE showing the fusion protein band intensities for the induced and uninduced controls at 2 and 4 hours incubation in Figure 4.4.13(A).

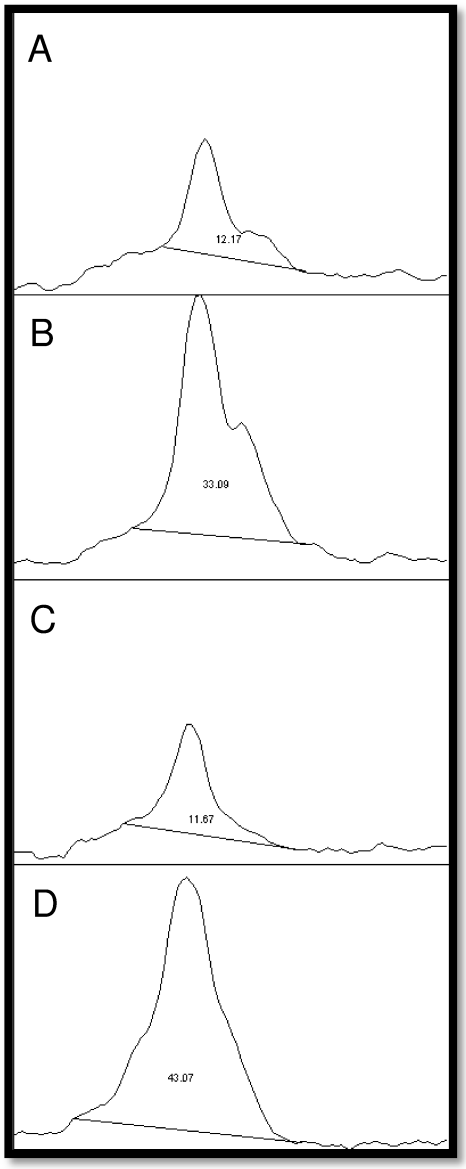

Figure 4.4.15 Image J plot showing the band intensity for the fusion protein following the WB in Figure 4.4.13 (B). Uninduced 2 hour incubation (A), induced 2 hour incubation (B), uninduced 4 hour incubation (C), induced 4 hour incubation (D).

4.4.7 Optimisation of the induction temperature

The experiment was carried out at different times as there were no two incubators with temperature control available to be used simultaneously. Inductions were carried out at 28 ^{o}C and 37 ^{o}C and the soluble fractions were subjected to SDS-PAGE. The bands representing the fusion protein were more prominent in the 28 ^{o}C induction compared to the 37 ^{o}C induction.

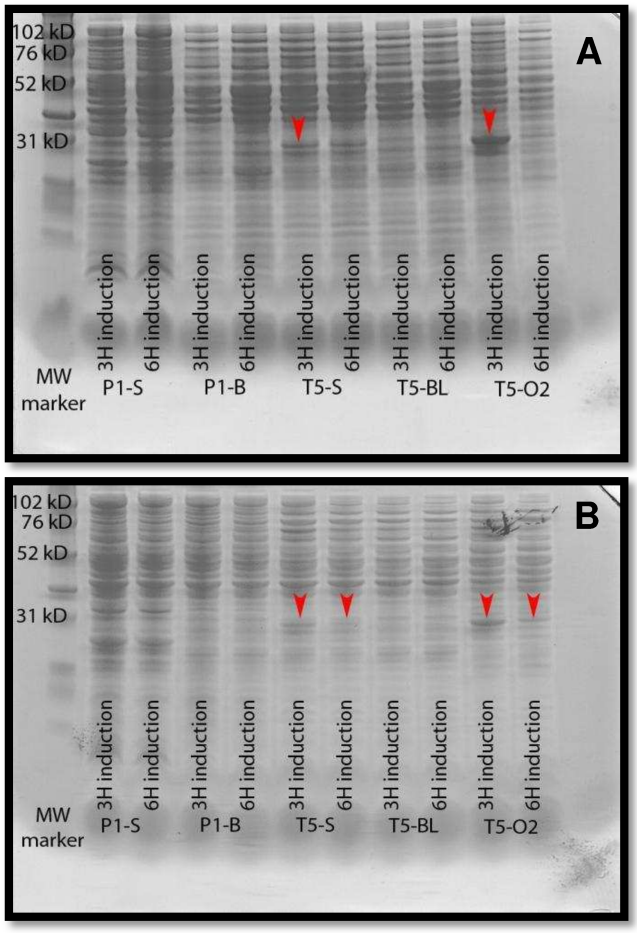

Figure 4.4.16 Photograph of the SDS-PAGE for induction at 28 °C (A) and 37 °C (B) showing the fusion protein (red arrow head). P1, native gene; T5, optimised gene; S, BL21(DE3)pLysS; B, BL21-A1; BL, BL21(DE3); O2, Origami 2 *E. coli* expression hosts.

4.5 Discussion

Expression in the BL21(DE3)pLysS resulted in a completely soluble fraction following lysis using the BugBuster (Merck Millipore, Watford, UK), protein extraction reagent, leaving no pellet of insoluble protein. This is in contrast to pLysE and Origami 2 strains which had both the soluble and insoluble fractions. In term of amount, the pLysS and Origami 2 strains produced higher amount of fusion protein. As such, BL21(DE3)pLysS was chosen as the expression host strain in the purification step. *E. coli* strains

co-expressing the lysozyme such as the BL21(DE3)pLysS and -pLysE, have the advantage in preventing basal expression of the recombinant plasmid as the co-expressed lysozyme binds to the T7 RNAP from unintended leaky expression of the bacterial genome. This is especially important for over-expression of potentially toxic peptide such as hBD9. However, it may also affect the overall target protein production [254].

Precise folding and prevention of aggregation are important in order to yield functional protein. This could be achieved by slow expression and several factors were demonstrated to be important. This includes reducing the IPTG concentration, reducing the induction temperature, reducing the shaking rate and shortening the induction duration.

Concerning the IPTG concentration, the fusion protein expression decreased from IPTG concentration of 0.3 mM to 0.7 mM before increasing again with peak band intensity at IPTG concentration of 1.0 mM. It was also found that for incubation at 24 ^{0}C for between 3 to 6 hours IPTG concentration between 0.75 to 1.0 mM was associated with highest fusion protein expression. With longer incubation, a slightly higher IPTG is required probably to accordingly maintain the activation of the lysogen to produce the T7 RNAP. Hence, induction with final IPTG concentration of 1.0 mM is recommended.

The induction time was shown to affect the amount of soluble fusion protein expressed and the formation of oligomeric hBD9. There was an obvious increment in band intensity as the induction time increased from 2 to 4, 6 and 8 hours. The biggest increment between two successive durations was recorded between 2 and 4 hours inductions with 5.8 fold. It was noted

from this study that longer induction increased the oligomerisation of fusion protein which could be due to the formation of intermolecular bonds. As such, induction is best carried out for 4 hours.

Lowering the rate of fusion protein production allows the protein time to fold properly and avoid aggregation into inclusion bodies [255]. The commonly used method is by reducing the induction temperature. It was found in this study that the amount of soluble fusion protein increased at 28 ^{0}C compared to 37 ^{0}C induction temperature after 3 hours incubation in Origami 2 expression host. San-Miguel *et al* reported successful expression of active soluble protein after 72 hour induction at 4 ^{0}C but overall protein yield may be low due to slower bacterial growth rate and low protein synthesis rate [256]. Activity of molecular chaperone can be reduced too at extremely low temperature [257]. Cold-adapted chaperones Cpn60 and Cpn10 in ArticExpress (Stratagene, Agilent Technologies, London, UK) expression host were reported to show folding activity at temperatures between 4 and 12 ^{0}C [258].

Heterologous protein expression in the cytoplasmic compartment of *E. coli* is associated with high yield but is not conducive for the formation of disulphide bonds. This was due to the presence of thioredoxin and glutaredoxin, maintained in reduced formed by the thioredoxin reductase and glutathione reductase, respectively. As such, *E. coli* with mutation in the *trxB* and *gor* genes encoding thioredoxin reductase and glutathione reductase is more suitable for expression of heterologous protein with disulphide bonds such as hBD9. Disulphide bond formation and proper folding of the target protein can be further enhanced by fusion to thioredoxin fusion partner [259].

In conclusion, the expression of hBD9 from the optimised *DEFB109* to be carried out using pET32a(+) which has the Trx tag to promote disulphide bond formation in BL21(DE3)pLysS *E. coli* strain as it has tight control preventing basal expression of the potentially toxic protein. Induction should be carried out with 1.0 mM final IPTG concentration at low temperature such as 28 ^{o}C for 4 hours.

Chapter 5

hBD9 purification

CHAPTER 5: hBD9 purification

5.1 Introduction

Purification is an important step in the recovery of the free target peptide from the recombinant expression system. Effective purification will yield high amounts of the highly purified peptide. Several steps are usually involved before the final elution of the free target protein. However, in each step, there can be loss of some protein as the recovery may not always be 100%. The more steps are involved in the purification process, the more likely loss will occur. As such, a planned and optimised strategy to obtain high amounts of the purified protein is essential, which depends on the features of the fusion protein. The proteolysis system employed affects the amount of the free target protein as the mixture of the cleavage reaction will require separation. Only with sufficient amount of highly purified soluble protein can subsequent experiments to characterise the structure and functions of the target protein be carried out successfully.

5.1.1 The fusion protein

The fusion protein in this research consisted of the fusion partner and the target peptide hBD9 pro-peptide. In the fusion partner, there were a few motifs which included the thioredoxin, HisTag and enterokinase cleavage site. Located immediately after the enterokinase cleavage site was the in-frame hBD9 pro-peptide sequence. The presence of thioredoxin in the fusion partner was to promote disulphide bond formation leading to proper folding of the protein in the cell cytoplasmic compartment and thus increase the solubility of the fusion protein.

Upon translation of the plasmid recombinant gene, the expressed fusion protein will have a combined 222 amino acid residues with molecular weight of 24.403 kD and a theoretical isoelectric point (pI) of 5.9. The total number of negatively charged (Aspartate and Glutamate) residues was 30 and positively charged (Arginine and Lysine) residues was 24, giving a nett charge of negative 6. The estimated half life (the time taken for half of the amount of protein in a cell to disappear after its synthesis, and depends on the identity of its N-terminal residues) of the fusion protein was more than 10 hours in *E. coli*, in vivo. The fusion protein instability index was calculated at 31.58 which classified the protein as stable. Its aliphatic index was 83.11. The grand average of hydropathicity (GRAVY) was -0.274.

5.1.2 The fusion partner

Fusion partners or tags can enhance the expression of soluble fusion proteins. Commonly used fusion partners include thioredoxin (Trx), glutathione S-transferase (GST), maltose binding protein (MBP) and others. Not all fusion partners work positively in all recombinant target proteins [260]. For example, GST was shown to suppress instead of enhancing the production of IL-11 cytokine which was expressed readily on its own or enhanced by HAT (natural histidine affinity tag) [252].

The proteolytic enzyme chosen in this research was the recombinant enterokinase (rEK) enzyme which would cleave the fusion partner after the DDDDK recognition site. Following cleavage, the fusion partner has 157 amino acid residues with molecular weight of 17.048 kD and theoretical isoelectric point (pI) of 5.48. The negative (Asp and Glu) charge outnumbered the positive (Arg and Lys) charge by 24 to 16 causing a nett

charge of negative 8. The estimated half life of the fusion partner was more than 10 hours in *E. coli*, in vivo. The fusion partner instability index was calculated at 18.03 which classified the protein as stable. Its aliphatic index is 83.11. Grand average of hydropathicity (GRAVY) was -0.373.

5.1.3 The free hBD9 pro-peptide

The pro-peptide sequence was subjected to the parameter tool in ExPasy (http://web.expasy.org/protparam/). It contained 65 amino acids with total molecular weight of 7.372 kD and an isoelectric point (pI) of 8.33. The total number of negatively charged (Aspartate and Glu) residues was 6 and positively charged (Arginine and Lysine) residues was 8, giving a net charge of positive 2. The estimated half life of the free pro-peptide was more than 10 hours in *E. coli*, in vivo. The pro-peptide stability index was calculated at 65.46 which classified the protein as unstable. Its aliphatic index was 90.00. The grand average of hydropathicity (GRAVY) was -0.034.

The detailed information regarding the chemical and physical properties of the fusion protein and the free pro-peptide was important to plan a strategy for the purification of the free pro-peptide.

Table 5.1.1 Comparison of the characteristics of the fusion protein, fusion partner and the free pro-peptide.

	Fusion protein	Fusion partner	Free pro-peptide
Amino acid	222	157	65
Molecular weight, kD	24.403	17.048	7.372
Isoelectric point, pH	5.9	5.48	8.33
Negative charge	30	24	6
Positive charge	24	16	8
Nett charge	-6	-8	+2
Instability status	Stable	Stable	Unstable
Aliphatic index	83.11	80.25	90.00

5.1.4 HisTag immobilised metal affinity chromatography (IMAC)

The underlying principle behind the IMAC is the reversible interaction between the amino acid side chains of the target protein and the immobilised metal ions of the resin matrix [261]. Depending on the immobile metal ions, different amino acid side chains can be extracted in the process. Among all of those, histidine, cysteine and tryptophan have been implicated in the protein binding to the immobilised metal ions.

In the resin matrix, there is a metal chelating ligand which binds to the electropositive transition metal ions. The chelating ligand such as the iminodiacetic acid (IDA) [262], nitrilotriacetic acid (NTA) [263] or carboxymethyl aspartate-agarose (CMA) [264] binds strongly to, and thus immobilises, transition metal ions. These chelating ligands are coupled to solid support resins. These matrices possess four coordination sites through which the transition metal ions will bind, while leaving the other two coordination sites of the metal ions available for interaction with the amino

acid side chains of the protein. The robustness against a wide range of protein denaturants and detergents makes it versatile, while the stability of the metal ion immobilisation allows regeneration and recycling of the matrices [265].

The Ni^{2+}–NTA matrix has a binding capacity of 5–10 mg protein/ml of matrix resin and a high binding affinity ($K_d = 10^{-13}$ *M*) for the hexahistidine tag at pH 8.0 [266]. The Co^{2+}–CMA also has been reported to bind less nonspecific protein than the Ni^{2+}–NTA resin, resulting in higher eluted protein purity with binding capacity of approximately 5–10 mg of protein/ml of resin too.

The immobilised ions commonly used in IMAC include transition metal ions such as the cobalt (Co^{2+}), nickel (Ni^{2+}), zinc (Zn^{2+}) and copper (Cu^{2+}) with six coordination sites. Four coordinations will bind with the ligands leaving another two sites for binding with the amino acid side chains [267]. Zn^{2+} and Cu^{2+} have been frequently used for binding of untagged protein although both can also be used to bind HisTagged protein [268]. The cobalt-based resins bind to the histidine more specifically and as such have better purity compared to nickel-based resin. This gives rise to better purity at the expense of yield. Both the cobalt-based and nickel-based resins can be used in the gravity-flow columns, spin columns or high flow columns.

Polyhistidine would have higher affinity for nickel than isolated histidine. They would bind more strongly than would an antibody bind to an antigen, by sharing the electron of the nitrogen with the electron deficient orbitals of transition metals ions. As there were only two coordination sites on the metal ions available for covalent binding, only two histidines can bind

simultaneously to the metal ion. Other amino acids which could be used in IMAC were cysteine and tryptophan [252].

Imidazole, on the other hand, would compete for nickel but has less affinity compared to HisTag. The presence of low concentrations of imidazole in the bind buffer would saturate the Ni^{2+}, and prevent binding of non-tagged contaminants and could only be displaced by the HisTag from the lysate passing through the column. The specificity of the affinity chromatography can be enhanced by increasing the concentration of sodium chloride (NaCl) in the buffer solution, or by decreasing the acidity of the solution. It was reported that a double hexahistidine tagged protein bound better to Ni-NTA matrix and increased the yield of protein significantly [269].

During elution, the high concentration of imidazole forces the release of the HisTagged protein from the nickel matrix and replacement by the imidazole. In this way, the purified HisTagged protein can be eluted. Imidazole in the wash buffers minimises non-specific binding and reduces the amount of contaminating non-polyHis protein. Nickel-based IMAC resins often bind unwanted hosts protein containing His residue.

IMAC demonstrates a number of advantages which include stable immobilisation of the transition metal ions, high protein loading, mild elution conditions, easy regeneration of the affinity matrix and low cost [270]. The pET32a plasmid used as the expression vector has two histidine tags readily available for manipulation in the purification of the fusion protein. For the purpose of this study, the amino (N-) terminal HisTag was used. This motif, being part of the fusion partner of the recombinant fusion protein, can be

utilised to purify the free pro-peptide from the fusion protein by IMAC after the proteolysis.

5.1.5 Desalting by gel filtration chromatography

Desalting is a process where small molecules such as salt are removed from the buffer while buffer exchange refers to replacement of a set of buffer salts with another set. Both processes can be done by using size exclusion chromatography (SEC) which is also known as molecular sieve, gel filtration chromatography or gel permeation chromatography. This step is important as certain components of the histidine purification buffer are not compatible and hinder effective cleavage of the fusion protein. Such components included NaCl and imidazole in high concentration.

In this research desalting was performed by gel filtration chromatography using the PD10 desalting column, which contains porous resins. When the column is pre-equilibrated with the water, the samples of purified fusion protein are allowed to pass by gravitational force. The larger molecules of fusion protein will pass rapidly between resins while the smaller salt molecules will enter the pores within the resins, making their passage slower. The original sample buffer will displace the equilibrium buffer. At the end of this process, the fusion protein will be eluted into double distilled water, without the NaCl and the imidazole, which would be more compatible for the downstream proteolysis.

5.1.6 Cleavage using the enterokinase enzyme

The fusion partners need to be removed as they may alter the important characteristics of the target protein. There are several ways to achieve this.

The more commonly used method was by using the proteases such as thrombin and factor Xa [271], Tobacco etch virus (TEV) protease [272] or enterokinase [273]. A non-protease method using self-splicing inteins has also been reported [274].

Enterokinase (EK) is a heterodimeric serine protease which plays a key role in initiating the proteolytic digestion cascade in the mammalian duodenum. The enzyme acts by converting trypsinogen to trypsin via a highly specific cleavage site of which the recognition sequence is pentapeptide $(Asp)_4$-Lys (DDDDK). This stringent site specificity gives EK great value as a cleavage reagent of a fusion protein. A study had previously shown that recombinant light chain of bovine enterokinase could be expressed in *E. coli* system and autocatalyse its separation from the fusion partner. The resultant rEKL had a property indistinguishable from that derived from mammalian cells [275].

In this research, the cleavage of the fusion partner and the target protein was achieved by using recombinant enterokinase enzyme (rEK) (Novagen, Merck Millipore, Watford, UK). Because of non-specific cleavage, optimisation steps were conducted to verify the optimal reaction conditions. The rEK was removed from the target protein by using agarose which binds to the rEK and is removed by using a spin column. The ratio of the rEK in unit with the agarose amount used needs to be optimised to achieve the best possible result.

The pET32a(+) plasmid vector had an in-built enterokinase cleavage site, nucleotide sequence of which was GACGACGACGACAAG. It coded for the AspAspAspAspLys (DDDDK) amino acid sequence. Proteolytic enzyme

recombinant enterokinase (rEK) would be able to recognise this site and cleave immediately after the lysine (Lys, K) amino acid, separating the fusion partner and the target pro-peptide. One has to bear in mind that rEK would not cut between lysine and proline. Therefore, it is important to not to have a proline residue immediately after the enterokinase cleavage site in the recombinant plasmid DNA. Should this be the case, a serine can be added into the target peptide N-terminus. In the case of hBD9, the N-terminal amino acid is glycine (Gly, G) which is compatible with effective cleavage by using rEK.

5.1.7 Ion exchange chromatography

This method of protein purification is based on the difference in strength of the reaction between charged molecules and an oppositely charged support (static phase) in a column. It can be divided into cation and anion exchange. In cation exchange, a weak base or strong acid is used to react with the positively charged molecules. On the other hand, strong base is used in the anion exchanger to form reaction with negatively charged molecules (anions).

Ion exchange chromatography was chosen as the method to separate the target protein from the fusion partner after successful rEK cleavage and removal. This method utilised the difference in the pI of the two proteins. The target protein, having a pI of 8.3, would be ionised in the environment of low pH in the static phase of the cation exchanger (pH 5.0).

Amphoteric molecules called zwitterions contain both positive and negative charges simultaneously depending on the functional motifs of the molecules. The nett charge of the molecules depends on the pH of its

surrounding solutions and may change after gaining or losing a proton (H^+). The pI is the pH value at which the molecule carries no electrical charge or the negative and positive charges are equal.

As the target pro-peptide was a cation with isoelectric point (pI) of 8.33, a cation exchange chromatography was performed. A cation exchanger column contains negatively charged resins. When using a buffer with pH lower than the pI of the target pro-peptide, the molecules would have been positively charged. Therefore it would bind to the resins (static or immobilised phase) in the column. The chosen pH of the buffer needs also to be higher than the pI of the fusion partner (5.48). In this condition, the fusion partner would have been negatively charged, and washed out of the column.

The samples contained a mixture of fusion tag with pI 5.48 and target protein with pI 8.33. The two peptides can be separated by gradient or fixed pH of the elution buffer. At the chosen buffer with pH 6.0 the fusion tag is negatively charged in contrast to the target protein which was positively charge. As such, upon loading of the cleavage reaction onto the negatively charged matrix in the cation exchanger column, only the target protein will bind while the fusion tag would be washed through. In the elution step, increasing the ionicity of the mobile phase will eventually overcome the strength of the interaction between the target protein and the matrix, resulting in the displacement of the positively charged target protein out of the column and into the buffer.

5.2 Objectives

In general, the objective of this chapter is to describe the process of purifying the free hBD9 pro-peptide from the soluble fraction of the expression host cell lysate by using various molecular steps.

The specific objectives included:

a. To describe the Histidine-tag purification of the fusion protein
b. To describe the desalting of the purified fusion protein using the PD10 column gravity flow gel filtration chromatography.
c. To describe the optimisation of the proteolysis using the rEK for the cleavage of the fusion partner from the hBD9 pro-peptide.
d. To describe the purification of the free hBD9 pro-peptide following proteolysis using the cation exchange chromatography.

5.3 Methods

5.3.1 HisTag IMAC

The histidine tag purification was performed using two separate methods. In the earlier part of the research, the gravity-flow column was used. This was because of the unavailability of the fast flow system in the earlier phase of the research.

5.3.1.1 HisTag IMAC using gravity-flow column

In this experiment, the HisTag Ni-NTA resin with gravity flow column of the histidine purification was purchased from Thermo Scientific, Loughborough, UK and used according to the manufacturer's

recommendation. 4 ml of slurry (2.0 ml bed volume) was placed in a tube and allowed to settle completely and the supernatant was carefully removed. The resin was equilibrated with two resin-bed volumes of equilibrium buffer (20 mM sodium phosphate, 300 mM sodium chloride with 10 mM imidazole, pH 7.4) and mixed until the resin was fully suspended. The equilibrated resin mixture was loaded onto the column and allowed to settle.

The sample was prepared by mixing the soluble fraction with an equal volume of equilibrium/wash buffer. 4 ml of sample mixture was then loaded into the equilibrated column and the binding follow-through was collected. The column was then washed with 2 resin volume of wash buffer (PBS with 25 mM imidazole, pH 7.4) twice and the follow through was collected. The wash follow-through was collected in two separate tubes. Elution of bound HisTagged protein was performed with two resin-bed volumes of elution buffer (PBS with 250 mM imidazole, pH 7.4), collected in fractions of 1.0 ml.

5.3.1.2 HisTag IMAC using HPLC column

In this experiment, the 5 ml HisTrap (GE Healthcare Life Sciences, Little Chalfont, UK) purification column was used. This was connected to the purification system (Bio-Rad, Hemel Hempstead, UK), without UV detector, pH sensor and the computerised analytical software. In brief, the machine was set to equilibrate column with 4 column volumes (CV) of the start buffer. 10 ml of the soluble fraction of the fusion protein was equilibrated with 10 ml of the start buffer and loaded into the column. The column was then washed with five CV of start buffer before elution with 5 CV of elute buffer. The elution was collected in 2.5 ml fractions. The bind and wash follow-throughs were also collected for SDS-PAGE analyses.

The start buffer contained 40 mM of imidazole and the elute buffer contained 500 mM of imidazole. The loaded samples, bind follow-through, wash follow-through and the eluted fractions were subjected to SDS-PAGE to verify the result.

5.3.2 Desalting using PD10 column

The PD10 desalting column (GE Healthcare Life Sciences, Little Chalfont, UK) was used in the gravity force method. The column was first pre-equilibrated using 4 column volumes (CV) of double distilled water as this would be the final elute buffer. 2.5 ml of the histidine purified sample was then loaded and allowed to enter the packed bed completely and the follow-through was discarded. The final elution was performed using 3.5 ml double-distilled water and 0.5 ml fractions were collected. The protein eluted was quantified using the nanodrop spectrophotometer and subjected to SDS-PAGE.

5.3.3 Proteolysis using the rEK cleavage

The desalted histidine-purified sample was subjected next to the rEK cleavage step. In this step, the protein to enzyme ratio, temperature and duration were optimised. The cleavage product was then run in SDS-PAGE for verification of the cleavage result.

The Enterokinase Cleavage Capture Kit (Novagen, Merck Millipore, Watford, UK) was used. In brief, 50 µl of sample was added to 5 µl 10x cleavage buffer and 1 iu of rEK. The sample was incubated at 4^{o}C incubation, and 21^{o}C. 10 µl of sample was removed at 2, 4, 6 and 16 hour time points and were subjected to SDS-PAGE.

5.3.4 Cation exchange chromatography

Cation exchange chromatography was performed using the HiScreen Capto S (GE Health System, Little Chalfont, UK) cation exchange column. The pre-packed column with column volume of 4.7 ml was attached to the protein purifier system (Bio-Rad, Hemel Hempstead, UK) with no UV spectroscopy monitoring and computerised analysis software.

The experiment was conducted according to the manufacturer's recommendation. In brief, the column was washed with 1 CV of distilled water followed with 5 CV of start buffer (50 mM sodium acetate, pH 5.0). The hBD9 fusion protein sample which was adjusted to the start buffer was loaded into the column followed by washing with 5 CV of start buffer. Linear gradient elution was performed using 10 CV elution buffer (50 mM sodium acetate, 1 M NaCl pH 5.0). The eluted fractions were subjected to nanodrop spectroscopy for evidence of eluted free hBD9 pro-peptide.

5.3.5 Size exclusion chromatography

Size exclusion chromatography was the only step performed with attachment to the ÄKTA HPLC machine (GE Healthcare Life Sciences, Little Chalfont, UK) equipped with computerised analysis software. The HiPrep 16/60 sephacryl S200 HR column (GE Healthcare Life Sciences, Little Chalfont, UK) which has 120 ml column volume (CV) was attached to the ÄKTA prime HPLC system. The column was equilibrated with one-half CV with distilled water at a flow rate of 0.5 ml/min followed by 2 CV of start buffer (0.05 M sodium phosphate, 0.15 M NaCL, pH 7.2) at 1 ml/min. A volume of 1.2 ml (1% of CV) of HisTag-purified desalted hBD9 fusion protein sample was loaded followed by 2 CV of the buffer (0.05 M sodium phosphate, 0.15 M

NaCL, pH 7.2), at a flow rate of 1 ml/min. Eluted fractions were collected in 1 ml fractions up to 150 ml.

5.3.6 SDS-PAGE

The samples were collected and separated in the SDS-PAGE using conditions described in previous chapter. The molecular weight marker (GE Healthcare Life Sciences, Little Chalfont, UK) was loaded as protein size reference (Figure 5.3.1).

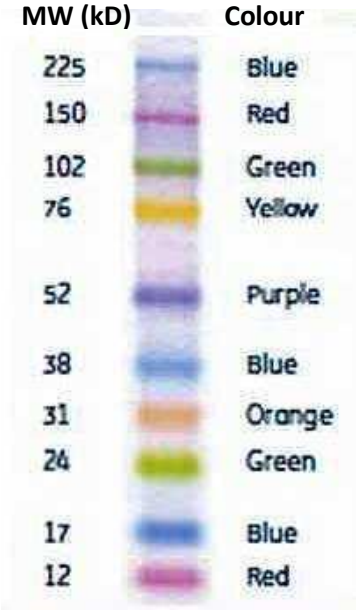

Figure 5.3.1 Molecular weight full range marker (Catalogue No. RPN800E, GE Healthcare Life Sciences, Little Chalfont, UK) which was used in the SDS-PAGE for fusion protein size reference - http://www.gelifesciences.com/.

5.4 Results

5.4.1 Histidine purification

The soluble fraction of the cell lysate was always kept in ice while on the bench. This is following the observation that precipitation would occur in

the soluble fraction with time when left at room temperature. The pH of the BugBuster (Novagen, Merck Millipore, Watford, UK) was 7.8. The pH of the soluble protein fraction was 8.0. It was calculated that the pI of the fusion protein was 5.9. Therefore, theoretically, the BugBuster (Novagen, Merck Millipore, Watford, UK) would have kept the fusion protein to be soluble. However, it was found that precipitation occurred if kept for more than 24 hours even at 4 ^{o}C.

5.4.1.1 The gravity method

The SDS-PAGE of the IMAC using Ni-NTA gravity column resulted in satisfactory yield of fusion protein in the fractionated eluates. The binding of the fusion protein from the loaded sample was good and the washing buffer was effective in removing the other non-tagged protein. The elution mostly occurred during the first two ml of elution which was associated with some oligomeric coelution.

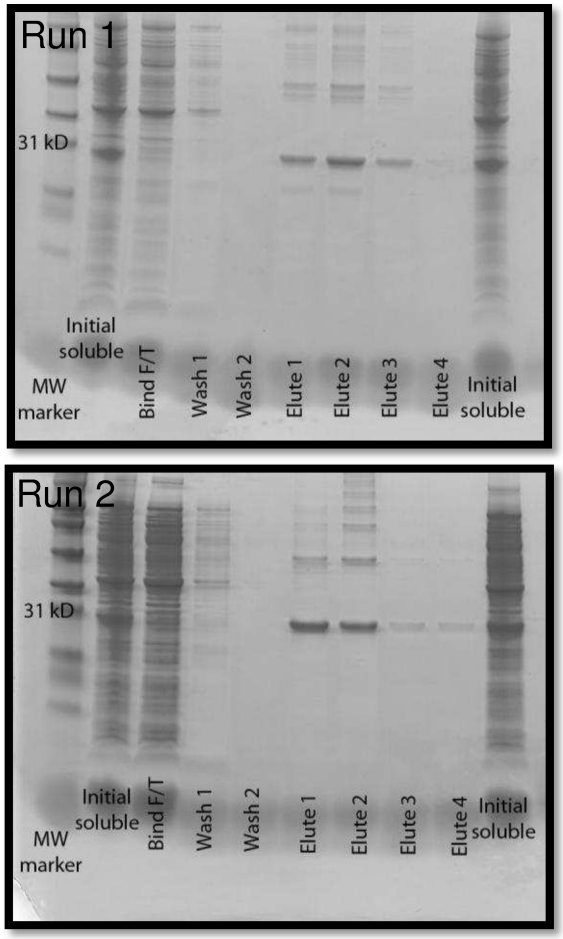

Figure 5.4.1 Photographs of the SDS-PAGE gels showing the fusion protein bands in the elution samples from the HisTag IMAC using the gravity flow column Run 1 and Run 2.

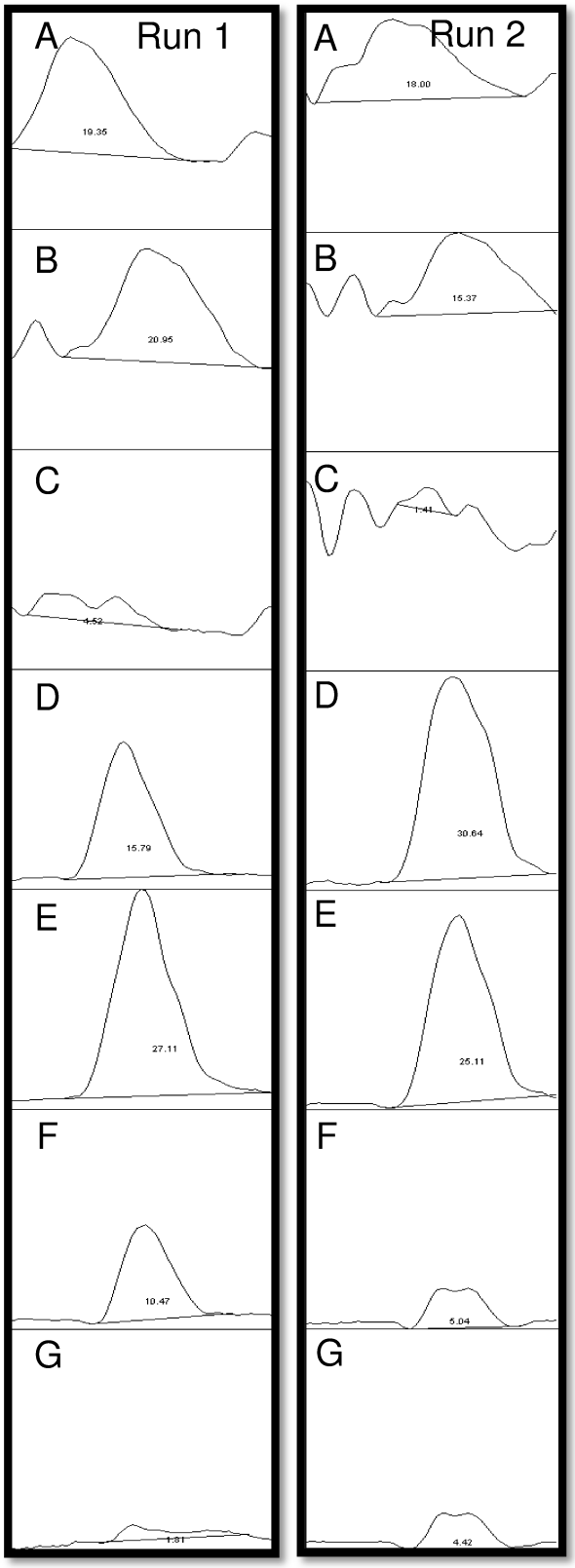

Figure 5.4.2 Image J plot for the SDS-PAGE in Figure 5.4.2, showing the fusion protein band intensity for Run 1 and Run 2. Lysate sample 1 and 2 (A and B), bind follow through (C), Elute 1 to 4 (D to G).

Table 5.4.1 Table summarising the relative band intensity from Image J plot and the protein recovery

	Run 1	Run 2	Average Run	%
	Band intensity			
Loaded 1	10201	9175.8		
Loaded 2	11044	7834	9563.7	-
Average loaded	10623	8504.9		
Bind F/T (loss)	1190	718.2	954.2	9.97
Elute 1	8323.4	15618		
Elute 2	14290	12801		
Elute 3	5519.2	2570.1		
Elute 4	952.1	2253.5		
Average eluted	7271.3	8310.7	7791	81.46

From Table 5.4.1, the average fusion protein loss in the bind follow through between the two runs was 9.97% and the average fusion protein recovery was 81.46%.

5.4.1.2 HPLC method

This result was obtained using the Bio-Rad protein purifier (Bio-Rad, Hemel Hempstead, UK) without the computerised facility to detect the UV level and the pH changes in the eluted samples. The purifier was not attached to computerised analysis software, so that no graph could be printed and shown in this thesis. In this method, the elutions were fractionated into 2.5 ml samples. The fractionated samples were subjected to nanodrop spectrophotometry. For verification, the samples were also subjected to SDS-PAGE. A few runs were conducted for the HisTag IMAC and the concentrations of the fusion protein in the eluted fractions are summarised in Table 5.4.2.

The SDS-PAGE of the HisTag IMAC showed presence of fusion protein with highest concentration, as determined by nanodrop spectroscopy, between fractions 12 to 17 (Figure 5.4.3) in all runs. The fusion proteins were also demonstrated in the form of monomeric and oligomeric protein. The purity of the eluted fusion protein was high and no contaminant band was seen (Figure 5.4.4).

Table 5.4.2 Table showing the concentration of HisTagged-purified fusion protein following IMAC.

Elute No.	Concentration (mg/ml)			
	Run 1	Run 2	Run 3	Run 4
Elute 1	-	0.89	-	-
Elute 2	-	0.16	0.45	1.74
Elute 3	1.91	0.1	0.23	0.9
Elute 4	1.31	0.09	0.17	0.65
Elute 5	0.69	0.1	0.13	0.47
Elute 6	0.52	0.11	0.14	0.37
Elute 7	0.48	0.12	0.15	0.34
Elute 8	0.51	0.16	0.26	0.46
Elute 9	0.53	0.32	0.4	0.56
Elute 10	0.59	0.4	0.54	0.82
Elute 11	0.54	0.63	0.76	0.88
Elute 12	0.54	0.82	0.92	0.96
Elute 13	0.66	1.05	1.14	1.35
Elute 14	0.71	1.18	1.64	2.12
Elute 15	0.75	1.36	2.33	2.64
Elute 16	0.79	1.69	2.24	2.6
Elute 17	0.8	1.42	1.75	1.47
Elute 18	0.79	1.11	1.32	1.14
Elute 19	0.79	0.93	1.15	1.01
Elute 20	0.77	0.85	1.04	0.92
Elute 21	0.77	0.81	0.95	0.89
Elute 22	0.77	0.83	0.9	0.84
Elute 23	0.76	0.75	0.87	0.82
Elute 24	0.76	0.76	0.85	0.81

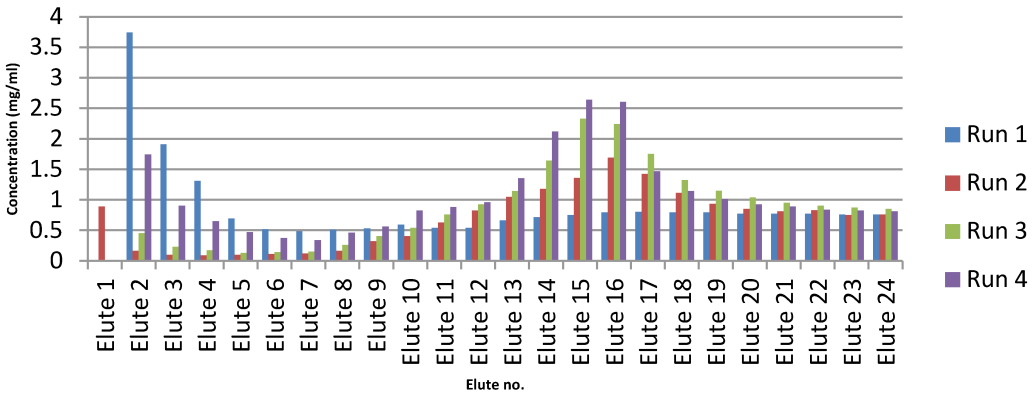

Figure 5.4.3 Histogram showing the concentration of the eluted fusion protein following histidine tag IMAC.

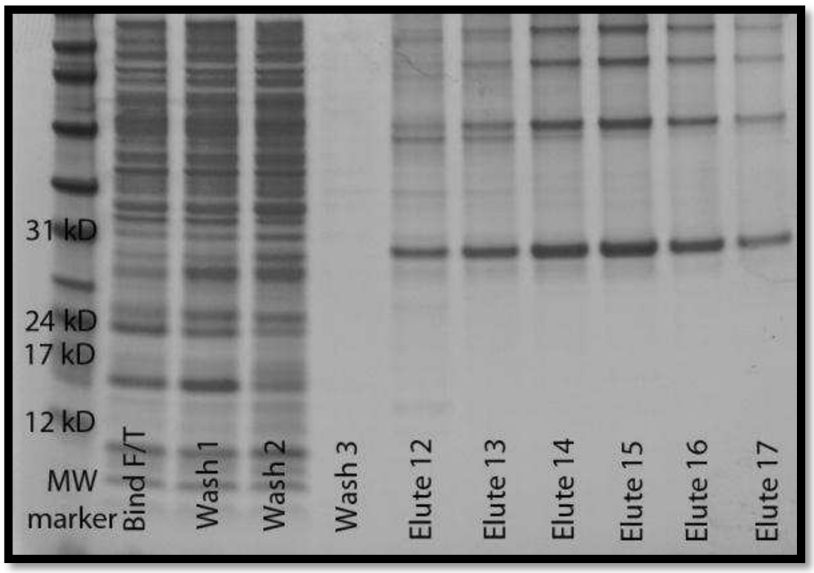

Figure 5.4.4 Photograph of SDS-PAGE gel of HisTag purification using IMAC (Run 4). Elutes 12 to 17 contained fusion protein mainly as monomer but there were fusion protein oligomers too.

Image J software was used to quantify the relative band intensity in elute 12 to 17 (Figure 5.4.4). The average percentages for monomer and dimers were 45.70% and 31.43%, respectively. The rate of the protein recovery could not be determined from the above SDS-PAGE gel as the loaded soluble fraction was not included in the electrophoresis.

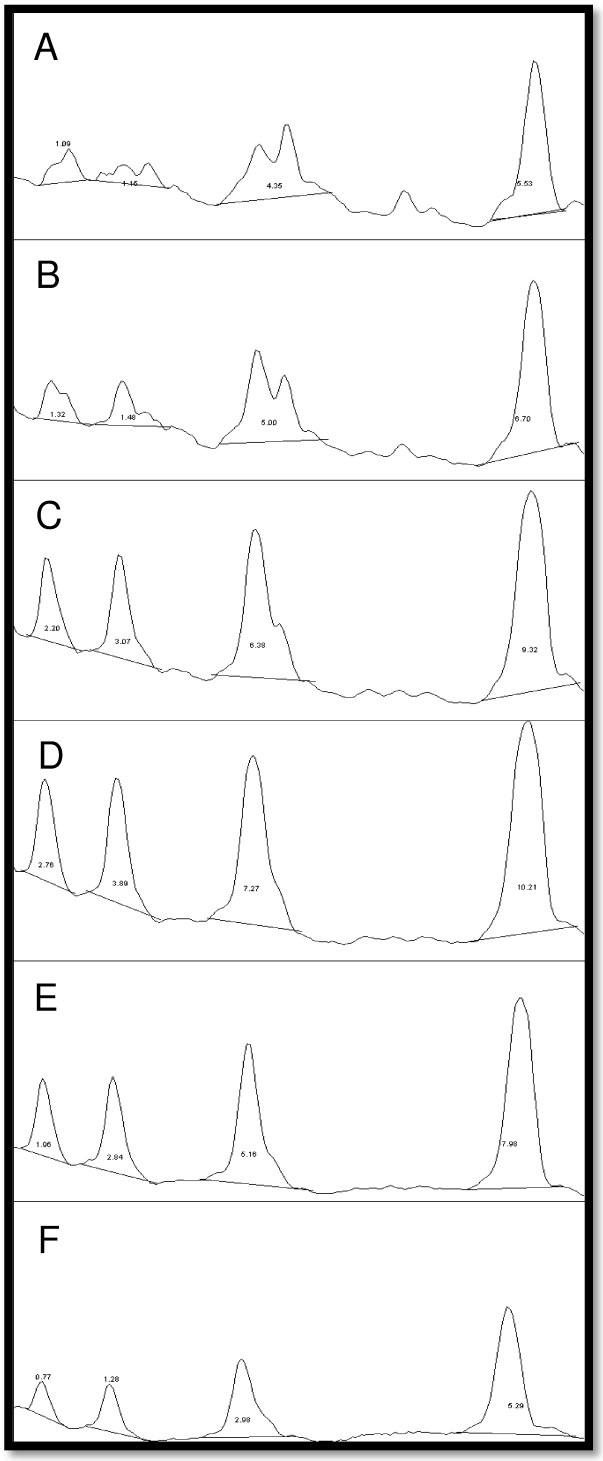

Figure 5.4.5 Image J plot for bands in Elute 12 to 17 (A to F) from Figure 5.4.4 to determine the relative band intensity for the monomers and oligomers of the fusion protein.

5.4.2 Desalting of the fusion protein

The histidine-purified samples of different concentrations were subjected to PD10 desalting steps. The eluted samples were subjected to

nanodrop spectrophotometry for protein quantification and the results were represented by the chart below. For verification, the eluted samples were also subjected to the SDS-PAGE with the following results.

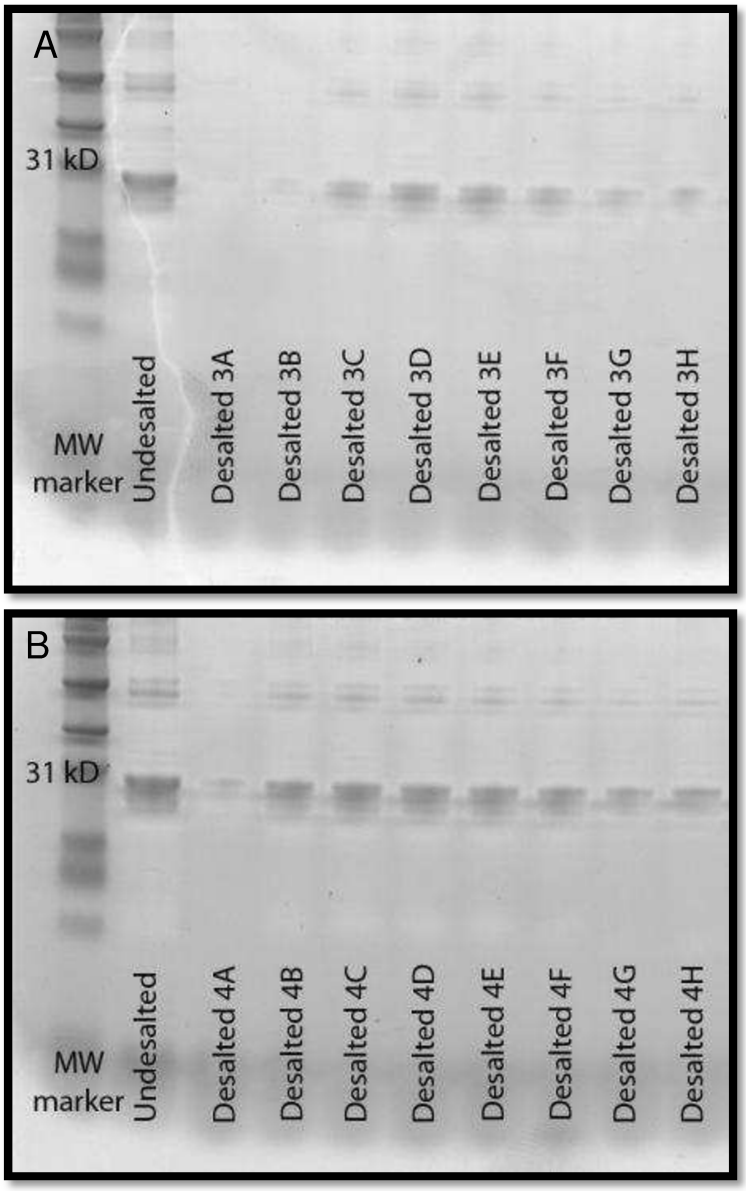

Figure 5.4.6 Photographs of the SDS-PAGE of the histidine-purified samples Elute 3 (A) and Elute 4 (B) following desalting. The bands corresponding to the fusion protein were detected with different intensity in the different elutes.

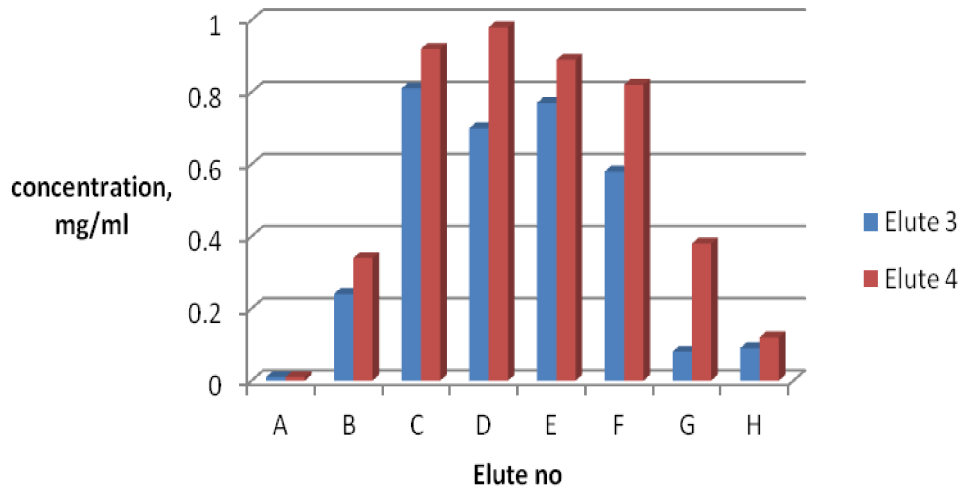

Figure 5.4.7 Concentration of the fusion protein in different elutes following desalting of histidine-purified samples of Elute 3 (0.96 mg/ml) and 4 (1.16 mg/ml).

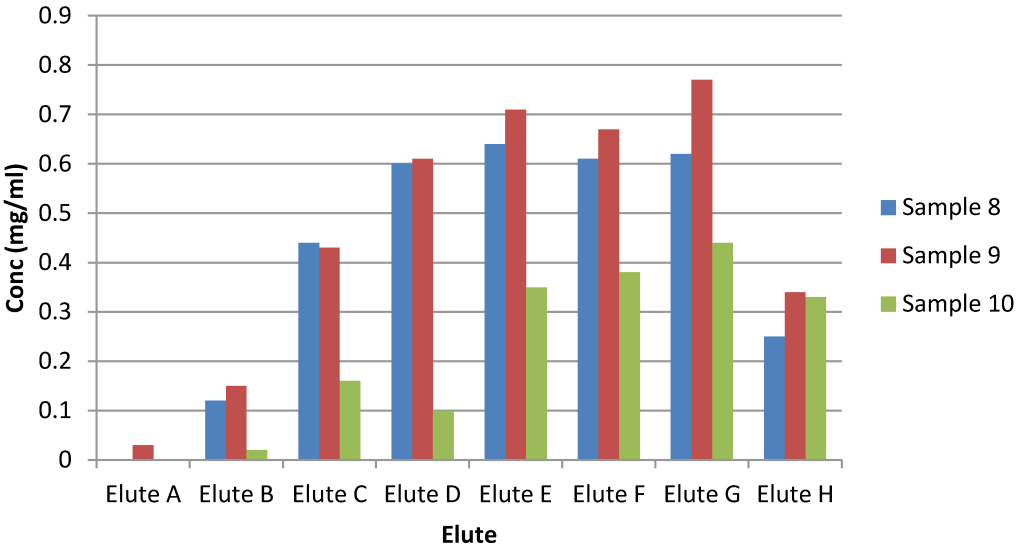

Figure 5.4.8 Histogram showing the desalting of histidine-purified samples 8 (0.78 mg/ml), 9 (0.8 mg/ml), and 10 (0.6 mg/ml). 2.5 ml of samples were loaded into the column and eluted using 4 ml deionised water into 0.5 ml fractions A to H.

Table 5.4.3 Concentration of the fusion protein in different elutes following desalting of histidine-purified samples.

Sample		Protein concentration (mg/ml)								Total eluted (mg)	Percentage recovery
		Elute A	Elute B	Elute C	Elute D	Elute E	Elute F	Elute G	Elute H		
Elute 3	Conc. (mg/ml)	0.01	0.24	0.81	0.70	0.77	0.58	0.08	0.09		
	Amt (mg)	0.05	0.12	0.41	0.35	0.38	0.29	0.04	0.05	1.69	70.42
Elute 4	Conc. (mg/ml)	0.01	0.34	0.92	0.98	0.89	0.82	0.38	0.12		
	Amt (mg)	0.05	0.17	0.46	0.49	0.45	0.41	0.19	0.06	2.28	78.62
Elute 8	Conc. (mg/ml)	0	0.12	0.44	0.60	.064	0.61	0.62	0.25		
	Amt (mg)	0.	0.06	0.22	0.30	0.32	0.31	0.31	0.13	1.64	84.10
Elute 9	Conc. (mg/ml)	0.03	0.15	.043	0.61	0.71	0.67	0.77	0.34		
	Amt (mg)	0.02	0.07	0.22	0.30	0.35	0.33	0.38	0.17	1.85	92.75
Elute 10	Conc. (mg/ml)	0	0.02	0.16	0.10	0.35	0.38	0.44	0.33		
	Amt (mg)	0	0.01	0.08	0.05	0.18	0.19	0.22	0.16	0.89	59.33

From the above table, the average calculated percentage recovery for the desalting step was 77.04% ± 12.81% (mean ± SD).

5.4.3 Cleavage of the fusion protein

5.4.3.1 Detection of free hBD9 propeptide following cleavage

Following cleavage at 21 ^{o}C for 4 hours, the cleavage reaction was subjected to SDS-PAGE and western blot analysis. In the SDS-PAGE gel photograph, the uncut fusion protein and the cleaved fusion partner could be detected at the appropriate location for their molecular size. However, in the gel photograph the free target peptide could not be detected (Figure 5.4.9 A).

Nevertheless, the free hBD9 propeptide was seen at approximately 8 kD MW on the western blot membrane (Figure 5.4.9 B).

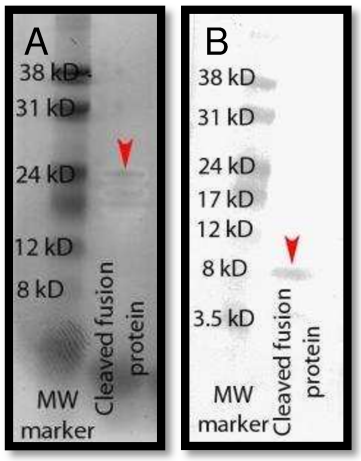

Figure 5.4.9 Photograph of the SDS-PAGE gel (A) and the WB membrane (B) showing presence of a band corresponding to fusion partner in the SDS-PAGE and a smaller band corresponding to the free hBD9 pro-peptide by WB.

5.4.3.2 Cleavage at 21 ^{o}C

5.4.3.2 (a) Cleavage at 21 ^{o}C compared with 4 ^{o}C

The cleavage at 21 ^{o}C for 16 hours (Lane 5) gave better result than at 4 ^{o}C for 16 hours (Figure 5.4.10, Lane 2). The uncleaved proportion at 4 ^{o}C incubation temperature was more than that in the 21 ^{o}C incubation temperature. However, 4 ^{o}C incubation gave a significantly higher proportion of appropriately cleaved protein than 21 ^{o}C incubation. Likewise, the 4 ^{o}C incubation also produced lower miscleaved protein than 21 ^{o}C. We concluded although both incubation temperatures were effective, long duration cleavage at 4 ^{o}C was more preferred because although it had higher uncleaved protein, it had the higher appropriately cleaved proportion.

5.4.3.2 (b) Cleavage at 21 ^{o}C for various durations

Cleavage of the desalted HisTag-purified fusion protein was carried out to investigate the effect of cleavage time on the cleaved protein amount. Cleavage was carried out at 21 ^{o}C for 2, 4, 6 and 16 hours duration (Figure 5.4.10). SDS-PAGE for the cleavage product was conducted with the lane allocation shown in Table 5.4.4.

Table 5.4.4 Lane allocation for the SDS-PAGE following the cleavage.

Lane	Description
Lane 1	Molecular weight marker
Lane 2	Cleavage at 4 ^{o}C, 16 hours
Lane 3	Cleavage at 21 ^{o}C, 2 hours
Lane 4	Cleavage at 21 ^{o}C, 4 hours
Lane 5	Cleavage at 21 ^{o}C, 6 hours
Lane 6	Cleavage at 21 ^{o}C, 16 hours
Lane 7	Uncleaved control

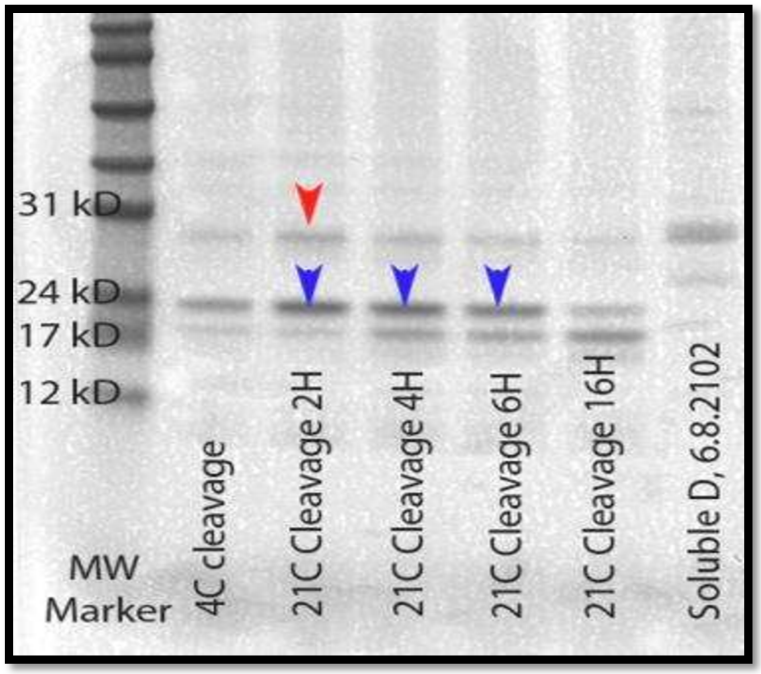

Figure 5.4.10 Photograph of the SDS-PAGE showing the cleavage result at 2, 4, 6 and 16 hour incubations. The cleavage was highest at 16 hours compared to the shorter durations. The miscleaved proportion also increased with longer incubation.

Cleavage for different incubation duration was also reviewed (Figure 5.4.11). The amount of uncleaved protein was similar after 2, 4 or 6 hours incubation but less after 16 hours incubation. The amount of the appropriately cleaved protein increased in parallel to the increment of miscleavage, with increment in the incubation durations. At 21 ^{o}C incubation temperature, 2 hour incubation had the highest proportion of appropriately cleaved protein and the lowest miscleaved protein. The non-cleavage rate was 16.4% (2.5 µg). Cleavage for 16 hours was associated with reduced proportion of uncleaved protein. However, allowing cleavage for a longer period was associated with a higher proportion of non-specific cleavage, and reduction in the properly cleaved protein. In conclusion, 2 hour cleavage gives the highest appropriate cleavage rate and lowest miscleavage rate (Figure 5.4.12.

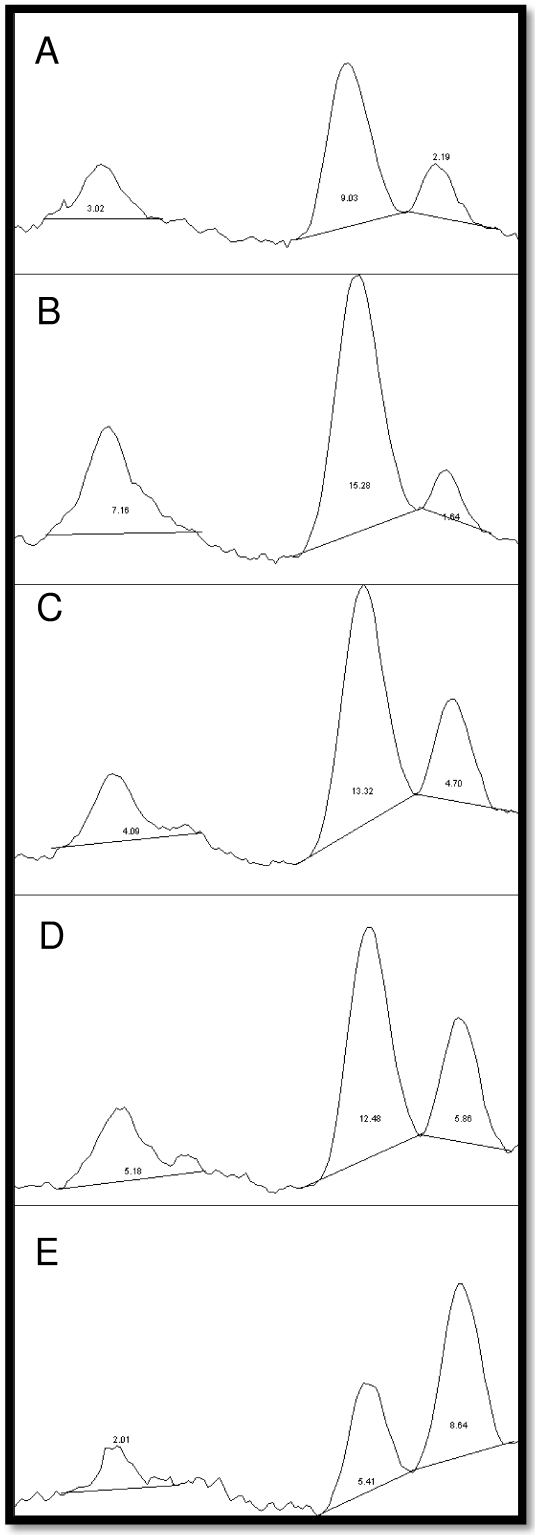

Figure 5.4.11 Image J plot of the bands in showing the comparison between the uncleaved, cleaved and miscleaved protein for 4 ^{o}C 16 hours (A), 21 ^{o}C 2 hour (B), 21 ^{o}C 4 hours (C), 21 ^{o}C 6 hours (D) and 21 ^{o}C 16 hours (E) incubations.

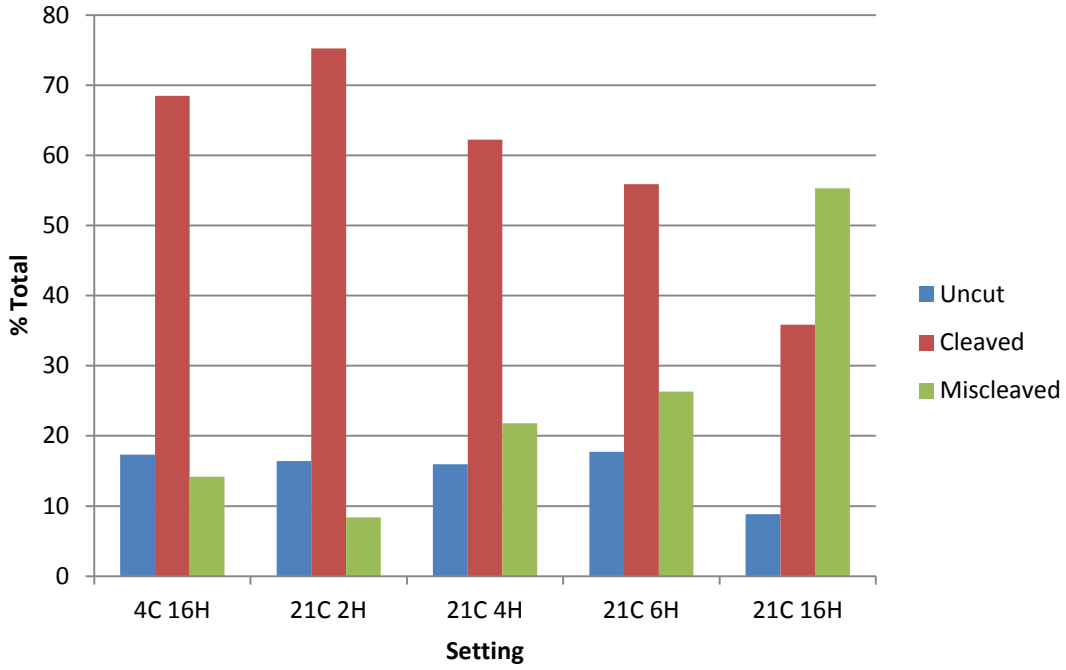

Figure 5.4.12 Histogram showing the relationship between the uncleaved, appropriately cleaved and miscleaved fusion protein at different cleavage conditions.

5.4.3.3 Cleavage at 21 ^{o}C for different protein concentrations

The cleavage carried out at 21 ^{o}C for several incubation durations showed that the rEK cleaved the fusion protein better at 30 µg compared to 40 µg or 50 µg. The non-specific cleavage was seen at four hours for concentration of 50 µg. With longer incubation, more non-specific cleavages in terms of prominence and number of the miscleaved bands, were detected (Figure 5.4.13).

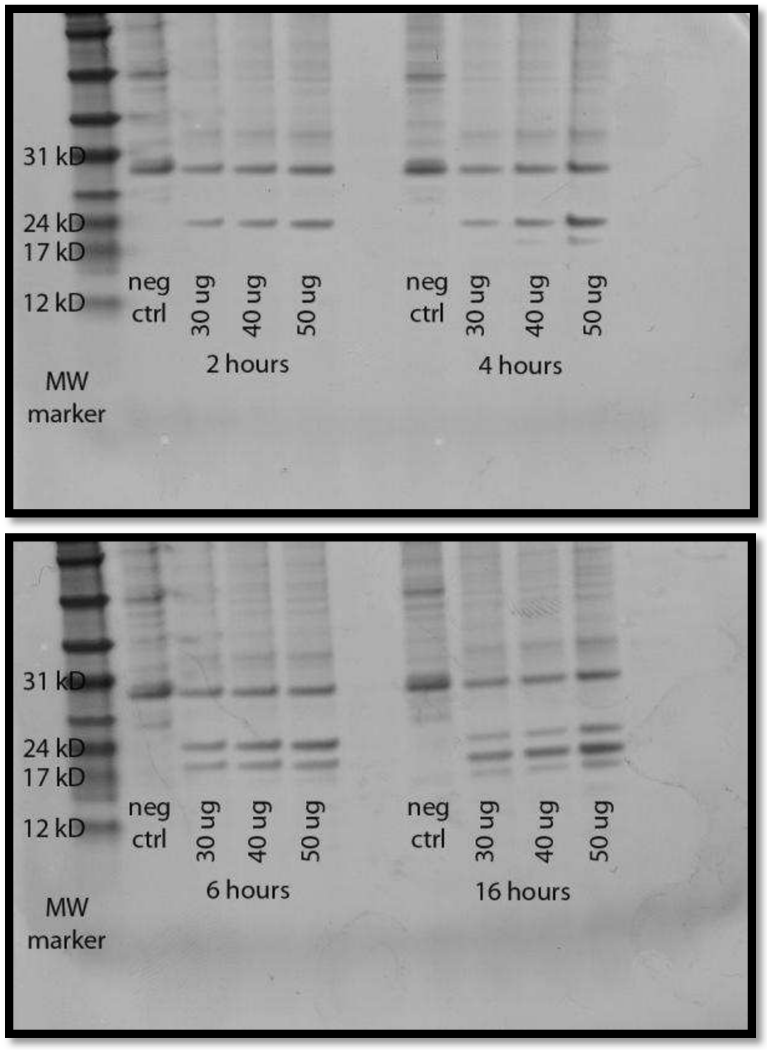

Figure 5.4.13 Photograph of the SDS-PAGE showing the proteolysis using rEK at different fusion protein concentrations and durations.

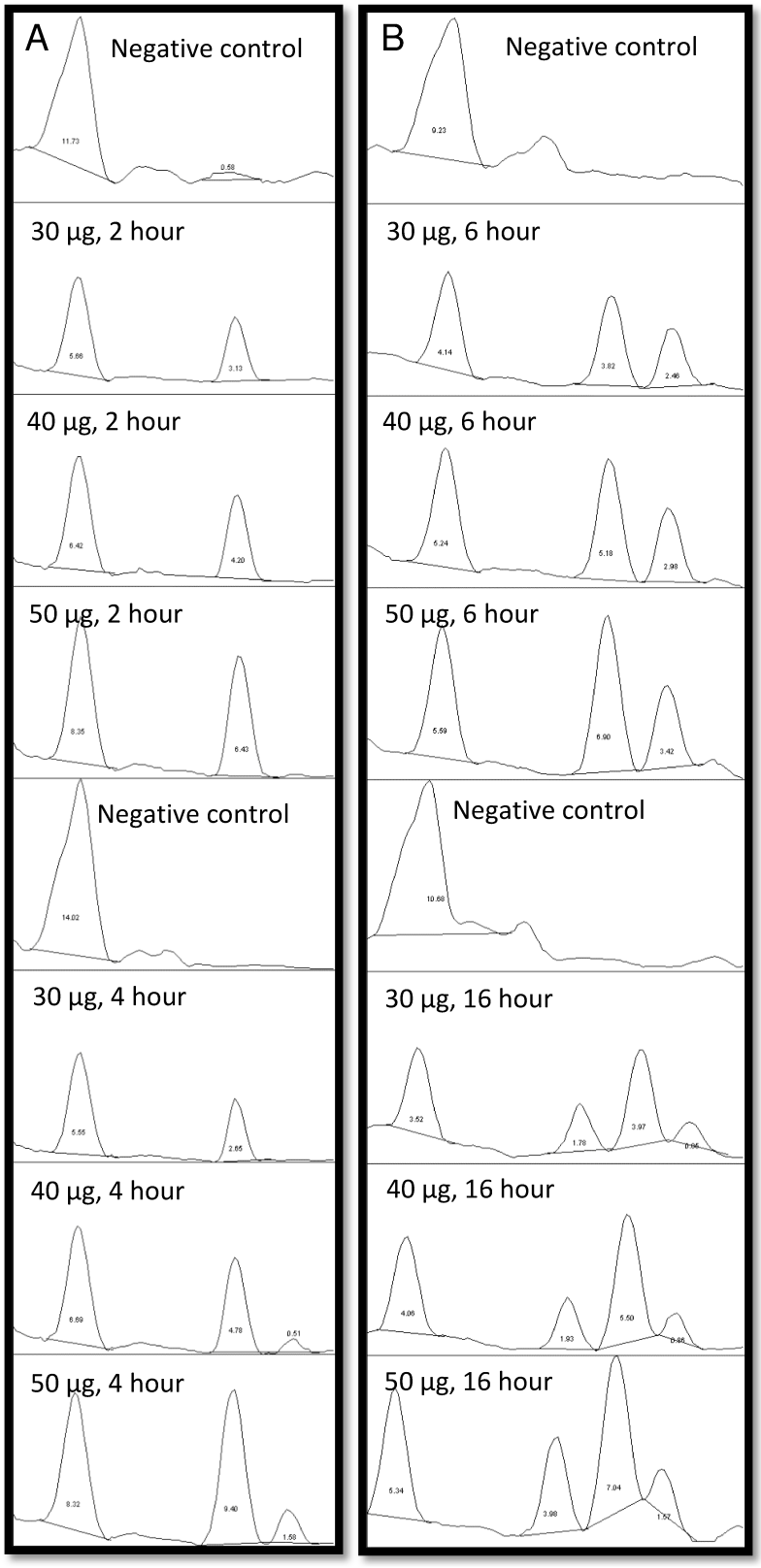

Figure 5.4.14 Image J plot for the bands in SDS-PAGE showing the comparison between the uncleaved, cleaved and miscleaved protein in Figure 5.4.13.

Based on the reactions of 50 µg starting protein amount, the percentages of uncut fusion protein were 71.1% (after 2 hours incubation), 59.37% (4 hours), 60.64% (6 hours) and 49.93% (16 hours). The percentage of cleaved fusion protein increased with duration of incubation. From the 50 µg for 2 hours reaction, the produced fusion protein was 19.90% of the loaded protein (50 µg) which was 10.23 µg. The free target protein should theoretically be 4.21 µg/50 µl. Theoretical percentage of cleavage was 4.21 µg from the potential 14.53 µg ie 28.9 %. However, the corresponding band for the free target protein was not detectable as the amount (4.21 ug) was too small for detection. The same calculation method could not be applied to the 4, 6 and 16 hour incubations as the exact sizes of the miscleaved fusion tags could not be determined. As for the 30 µg and 40 µg loaded protein, the percentage of uncleaved fusion protein could not be determined as there were no corresponding controls. Therefore, the amount of yield of efficiency of cleavage could not be calculated as well.

5.4.4 Cation exchange chromatography

The rEK cleavage reaction of 50 µl was loaded to the cation exchange column for free hBD9 propeptide purification. However, there was no protein retrievable from the small volume of the cleavage reaction subjected to the chromatography step. As such, no result could be presented in this section.

5.4.5 Size exclusion chromatography

From the SEC described earlier (5.3.5, page188), there were several spikes of UV A_{280} absorbance seen in the graph tracing. The corresponding fractions of eluted samples for these spikes were identified and subjected to

the SDS-PAGE. The gel was stained and photographed in Figure 5.4.15. It can be seen that in general, the high MW higher order oligomers eluted in the earlier phase compared to the smaller lower order oligomers and monomer. However, the SEC system applied in this experiment failed to single out each oligomeric form into one specific elute of different MW sizes.

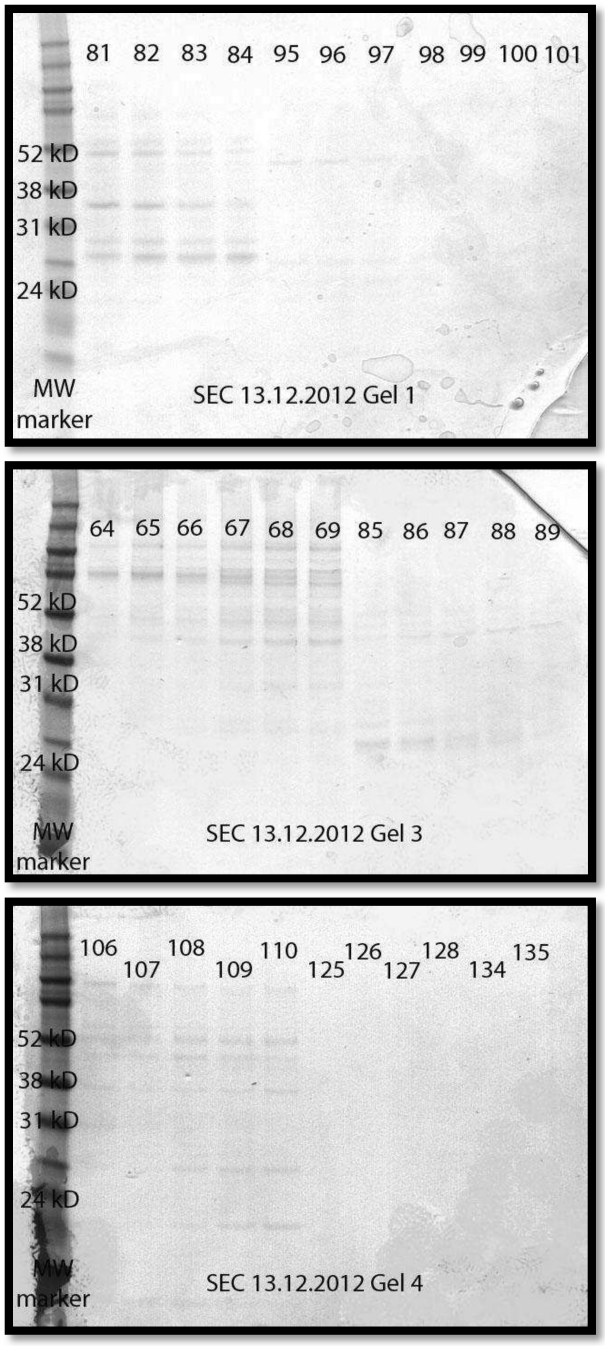

Figure 5.4.15 SDS-PAGE photographs for eluted samples from the SEC showing presence of multiple bands of widely ranged molecular weight in the samples. It seemed that the SEC failed to separate the bands of different molecular weight effectively.

5.5 Discussion

Purification of different target proteins in various plasmid systems with wide range of success showed that there is no one ideal way to express all proteins using genetic engineering recombinant system. Therefore, depending on the characteristics of the desired protein, an expression strategy needs to be carefully chosen and meticulously optimised to maximise the purity and recovery of the free target protein. The purification steps need to be minimised as any additional step is associated with further loss of protein.

5.5.1 HisTag purification

In this research, the gravity column and the fast flow column was used. Both methods showed good results. However, for the efficient upscaled purification of large amount of desired fusion protein, the fast flow method using HPLC column is recommended. This should be connected to a computerised detection system and software for analyses and precise detection of the eluted protein.

Although the resin used was Ni-NTA and no comparison was made with Co-NTA, the resultant level of purified fusion protein was high both in concentration and purity. The histidine purification step in this project has been successful to purify the fusion protein at a high level of purity. This was evident from the SDS-PAGE in which only one band corresponding to the size of the fusion protein was detected. In term of protein recovery, the amount of the protein which was recovered was also high.

A common issue when using the histidine tag IMAC is nonspecific binding of untagged protein. Although histidine only occurs as less than 2% of cellular membrane amino acids, some of the proteins contain two adjacent histidines and thus may bind to the matrices and coelute with the target protein [276]. This may lead to the contamination and reduce the purity of the final product. Disulfide bonds between the fusion protein and other proteins are another source of nonspecific binding which contribute to contamination of the final product. Addition of 10 mM 2-mercapto-ethanol in the buffers used would overcome this problem. Inclusion of Triton X or Tween 20 in the buffers may ease this interaction without jeopardising the IMAC of the target protein [266]. Inclusion of salt (500 mM of NaCl or less), glycerol (less than 20%) or ethanol (less than 20%) can also reduce the nonspecific hydrophobic interactions. It can never be emphasised too much that the optimal IMAC condition for every target protein requires a process of optimisation.

5.5.2 Desalting by gel filtration chromatography

The buffer exchange for hBD9 in this research worked well with purity of 100% and average recovery of 77.04%. This result was reasonable but comparison was not possible as other similar studies did not report on the fusion protein purity and recovery following desalting [242, 253].

5.5.3 Cleavage using the enterokinase enzyme

Efficient site specific proteolysis is crucial in the process, and rEK is known for its nonspecific proteolysis at non-canonical or non-target sites. Lowering the reaction's pH from 7.6 to 7.0 did not have any effect on the

cleavage rate but increasing pH to 8.0 had an inhibitory effect on cleavage [269]. Lowering the temperature from 37 ^{o}C to 25 ^{o}C was reported to have no effect on cleavage [277]. This was in contrast to our finding that lowering the temperature from 21 to 4 ^{o}C showed some improvement in the non-specific proteolysis rate of the fusion protein by the enterokinase. Cleavage at higher temperature was associated with higher non-specific proteolysis.

Depending on the recombinant expression strategy used, several authors have described cleavage of β-defensin with different success rates. Tay *et al* used pET48b(+) to express hBD28 and used TEV(p) to cleave the target protein from the fusion partner [277, 278]. They reported 71% purity and 57% protein recovery during the cleavage. Xu *et al* expressed hBD2 using the pET32 and used rEK at 25 ^{o}C for 12 hours, to cleave the fusion protein. However, they did not report on the purity and protein recovery rates of this step [279]. Huang *et al* used pET32 for recombinant expression of hBD3 and found rEK cleavage step allowed recovery rate of 86% [242]. Xu *et al* had reported on the expression of the synthetic mature hBD4 in pET32 system and found a cleavage of 95% after incubation at 25 ^{o}C for 18 hours [245].

Although the proteolysis using rEK enzyme is technically relatively easy to perform, it is subject to a few constraining issues. First, the sample buffer has to be free of high NaCl and imidazole content. Secondly, the relatively expensive rEK has a low substrate to enzyme ratio for effective and yet economical cleavage. This will limit the amount of fusion protein cleaved and thus the amount of the resultant free target protein. Thirdly, it is associated with non-specific cleavage. And lastly, the rEK has no tag and can only be

separated by spin column, which itself risks for further protein loss. An alternative strategy would be to use a relatively cheaper enzyme with much higher substrate to enzyme ratio, more tolerance to the salt content and pH level, and more easily removed via HisTag such as SUMO protease [253].

Longer duration of cleavage causes more fusion protein to be cleaved across all incubation temperature. However, nonspecific cleavage started to occur at four hours incubation at 21 ^{o}C.

5.5.4 Size exclusion chromatography

Size exclusion chromatography was conducted following the findings that the purified desalted fusion protein contained mixtures of monomeric and oligomeric fusion protein. In the oligomeric peptide, enterokinase recognition site may be hidden away from binding with the enterokinase and lead to less efficient cleavage. Therefore, the HisTag-purified desalted samples were subjected to size exclusion chromatography, before performing the cleavage only for the monomeric peptide. The cleavage of the monomer peptide would be more efficient, yield higher amount of free hBD9 peptide and avoid high level of enzymatic requirement for the enterokinase proteolysis.

The separation of the oligomers from the monomers was however not efficient. Mixture of monomers and oligomers were found in elutes following the size exclusion chromatography. As such, efficient cleavage to yield retrievable amount of free target protein from the monomeric fusion protein could not be performed. This can be further improved by optimising the conditions such as changing to the S100 HR column and reducing the flow rate to 0.8 ml/min in the size exclusion chromatography.

5.6 Closing and recommendation

In general, the purification of the hBD9 pro-peptide in this project has not been very successful as it did not reach the end of the planned expression strategy to purify the free hBD9 propeptide. The first part of the purification which was the IMAC worked well with protein recovery of about 80% highly pure fusion protein. The subsequent purification step which was the PD10 desalting worked well too with recovery of approximately 70%. Although the proteolysis using rEK cleavage worked under given reaction conditions, the amount cleaved was too small, and recovery of the free hBD9 pro-peptide has not been successful in the subsequent cation exchange chromatography. The size exclusion chromatography to separate the oligomeric from the monomeric fusion protein needs refinement too. Because of failures at these stages, the free hBD9 could not be purified from the cleavage reaction mixture.

A better recombinant system which is easier to manage in terms of expression, proteolysis and subsequent purification should be adopted based on the inadequacy of this project. The optimum utilisation of the computerised FPLC system should be made available from the start as effective purification will depend very much on parameters indicated on this machine such as the UV, pH and buffer percentage which can be incorporated with computerised software analysis into the FPLC machine.

Collaboration with researchers from the molecular medicine department who are familiar with peptide purification shall enhance the success of the free hBD9 purification.

Chapter 6

Antimicrobial property of hBD9

CHAPTER 6: Antimicrobial property of hBD9

6.1 Introduction

The designation of hBD9 into the β-defensin family has led to the presumption of an antimicrobial role for this peptide. This presumption was further enhanced by the demonstration of antimicrobial effect of many tested β-defensin family members thus far including the hBD1-3 [280], hBD4 [88, 180], hBD5-6 [253, 281], hBD19, -23, hBD27-28 [282] and hBD29 [283] although their efficacy against different organisms was variable. To date, there has been no report describing the antimicrobial property of the hBD9 peptide. Nevertheless, a few studies have attempted to correlate its expression at the mRNA level with disease process including infection [284].

6.1.1 Historical perspective

The first mammalian β-defensin was isolated from bovine tongue (tracheal antimicrobial peptide, TAP) [106]. Following this discovery, 13 other β-defensins were purified from bovine neutrophils. The three-dimensional structure including the disulfide array of one β-defensin has been successfully characterised [107].

The first human β-defensin, human β-defensin-1 (hBD-1), was originally purified from the plasma of renal dialysis patients in 1995 [285], and was later discovered in the male urinary tract as gram-negative bacteria-killing natural antibiotic. It was also shown to be detectable in the female reproductive tract [108]. The mRNA of hBD1 was constitutively expressed in various epithelia [109]. The second human beta defensin, human β-defensin-2 (hBD2), was discovered in the extract of psoriatic scales [108, 109]. hBD2

was expressed in inflamed skin and lung and was induced in epithelial cells upon treatment with TNFα, IL-1β and contact with *Pseudomonas aeruginosa*.

The hBD3 was first isolated from the scales of psoriatic lesions in 2001 by Harder *et al* [97, 286]. The hBD4 was first reported at almost the same time as hBD3 by Garcia *et al* [98, 180]. The hBD5 and -6 were first reported from the computerised human genome analysis [281].

6.1.2 Post-translational processing of β-defensins

The human α-defensins are secreted in the proform into the granules. In the mice, matrilysin, which cleaves the cryptdin proprotein, digests the pro-piece to form functional mature defensins. In humans, trypsin stored in the granule of the Paneth cells is the processing enzyme which cleaves the mature HD-5 from the pro-piece [287]. The function of the pro-piece is to protect the host cells from the toxic effect of the mature peptide. However, there are conflicting reports with regard to the pro-protein. Insect proHD-5 was reported to possess antibacterial activity against *Listeria monocytogenes* but not against *Salmonella typhimurium*. A recent report failed to show activity in chemically synthesised proHD-5 against *E. coli* or *Staphylococcus aureus* [288].

In contrast to the α-defensin, the pro-pieces of the β-defensins are relatively short. The suspected pro-piece of the hBD3 was reduced to only a single glycine residue. It is believed that the pro-piece in β-defensin does not function to negate the effect of mature protein and therefore the pro-peptide of β-defensin has the antimicrobial effect [288].

The currently available data on defensin post-translation processing was based solely on the experiment for α-defensins. The only β-defensin

which had been clearly cleaved was the hBD-1. The hBD-1 has many isoforms which resulted mainly from the truncation at the amino terminal of the peptide. Nevertheless, there was also at least one hBD1 isoform which was produced as a result of the carboxy terminal removal of the lysine residue.

Premratanachai *et al* conducted a study on *DEFB4* and 10 other novel β-defensin gene (DEFB105-114) expression in gingival keratinocytes [289]. They found three defensin genes were constitutively expressed, four were inducible and another three were not expressed in the gingival keratinocytes. *DEFB109* mRNA was reported to be constitutively expressed in gingival keratinocytes. They also noted that *DEFB109* mRNA expression in the gingival keratinocytes was down regulated in the presence of *Candida albicans* infection [188]. They had postulated that this phenomenon occurred as part of the host-pathogen interaction to allow *Candida albicans* to become an oral commensal. However, no protein work to confirm this has been reported to date.

Abedin *et al* conducted research on ocular surface defensin and noted that hBD9 was constitutively expressed on the ocular surface tissue but further added that the hBD9 was down-regulated in all eyes with surface infection and inflammation. They postulated that this may either be the cause or the effect of infection. They suggested hBD9, because it was down-regulated in infection, may play an insignificant role in host defence [187]. The down-regulation phenomena was also reported by Islam *et al* [189]. LL37 and hBD1 expression was down-regulated by shigellosis from the lower

gut epithelial cells. This has been hypothesised to be a case of immune escape strategy in order for the *Shigella* to invade the gut mucosa.

Host defence peptides showed great variance of effects and interactions. The major function of HDP is to inactivate the invading microbes which included bacteria, fungi, parasites and viruses through direct effects on their membranes. HDP has the ability to specifically attack external targets simultaneously such as the cytoplasmic membrane of bacteria, by building perturbing peptides and attacking internal targets by invading the bacterial cell wall and permitting passage of molecules into the cells. Human β-defensins also promote histamine release and prostaglandin-2 production in mast cells [189]. They play important roles in connecting the innate and adaptive immune system by chemo attraction of immature dendritic cells and T-lymphocytes [145, 146], and increase the expression of TNF-α and IL-1 in human monocytes following activation by bacterial stimulus [47].

Several studies have demonstrated the efficacy of various β-defensins against different organisms including the resistant strains. Sahly *et al* examined the antimicrobial effect of hBD2 and hBD3 against extended spectrum β-lactamase (ESBL) produced by *Klebsiella* strains. Both hBD2 and hBD3 were reported to be efficacious against almost all of the ESBL-producing strains with lethal dose (LD) and MBC of less than 12.5 mg/L, making them potential antibiotic candidates against the *Klebsiella* infections [290].

6.1.3 Factors affecting the antimicrobial property of the hBD9

Structural aspect of β-defensins that have been studied in the past included the disulphide connectivity, amino acid exchange, peptide length,

charge or ionicity and hydrophobicity. These factors were correlated mainly to the antimicrobial function and extended to the cytotoxicity or chemotactic activity of the β-defensins.

6.1.3.1 Conserved cysteine residues

The low degree of sequence homology between members of mammalian β-defensins apart from the six highly conserved cysteine residues and two relatively conserved glycine residues, has raised the question whether the hallmark antimicrobial property of the β-defensins depends on these conserved cysteines. A few studies showed that this feature was not critical for antimicrobial activity. Wu *et al* [291] had demonstrated that the disulphide bonds were not necessary in the antimicrobial effect of the beta defensins. In addition to this claim, it was reported that short segments derived from hBD1 and hBD3 had potent antimicrobial property [292].

The current understanding generally accepts that the presence and distribution of cysteines, and thus the formation of disulphide bonds between the six conserved cysteines, are not crucial for the antimicrobial property of the β-defensins. This claim was supported by a study on bovine β-defensin 2 (BNBD2) and -12 (BNBD12) against common gram positive and gram negative organisms. The antimicrobial property of these peptides was conferred by the hydrophobic C-terminal part of the protein which had the characteristic form of β-hairpin structure [292-295]. Shorter defensin C-terminal analogues have also been shown to improve antimicrobial activities with minimal cytotoxicity. C-terminal analogues of hBD3 were amplified and

their tertiary structures and interactions with membrane lipids were studied. Ability to dimerise enables the protein to increase surface positive charge density. Formation of specific structure with highest density of positive charges leads to a more potent bactericidal activity.

The presence and the distribution of the conserved cysteine residues were more important for the folding and general structural property of the molecule [296, 297] and for the receptor dependant chemotaxis property [298].

6.1.3.2 Amphipathicity

Amphipathicity is the extent of separation between the hydrophobic cluster and polar residues. It is another important feature of HDPs and influences the antimicrobial activity and toxicity of the peptides. By being amphipathic, a peptide could bind and insert into the lipid bilayer and interact with hydrophobic acyl chains of the phospholipids, leading to permeabilisation of the membrane [299]. A study in margainin-2 peptide revealed that increasing the amphipathicity while keeping other factors constant resulted in increase of the bactericidal activity and the cytotoxicity alike [142].

6.1.3.3 Hydrophobicity

Hydrophobicity is the state of the molecule which repels water. A hydrophobic molecule does not have a charge, meaning it is non-polar. Hydrophobicity is an important factor for antimicrobial efficacy and target cell predilection [300]. Amphipathic peptides vary widely in terms of their hydrophobicity, and hydrophobicity itself was shown to have inverse

relationship with cell selectivity when the cationicity and amphipathicity were constants in magainin [301].

6.1.3.4 Salt concentration

The concentration of salt such as the NaCl and $MgCl_2$ had been reported to be influential on the activity of AMPs. Different defensins and their C-terminal analogues were shown to have reduced activity levels in the presence of high salt concentration [302]. In general, it was found that hBD1 [88, 303], -2 [108, 304] and -4 were salt-sensitive [97, 305] whereas hBD3 was salt insensitive [281].

Huang *et al* reported that hBD5 and -6 had salt-sensitivity profile similar to that of hBD2 and -4 [98, 306]. The antimicrobial effects of hBD5 and -6 were suppressed in the presence of NaCl concentration from 10 to 100 mM. In NaCl concentration above 100 mM, survival of *E. coli* reached almost 100% which indicated that the effect of hBD5 and -6 were almost completely inhibited [282]. The presence of salt such as NaCl and reducing agents such as DTT reduced the antimicrobial efficacy of hBD23 [282].

6.1.3.5 Monovalent and divalent cations

The presence of mono- and divalent cations such as K^+, Na^+, Ca^{2+} and Mg^{2+}, had also been implicated for the poor activity of the AMPs [284]. It was believed that these cations would compete with the AMPs for the negatively charged electrostatic binding sites on the bacterial surface. A study had shown that the reduction in the hBD2 antimicrobial activity was less affected by monovalent cations such as K^+ and Na^+ compared to the divalent cations

such as the Ca^{2+} and Mg^{2+}. In contrast, concentration of anions such as the Cl^- and the SO_4^{2-} had not affected the antimicrobial activity of hBD2 [98, 281].

6.1.3.6 Oligomerisation

Oligomerisation contributes to the quaternary structure of the β-defensins. The capacity to form oligomers, in addition to amphipathicity and hydrophobicity, is important in regulating the microbial activity of β-defensin [307]. hBD1 was shown to exist in a dimeric form while in crystalised state but not when in solution [142]. hBD2 also form oligomers and higher orders as much as an octameric form have been reported [144]. This finding of hBD2 propensity to form higher order oligomers, and the electrostatic property of hBD2, support the electrostatic-based mechanism rather than the lipid bilayer-spanning pore formation of antimicrobial action. HNP3 [143] and hBD3 [104] were also reported to exist in oligomeric forms.

Despite being first sequenced as early as 2002 [98, 308] and subsequently localised intracellularly in 2010 [222], the hBD9 peptide has never been reportedly isolated. This has contributed to our limited current knowledge with regard to the biological function of hBD9. This study is important to confirm the presumed antimicrobial effect of the hBD9. Nevertheless, because of failure in retrieving the free target peptide following rEK proteolysis step of the hBD9 purification, only the interim fusion protein was successfully purified and used for antimicrobial work in this research.

6.2 Objectives

The objectives of this study were:

a. To profile the efficacy of hBD9 fusion protein against *Staphylococcus aureus* and *Pseudomonas aeruginosa*.

b. To estimate the effective dose of hBD9 fusion protein to inhibit the growth of *Staphylococcus aureus* and *Pseudomonas aeruginosa*.

6.3 Methods

6.3.1 CFU count reduction method

The bacterial cultures were subjected to 10-fold serial dilution. 50 µl of each dilution were then inoculated onto the LB media plate and the plates were then incubated in the incubator at 37 ^{o}C overnight. On the following day, the plates were examined for growth and the number of colonies in each serial dilution was determined. The first dilution with countable colonies was chosen as the reference and the initial culture concentrations were calculated in term of its CFU/ml.

6.4 Results

6.4.1 CFU count

The CFU count was determined for each of the bacteria used in the antimicrobial assay experiment, namely the *Staphylococcus aureus* and the *Pseudomonas aeruginosa*.

6.4.1.1 Staphylococcus aureus

Staphylococcus aureus was chosen as the representative for gram positive organisms. It is a common causative factor for several human

infections such as lung abscess [231] and diabetic foot ulcer [309]. The first experiment did not show any countable colonies in any serial dilution. This indicated that the initial bacterial concentration was too high (Figure 6.4.1).

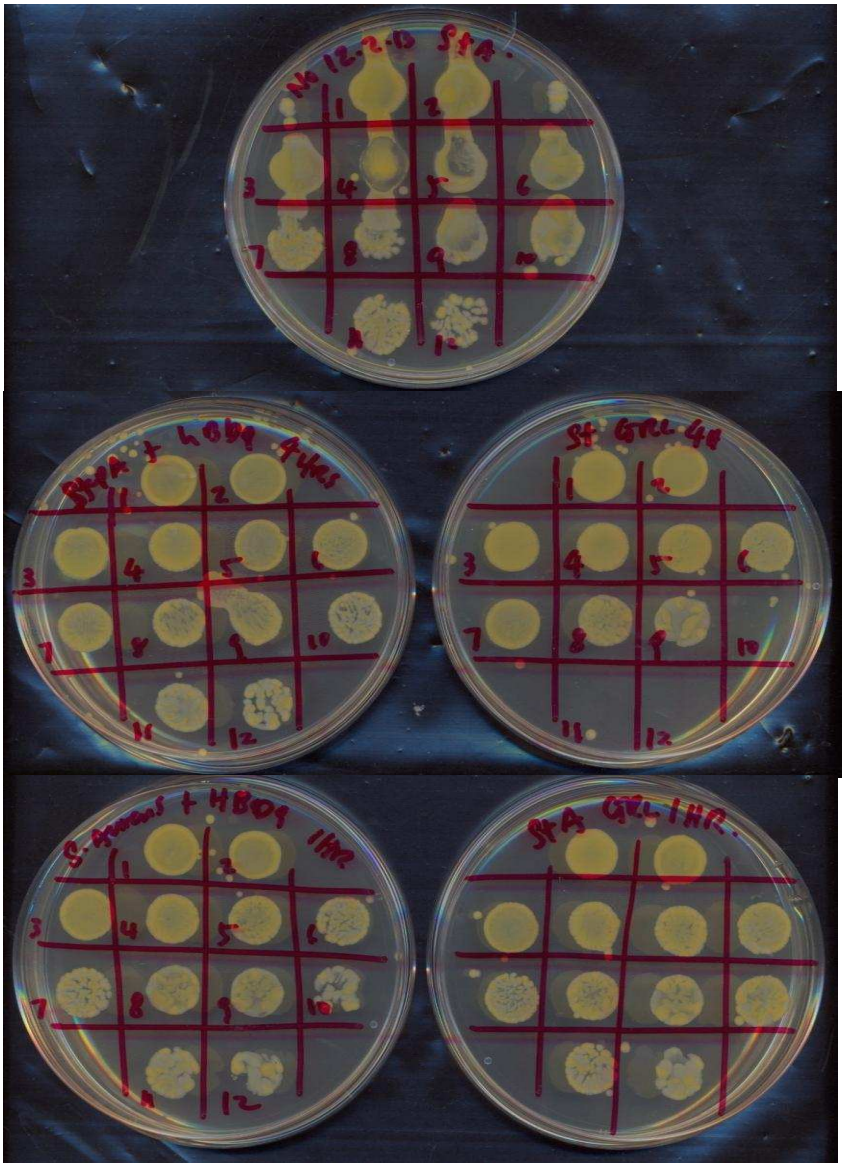

Figure 6.4.1 Photograph of culture plates comparing hBD9-treated *Staphylococcus aureus* against untreated control at 0, 2 and 4 hours time points showed no countable colony as the bacteria were confluent.

6.4.1.2 *Pseudomonas aeruginosa*

Pseudomonas aeruginosa represents the gram negative bacteria, often causing severe keratitis [310]. The wild strain of the organism, retrieved from the patients' specimens was used in this experiment. As with the *Staphylococcus aureus* experiment, there were confluent colonies of *Pseudomonas aeruginosa* found in the culture plate representing all the

serial dilutions. The conclusion made was that the initial bacterial concentration (OD_{600} 0.65) was too high (Figure 6.4.2).

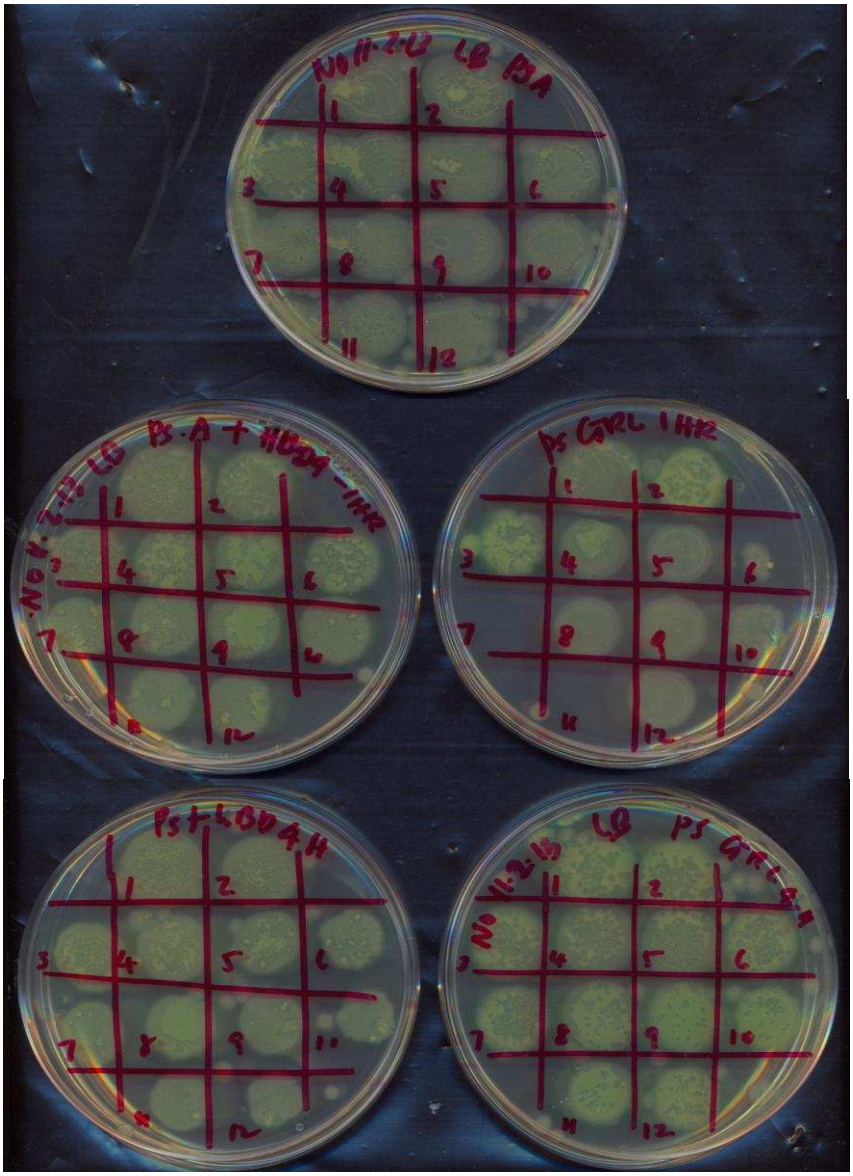

Figure 6.4.2 Photograph of culture plates comparing hBD9-treated *Pseudomonas aeruginosa* against untreated control at 0-, 2- and 4-hour time points showing no countable colony as the bacteria were confluent.

6.4.2 Repeat of CFU count

The repeat experiment for this purpose was carried out and the culture plates were examined. The initial culture spectrophotometry readings were

OD_{600} 0.07 and 0.08 for *Pseudomonas* and *Staphylococcus*, respectively. Serial 10-fold dilutions were carried out until the 12th dilution. 50 µl of each dilution was plated onto a culture plate and incubated at 37 ^{o}C overnight. The CFU counts were calculated from the findings of the culture. The OD_{600} 0.07 *Pseudomonas aeruginosa* contained 2.2 X 10^{14} CFU/ml and 0.08 *Staphylococcus aureus* contained 1.36 X 10^{9} CFU/ml (Figure 6.4.3).

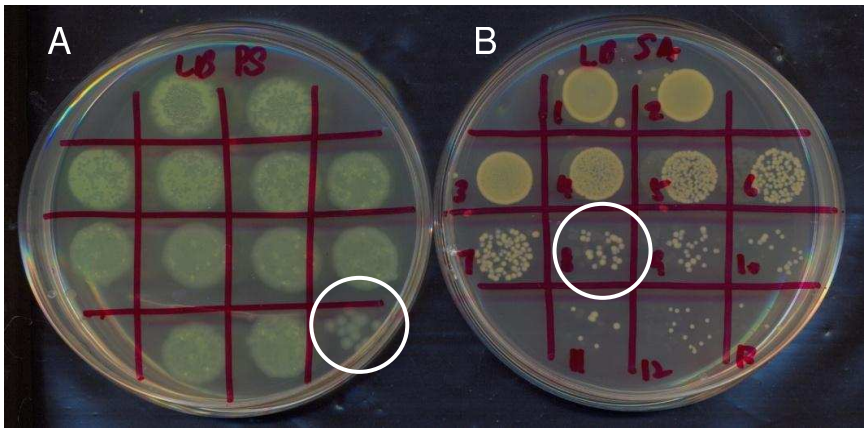

Figure 6.4.3 Colony forming unit (CFU) count to determine the concentrations of the bacterial cultures for *Pseudomonas aeruginosa* (A) and *Staphylococcus aureus* (B).

The CFU count for the *Pseudomonas aeruginosa* and *Staphylococcus aeruginosa* is summarised in Table 6.4.1.

Table 6.4.1 Colony forming unit per ml (CFU/ml) for *Pseudomonas aeruginosa* and *Staphylococcus aureus* at a given OD_{600}.

	OD_{600}	CFU count
Pseudomonas aeruginosa	0.07	2.20 X 10^{14} CFU/ml
Staphylococcus aureus	0.08	1.36 X 10^{9} CFU/ml

6.4.3 Incubation of bacteria with hBD9 fusion protein

Based on the CFU count result, approximately 1 X 10^6 of each bacterium was incubated with hBD9 at a final concentration of 100 µg/ml for 4 hours. 100 µl of reaction were collected at 0, 2 and 4 hour time points, and serially diluted 10-fold for 10 dilutions. 50 µl of each dilution were then plated onto LB plates for CFU determination. This was performed to investigate the incubation time required for hBD9 to exert its effect on the organisms.

6.4.3.1 CFU count at zero time point

The CFU count for the zero hour time point was set for the untreated and treated *Staphylococcus* and the *Pseudomonas*. This was performed to show that the concentration for both the treated and untreated samples were similar (Figure 6.4.4). The starting culture of *Staphylococcus aureus* contained 0.5 x 10^6 CFU/ml while *Pseudomonas aeruginosa* contained 1.4 x10^5 CFU/ml.

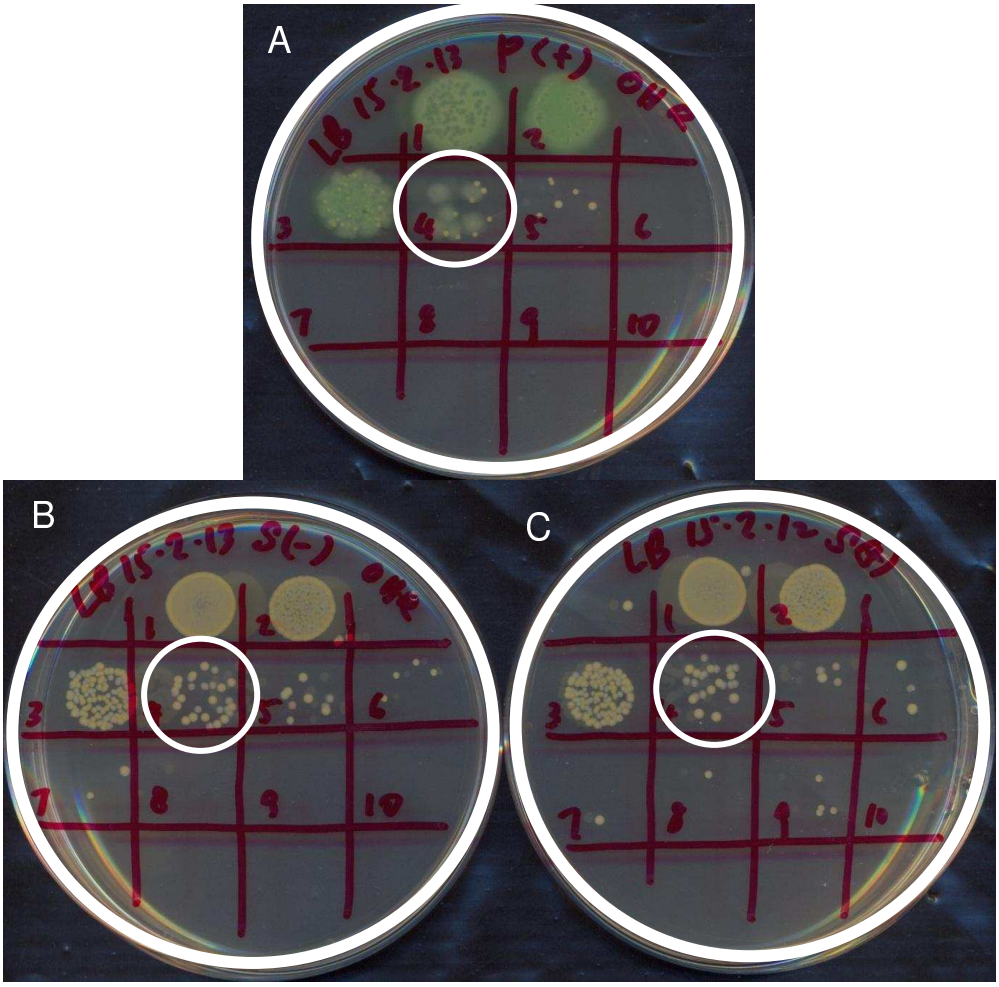

Figure 6.4.4 Photograph of culture plates showing CFU count in the untreated culture for *Pseudomonas aeruginosa* (A) and *Staphyloccus aureus* (B) and hBD9 treated *Staphylococcus aureus* (C).

6.4.3.2 CFU reduction at 2 hour time point

To investigate the effective incubation period for hBD9, the bacteria were exposed to the hBD9 for 2 hours and 4 hours.

6.4.3.2 (a) *Staphylococcus aureus*

After two hours incubation, there was a reduction in the CFU count in the hBD9-treated culture compared to the untreated control. The CFU/ml for *Staphylococcus aureus* was 2.8 x 10^7 in the treated culture compared to 3.6 x 10^{10} in the untreated control (Figure 6.4.5 A, B).

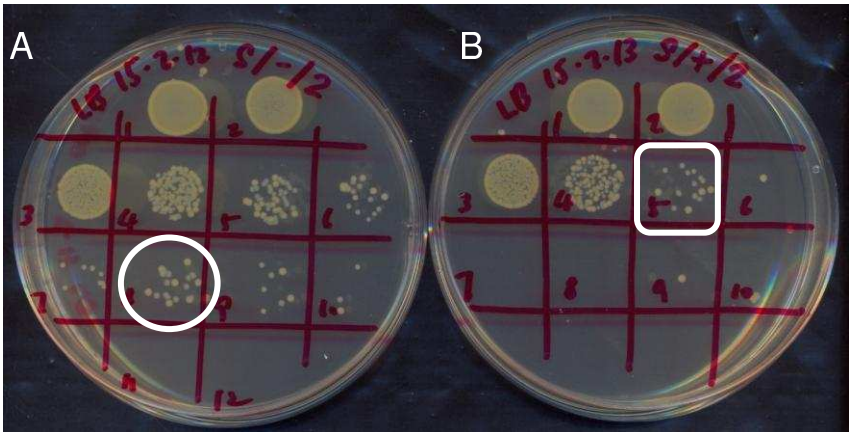

Figure 6.4.5 Photograph showing the colony formed in untreated control (A) and hBD9 treated *Staphylococcus aureus* after 2 hours of incubation.

6.4.3.2 (b) *Pseudomonas aeruginosa*

At two hour time point, *Pseudomonas aeruginosa* showed lower CFU count in the treated samples compared to the untreated sample. The CFU/ml was 3.6×10^7 in the treated culture against 2.0×10^{10} in the untreated control (Figure 6.4.6).

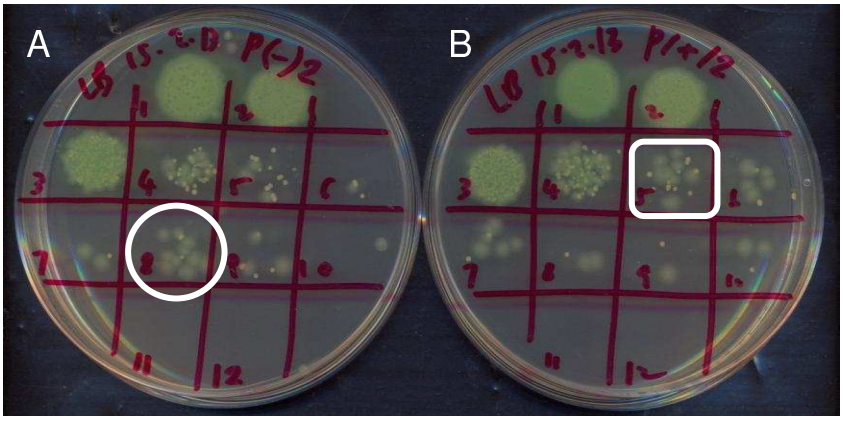

Figure 6.4.6 Photograph of the culture plates showing the CFU reduction in the untreated control (A) and the hBD9-treated (B) *Pseudomonas aeruginosa* at 2 hour time point.

6.4.3.3 CFU count at 4 hour time point

At 4 hours, both the *Pseudomonas aeruginosa* and *Staphylococcus aureus* grew to a similar concentration in the treated and untreated culture, preventing the determination of CFU count, and the difference between the treated and untreated control was obscured (Figure 6.4.7). The hBD9 fusion protein concentration was probably too low to have a sustainable effect on the bacterial growth over four hour period of incubation.

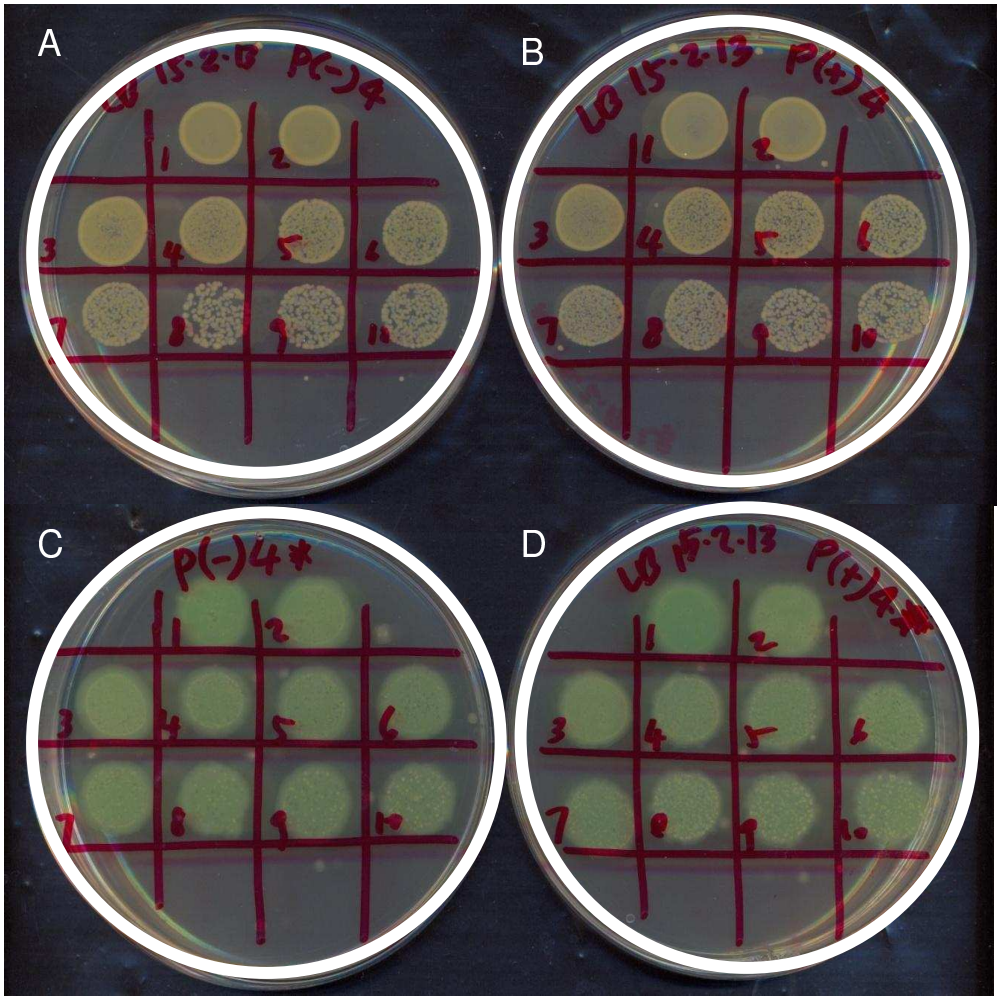

Figure 6.4.7 Photograph of the culture plates for untreated control (A) and hBD9 treated (B) *Staphylococcus aureus* and untreated control (C) and hBD9 treated *Pseudomonas aeruginosa* at four hour incubation. The plates show that there was no difference between treated and untreated *Staphylococcus aureus* or *Pseudomonas aeruginosa* after four hours of incubation.

The result of the CFU count reduction for both the bacteria in the untreated control and the hBD9 treated groups over the various time points is summarised in Table 6.4.2.

Table 6.4.2 Table showing the CFU/ml for the untreated controls and hBD9-treated organisms at variable time points. There was a reduction in the treated sample compared untreated controls for *Staphylococcus aureus* and *Pseudomonas aeruginosa* after two hours incubation.

	Colony forming unit per ml, CFU/ml			
	Staphylococcus aureus		***Pseudomonas aeruginosa***	
Incubation	Control	hBD9-treated	Control	hBD9-treated
0 hour	0.5×10^6	0.5×10^6	1.4×10^5	-
2 hour	3.6×10^{10}	2.8×10^7	2.0×10^{10}	3.6×10^7
4 hour	Undetermined	Undetermined	Undetermined	Undetermined

6.4.4 Susceptibility estimation

In this experiment we estimated the concentration of bacteria which would be susceptible to different concentrations of hBD9 fusion protein. The bacteria of were 10-fold serially diluted and each dilution was incubated with two different final concentrations of hBD9 fusion protein, in two independent experiments. After 2-hour incubation, 50 µl of each dilution were plated onto LB culture media and incubated overnight at 37 ^{o}C. The reduction in CFU counts were compared with the untreated control. For incubation with hBD9 fusion concentration of 71 ug/ml for 2 hours, growth inhibition was seen when the bacteria were diluted by 5 10-fold dilutions or more, for both *Pseudomonas aeruginosa* (Figure 6.4.8 A, B) and *Staphylococcus aureus* (Figure 6.4.8 C, D).

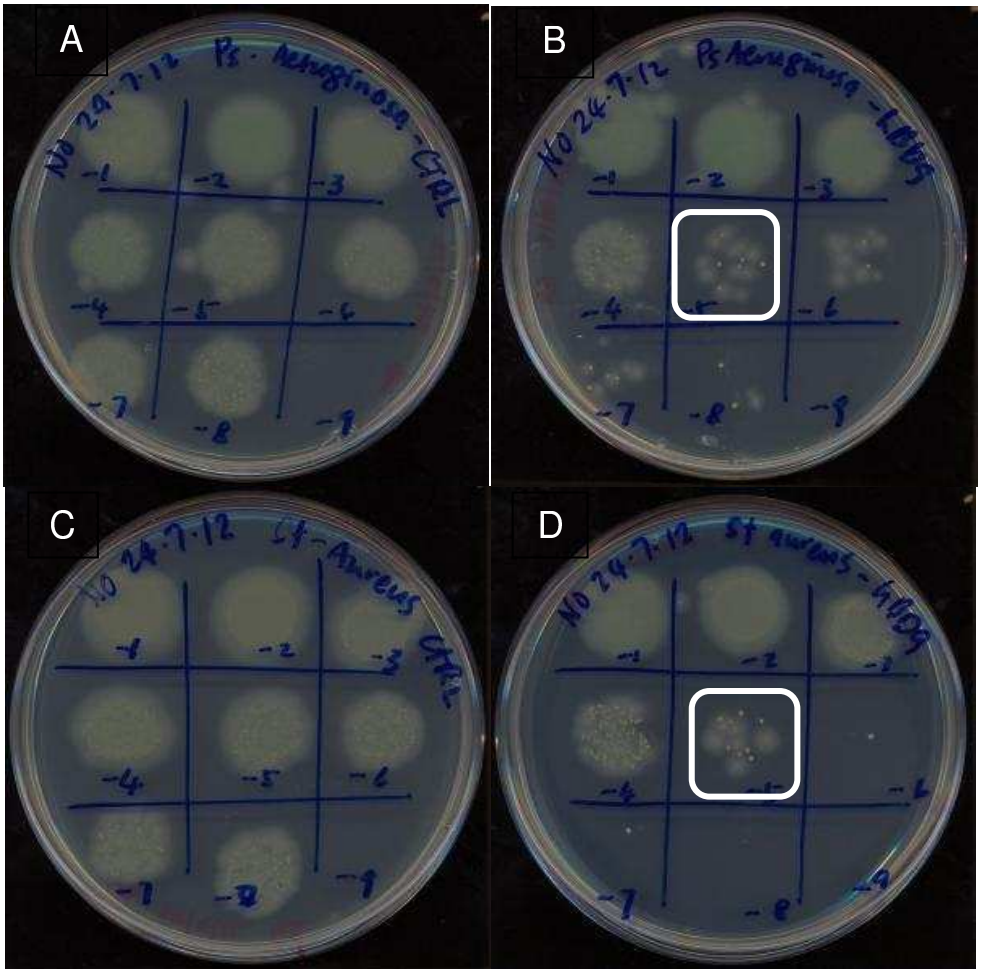

Figure 6.4.8 Photograph of the culture plates of colony forming unit (CFU) for the *Staphylococcus aureus* and *Pseudomonas aeruginosa*. (A), untreated *Pseudomonas aeruginosa* control; (B), hBD9-treated *Pseudomonas aeruginosa*; (C), untreated *Staphylococcus aureus* control; (D), hBD9-treated *Staphylococcus aureus*.

In line with the above finding, incubation with hBD9 fusion protein concentration of 38 ug/ml for 2 hours, showed growth inhibition when *Staphylococcus aureus* was diluted by 7 10-fold dilutions or more (Figure 6.4.9 A, C). As the concentration in this experiment was lower than that in the previous experiment, the inhibition observed was relatively less too. However, the hBD9 fusion protein concentration of 38 ug/ml seemed to be too low to show any inhibition in *Pseudomonas aeruginosa* (Figure 6.4.9 B, D).

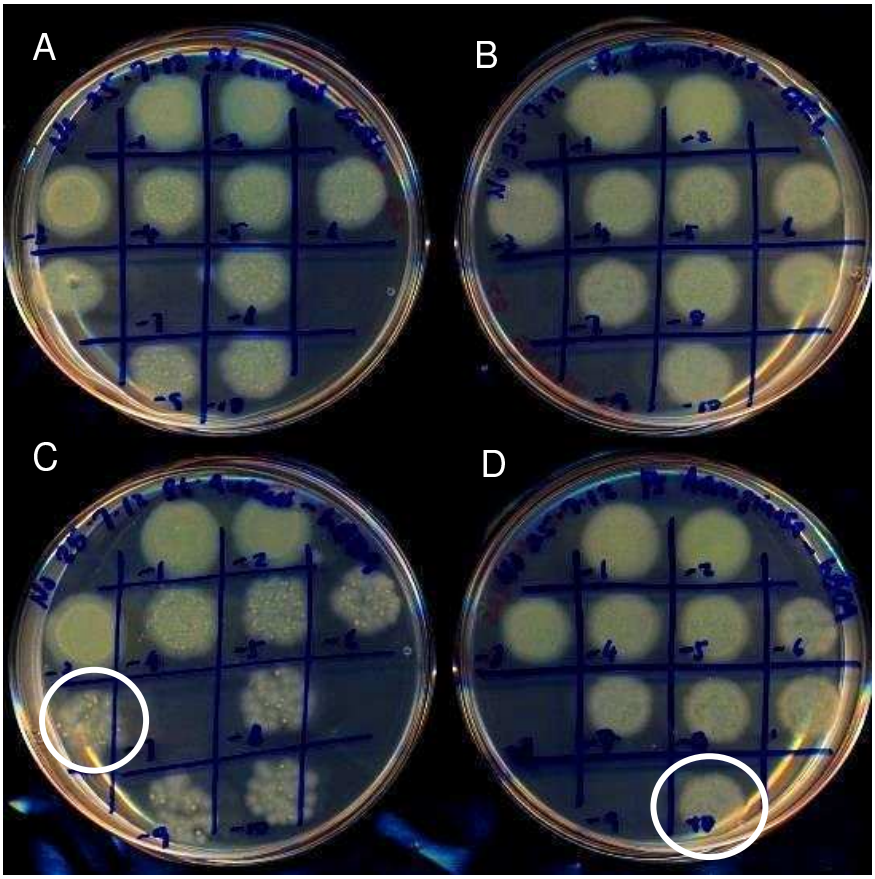

Figure 6.4.9. Photograph showing the culture plate of colony forming unit (CFU) for the hBD9 treated (A) and untreated control (B) of *Pseudomonas aeruginosa* and hBD9 treated (C) and untreated control (D) *Staphylococcus aureus*. The CFU reduced more markedly in the *Staphylococcus aureus* than in the *Pseudomonas aeruginosa*.

6.5 Discussion

The purified fusion protein in this study contained the hBD9 pro-peptide linked by a peptide linker to thioredoxin tag (Trx tag) which is a 109 amino acid peptide with a molecular weight of approximately 12 kD. Thioredoxins are ubiquitous proteins found in nearly all known organisms including the plants, prokaryotic and eukaryotic animals, and are essential for life in mammals [311]. They are oxidoreductase enzymes containing a dithiol-disulfide active site and act as antioxidants by facilitating the reduction of other proteins by cysteine thiol-disulfide exchange. This would catalyse the

reduction of the disulphide bonds and thus prevent the formation of the disulphide bonds.

Multiple *in vitro* substrates for thioredoxin have been identified, including ribonuclease, choriogonadotropins, coagulation factors, glucocorticoid receptor, and insulin. The mammalian thioredoxins are a family of small redox proteins that undergo NADPH-dependent reduction by thioredoxin reductase and in turn reduce oxidized cysteine groups on proteins [312]. The two main thioredoxins are thioredoxin-1, a cytosolic and nuclear form, and thioredoxin-2, a mitochondrial form. Thioredoxin-1 performs many biological actions including the supply of reducing equivalents to thioredoxin peroxidases and ribonucleotide reductase, the regulation of transcription factor activity, and the regulation of enzyme activity by heterodimer formation. Thioredoxin-1 stimulates cell growth and is an inhibitor of apoptosis [313].

Thioredoxin has a characteristic amino acid sequence due to the presence of two close-by cysteines, in a CXXC motif. Precisely, this is a canonical Cys-Gly-Pro-Cys (CGPC) catalytic motif. The two cysteines are the key to the ability of thioredoxin to reduce other proteins [314]. Thioredoxin proteins also have a characteristic tertiary structure termed the thioredoxin fold. The benefit of thioredoxin to reduce oxidative stress was demonstrated in transgenic mice that overexpress thioredoxin. It was reported that they became more resistant to inflammation, and live 35% longer than the non-transgenic mice [315].

In addition to the above finding, it was also reported in a study by Wu *et al* that the Trx tag in a control reaction did not have similar antimicrobial

effect compared to the Trx-BNBD12 fusion protein against gram positive and gram negative bacteria. Therefore, they concluded that the antimicrobial effect had resulted only from the hBD9 and not the Trx tag [316]. Based on these arguments, it is believed that any antimicrobial effect relating to Trx-hBD9 fusion protein is attributable to the hBD9 component.

Ideally, the antimicrobial assay for any molecule of interest should be conducted in three independent experiments in triplicate. This was not the case in this study. For all experiments involving antimicrobial assays, it is very important in that the starting amount of bacteria be standardised. From our preliminary experiment, the culture at mid logarithmic phase and diluted to with OD_{600} 0.07 and 0.08 for *Pseudomonas* and *Staphylococcus*, contained different CFU count (Figure 6.4.3). This suggests that the cultures with the above OD_{600} need to be diluted by 3 10-fold dilutions for *Staphylococcus aureus* and by 8 10-fold dilutions for *Pseudomonas aeruginosa*, in order to get an estimated concentration of 10^6 CFU/ml.

In this experiment the starting bacteria concentration was set to about 10^6 CFU/ml by using the spectrophotometer reading of the starting culture followed by the serial broth dilution culture. This concentration of bacteria was also used by several authors in their study in determining the antimicrobial property of the β-defensin [317].

The hBD9 fusion protein at 100 µg/ml final concentration showed efficacy against both the *Staphylococcus aureus* and *Pseudomonas aeruginosa* after 2 hours incubation. There was a 3 10-fold reduction in the CFU count in the hBD9 treated samples compared to the untreated controls for both *Staphylococcus aureus* and *Pseudomonas aeruginosa*. However,

this efficacy was not sustained over 4 hour incubation probably due to overwhelming bacterial load. Despite the initial inhibition of growth at 2 hour time point, the remaining bacteria outgrew the available hBD9 fusion protein toward the 4 hour time point. This could explain the lack of difference between the treated and untreated culture plates for *Staphylococcus aureus* and *Pseudomonas aeruginosa* at 4 hour time points.

Based on our findings in the CFU count reduction experiment (Result 6.4.3.2), we concluded that the fusion peptide was equally effective against the *Staphylococcus aureus* and *Pseudomonas aeruginosa*. The fusion protein had a nett positive charge of six. This was important to the binding of the protein to the bacterial lipid bilayer cell wall. The free target protein would have a nett positive charge of two. This finding was different to that reported by Huang et al [245, 253, 282]. They tested the antimicrobial effect of HBD5 and -6 in *Escherichia coli* K12 and *Staphylococcus aureus*. Against the *E. coli*, hBD6 was more efficacious than the hBD5. However, both hBD5 and -6 did not show any inhibitory effect on the growth of *Staphylococcus aureus* [282].

Our bacterial susceptibility test suggested that at least for a concentration of 77 µg/ml hBD9, the highest concentration of bacteria found susceptible was 5 10-fold dilutions from the initial OD_{600} 0.1 (Result 6.4.4). For final concentration of hBD9 fusion protein of 38 µg/ml, the highest concentration of bacteria showing reduction in CFU was found at 7 10-fold dilutions from the initial concentration with OD_{600} of 0.1 (Result 6.4.4). This indicated that there was a positive relationship between hBD9 fusion protein dose and its antimicrobial effect.

The quaternary structure of peptide may affect the antimicrobial potency of the peptide. In our research, we were not successful in separating the monomeric from the oligomeric forms of the fusion protein, and therefore our fusion protein comprised different oligomeric molecules. The effects of oligomerisation in hBD2 defensin homologues in various mammals were investigated by Verma *et al* [282]. The fact that some homologues existed in monomers in certain organisms while dimerised in others supported the suggestion that effective form of defensins may vary between the organisms involved. The quaternary structures of the AMPs play important roles in the bactericidal activity. HBD1 dimerised via symmetrical salt bridges between the molecules giving rise to a sickle shape structure with hydrophobic surface in the crystal form, but not in solution form. In contrast, hBD2 dimerised to form six-stranded β-sheets in the crystal form [318]. Meanwhile, the hBD3 forms stable dimers or oligomers in solution form [144]. This could explain why hBD3 exerts antimicrobial activity at physiological salt concentration [308].

It has been shown that the antimicrobial effect of hBDs was correlated with the concentration used. In our study, the higher concentration of the fusion protein resulted in more significant inhibition of the bacterial growth for both the *Staphylococcus aureus* and the *Pseudomonas aeruginosa*. hBD19 was reported to have antimicrobial activity against *Escherichia coli* and *Staphylococcus aureus* but little effect on *Pseudomonas aeruginosa*. At 100 µg/ml of hBD19, the number of colonies was reduced by 134-fold for *Escherichia coli* and 20-fold in *Staphylococcus aureus* but less than 10-fold in *Pseudomonas aeruginosa* [98]. Against *Mycoplasma pneumoniae*, hBD2

at concentration of 4 µM reduced the number of colonies by 100- to 1000-fold, compared to the control. hBD3 showed highest efficacy followed by the hBD2 while hBD1 showed the least efficacy in comparison to hBD2 and hBD3 [284]. Kuwano *et al* examined and reported on the efficacy of the human β-defensins on *Mycoplasma pneumoniae* which causes lower respiratory tract infection. Both hBD2 and -3 showed antimicrobial activities against *Mycoplasma pneumoniae* compared to hBD1 which showed minimal antimicrobial activity against this organism. They also described that in cultured pulmonary squamous cell line EBC-1 stimulated with IL-1β and *Mycoplasma pneumoniae*, hBD2 was upregulated but hBD1 and -3 were not upregulated [319].

Veldhuizen *et al* reported on the porcine β-defensin 2 (pBD2), the homolog of hBD1, against pathogenic intestinal pathogen including the *Staphylococcus aureus*, *Clostridium perfringens*, *Escherichia coli*, *Pseudomonas aeruginosa*, *Yersinia enterocolitica*, *Listeria monocytogenes*, *Erysipelothrix rhusiopathiae* and *Salmonella typhimurium*. The most susceptible organisms were *Listeria monocytogenes*, *Erysipelothrix rhusiopathiae* and *Salmonella typhimurium* whose survivals were reduced to below 100 CFU/ml at the pBD2 concentration of 16 or 32 µg/ml. Higher concentrations of pBD2 of 64-128 µg/ml were required for the similar effect on *Staphylococcus aureus*, *Clostridium perfringens*, *Escherichia coli*, *Pseudomonas aeruginosa* and *Yersinia enterocolitica* [319].

Both hBD1 and hBD2 showed microbicidal activity predominantly against gram-negative bacteria like *Escherichia coli* and *Pseudomonas aeruginosa*. In a skin keratinocytes culture study, it has been shown that

there was an upregulation in the hBD1 and -2 mRNA expression after exposure to these microorganisms and to tumour necrosis factor alpha (TNF-α) [320]. hBD2 was also demonstrated to be highly potent against *Candida albicans*. It was concluded that hBD2 confers innate immune defence against *Candida albicans* and has promising potential as a future antimicotic agent.

Sahl *et al* reported on the antimicrobial property of the hBD3 against gram positive and gram negative organisms. They concluded the antimicrobial efficacy of the hBD3 was high and broad-spectrum, and more so against gram negative than against gram positive bacteria possibly due to different mechanisms of actions exerted on both the bacterial types [97] .

Li *et al* introduced the hBD3 gene into pET30a and transformed this recombinant plasmid DNA into BL21(DE3)pLysS *E. coli*. The fusion protein consisted of 30.9% of the total cellular protein. Both recombinant hBD3 fusion protein and recombinant hBD3 had similar potency as the native hBD3 in inhibiting growth of both gram positive bacteria *Staphylococcus aureus* and gram negative *Escherichia coli* in a dose-dependent manner [142].

6.6 Limitations

This experiment was less than ideal due to failure to successfully retrieve the free target peptide of hBD9 despite getting the rEK cleavage successfully performed. As the target peptide was small and the reaction volume was also small due to the low substrate to enzyme ratio, the free target peptide was not purified. However, antimicrobial experiments were performed in order to get some understanding of the antimicrobial property of hBD9 propeptide.

When using the propeptide attached to the fusion partner in the antimicrobial assay, the effect of thioredoxin, if any, needs to be ruled out. For the purpose of objectively ruling out the influence of the fusion partner on the antimicrobial effect of hBD9 propeptide, the ideal control experiment would be using the purified and desalted translational product of pET32a(+) plasmid in the same expression host. The protein expressed by induction of the pET32a(+) is the protein J which has a molecular weight of 20.4 kD. It could be purified by using HisTag IMAC purification system. Upon desalting with PD10 buffer exchange chromatography, the purified peptide would contain the Trx tag along with several motifs. Unfortunately, this experiment was not included in this research because of plan to cleave and purify the target protein.

It was obvious in this project that the expressed hBD9 fusion protein existed in various quaternary forms in solution. The monomeric form was only approximately half of the total protein expressed. This high tendency to oligomerise may be attributed the amphipathicity of the hBD9 molecule. It is not certain if this effect could be due to the Trx fusion tag. Therefore, an appropriate purification strategy is to have these oligomeric forms separated before the monomers were subjected to cleavage, and thus allowing the hBD9 to be purified in its natural quaternary structure. This would enable us to confirm the propensity of the hBD9 to form oligomers in solution.

The CFU counts would best be conducted in multiple independent experiments and in triplicate. This would have allowed a statistical test to be performed. Following the CFU count determination and the susceptibility

estimation performed, a test to determine the MIC and the MBC would have been the best to do.

The salt sensitivity which has been proven to differ between various members of the hBDs was not addressed in this experiment. This was related mainly to the failure to purify the free propeptide. With a different expression strategy, a more efficient system may produce higher purified pro-protein in the future and pave the way for the complete antimicrobial pathway in the future.

Although ideally performed using the free target propeptide, the result shown using the hBD9 fusion protein is interesting. While it cannot be relied upon, it has some appeal to be further verified and validated in the future. Unless and until the free hBD9 peptide can be purified, the behaviour of this molecule in term of its propensity to form dimers and higher order oligomers in solution, and thus its functional properties could not be determined with high certainty.

A more effective fusion system is important in the recombinant expression of this protein. Although a fusion partner such as Trx tag important in the proper folding of this peptide, it must also not be detrimental to the cleavage step. This means the fusion partner must not have tendency to form oligomeric molecules that hide the proteolytic sites from the action of proteases and hinder the easy, efficient and economical cleavage.

Although the size of hBD9 peptide is small (65 amino acid residues), recombinant expression of this peptide in *E. coli* expression system is believed to be a better choice compared to chemical synthesis of this peptide. This is due to the high cost for chemical synthesis of adequate

amount of peptide and allowing proper folding of the over-expressed peptide in *E. coli* cytoplasmic compartment. Achieving these would enable various downstream experiments such as structural and physiological characterisation.

Reference

1. Akpek, E. and J.D. Gottsch, *Immune defense at the ocular surface.* Eye, 2003. **17**: p. 949-956.
2. Huang, L., Jean, D, Proske, RJ, Reins, RY, McDermott, AM., *Ocular surface expression and in vitro activity of antimicrobial peptide.* Curr. Eye Res., 2007. **32**(7-8): p. 595-609.
3. McDermott, A., *Defensins and Other Antimicrobial Peptides at the Ocular Surface.* Ocul. Surf., 2004 **2**(4): p. 229-247.
4. Oppenheim, J.J., et al., *Roles of antimicrobial peptides such as defensins in innate and adaptive immunity.* Ann. Rheum. Dis., 2003. **62**(suppl 2): p. ii17-ii21.
5. Mutwiri G, et al., *Innate immunity and new adjuvants.* Rev. Sci. Tech., 2007. **26**(1): p. 147-156.
6. Gordon, Y.J., E.G. Romanowski, and A.M. McDermott, *A review of antimicrobial reptides and their therapeutic potential as anti-infective drugs.* Curr. Eye Res., 2005. **30**(7): p. 505-515.
7. Knop, E. and N. Knop, *Anatomy and immunology of the ocular surface.* Chem. Immunol. Allergy, 2007. **92**: p. 36-49.
8. Forrester JV, et al., *Anatomy of the Eye and Orbit.*, in *The Eye: basic scienses in practise.* 1996, WB Saunders Company Ltd: London. p. 1-86.
9. Kobayashi, A., H. Yokogawa, and K. Sugiyama, *In Vivo Laser Confocal Microscopy of Bowman's Layer of the Cornea.* Ophthalmology, 2006. **113**(12): p. 2203-2208.
10. Reinstein DZ, A.T., Gobbe M, Silverman RH, Coleman DJ, , *Epithelial Thickness in the Normal Cornea: Three-dimensional Display With Very High Frequency Ultrasound.* J. Refract. Surg., 2008. **24**(6): p. 571-581.
11. Knupp, C., et al., *The Architecture of the Cornea and Structural Basis of Its Transparency*, in *Advances in Protein Chemistry and Structural Biology*, M. Alexander, Editor. 2009, Academic Press. p. 25-49.
12. Dua, H.S., et al., *Human Corneal Anatomy Redefined: A Novel Pre-Descemet's Layer (Dua's Layer).* Ophthalmology, 2013. **120**(9): p. 1778-1785.
13. Johnson, D.H., W.M. Bourne, and R.J. Campbell, *The Ultrastructure of Descemet's Membrane: I. Changes With Age in Normal Corneas.* Arch. Ophthalmol., 1982. **100**(12): p. 1942-1947.
14. Lesueur, L., et al., *Structural and Ultrastructural Changes in the Developmental Process of Premature Infants' and Children's Corneas.* Cornea, 1994. **13**(4): p. 331-338.
15. Price, N.C. and D.J. Barbour, *Corneal endothelial cell density in twins.* Br. J. Ophthalmol., 1981. **65**(12): p. 812-814.
16. Muller, A. and M.J. Doughty, *Assessments of Corneal Endothelial Cell Density in Growing Children and Its Relationship to Horizontal Corneal Diameter.* Optom. Vis. Sci., 2002. **79**(12): p. 762-770.
17. Hashemian, M., et al., *Corneal endothelial cell density and morphology in normal Iranian eyes.* BMC Ophthalmol, 2006. **6**(1): p. 9.
18. Van Buskirk, E., *The anatomy of the limbus.* Eye, 1989. **3**: p. 101-108.
19. Castro-Munozledo, F., *Review: corneal epithelial stem cells, their niche and wound healing.* Mol. Vis., 2013. **24**(19): p. 1600-1613.

20. Rene, C., *Update on orbital anatomy.* Eye, 2006. **20**(10): p. 1119-1129.
21. Ezra, D.G., M. Beaconsfield, and R. Collin, *Surgical anatomy of the upper eyelid: old controversies, new concepts.* Expert Rev Ophthalmol, 2009. **4**(1): p. 47-57.
22. VanderWerf, F., et al., *Eyelid Movements: Behavioral Studies of Blinking in Humans Under Different Stimulus Conditions.* J. Neurophysiol., 2003. **89**(5): p. 2784-2796.
23. Danjo Y, et al., *Alteration of Mucin in Human Conjunctival Epithelia in Dry Eye.* Invest. Ophthalmol. Vis. Sci., 1998. **39**: p. 2602-2609.
24. Goebbels, M., *Tear secretion and tear film function in insulin dependent diabetics.* Br. J. Ophthalmol., 2000. **84**(1): p. 19-21.
25. Khoury, N.J., et al., *Ductal Cysts of the Accessory Lacrimal Glands: CT Findings.* AJNR. Am. J. Neuroradiol., 1999. **20**(6): p. 1140-1142.
26. Zhang, X., et al., *Analysis of tear mucin and goblet cells in patients with conjunctivochalasis.* Spektrum der Augenheilkunde, 2010. **24**(4): p. 206-213.
27. Suzuki, T., A. Yamada, and M. Gilmore, *Host-pathogen interactions in the cornea.* Jpn. J. Ophthalmol., 2010. **54**(3): p. 191-193.
28. McCulley, J.P. and W.E. Shine, *The lipid layer of tears: dependent on meibomian gland function.* Exp. Eye Res., 2004. **78**(3): p. 361-365.
29. McCulley JP, S.W., *Meibomian gland function and the tear lipid layer.* Ocul Surf 2003. **1**(3): p. 97-106.
30. Dohlman, C.H., et al., *The glycoprotein (mucus) content of tears from normals and dry eye patients.* Exp. Eye Res., 1976. **22**(4): p. 359-365.
31. Saari, K.M., et al., *Group II PLA(2) content of tears in normal subjects.* Invest. Ophthalmol. Vis. Sci., 2001. **42**(2): p. 318-20.
32. Janeway CA, T.P., Walport M, et al., *Immunobiology: The Immune System in Health and Disease*. 5th edition. ed. 2001, New York: Garland Science.
33. Shiffman, M., *Vignettes of Medical History*. Int J Cosmetic Sur Aesthetic Dermatol, 2003. **5**(2): p. 213-214.
34. Heeg, K., *The Innate Immune System*, in *NeuroImmune Biology*, G.P.C. Adriana del Rey and O.B. Hugo, Editors. 2007, Elsevier. p. 87-99.
35. Medzhitov, R. and C.A. Janeway, *Innate immunity: impact on the adaptive immune response.* Curr. Opin. Immunol., 1997. **9**(1): p. 4-9.
36. Bals R, *Epithelial antimicrobial peptides in host defense against infection.* Resp Res, 2000. **1**: p. 141-150.
37. Gläser, R., J. Harder, and J.-M. Schröder, *Antimicrobial Peptides as First-Line Effector Molecules of the Human Innate Immune System*, in *Innate Immunity of Plants, Animals, and Humans*, H. Heine, Editor. 2008, Springer Berlin Heidelberg. p. 187-218.
38. Mackay, I.R., et al., *Innate Immunity.* N. Engl. J. Med., 2000. **343**(5): p. 338-344.
39. Fearon, D.T. and R.M. Locksley, *The instructive role of innate immunity in the acquired immune response.* Science, 1996. **272**(5258): p. 50-53.
40. Beutler, B., *Innate immunity: an overview.* Mol. Immunol., 2004. **40**(12): p. 845-859.
41. Janeway, C.A., Jr. and R. Medzhitov, *Innate immune recognition.* Annu. Rev. Immunol., 2002. **20**: p. 197-216.

42. Finlay, B.B. and R.E.W. Hancock, *Can innate immunity be enhanced to treat microbial infections?* Nat Rev Micro, 2004. **2**(6): p. 497-504.
43. Steinstraesser, L., et al., *Bioengineered Human Skin: Working the Bugs Out.* Mol Ther, 2009. **17**(3): p. 405-408.
44. Radek, K. and R. Gallo, *Antimicrobial peptides: natural effectors of the innate immune system.* Seminars in Immunopathology, 2007. **29**(1): p. 27-43.
45. Schröder, J.-M., R. Gläser, and J. Harder, *Antimicrobial peptides: Effector molecules of the cutaneous defense system.* International Congress Series, 2007. **1302**: p. 26-35.
46. Alberts B, J.A., Lewis J, et al., *Molecular Biology of the Cell.* 4th edition ed. 2002, New York: Garland Science.
47. Yang, D., et al., *Beta-defensins: linking innate and adaptive immunity through dendritic and T cell CCR6.* Science, 1999. **286**(5439): p. 525-528.
48. Ganz, T., *Defensins: antimicrobial peptides of vertebrates.* Comptes Rendus Biologies, 2004. **327**(6): p. 539-549.
49. Hancock, R.E. and L.R. I, *Cationic peptides: a new source of antibiotics.* Trends Biotechnol., 1998. **16**: p. 82-88.
50. Zasloff, M., *Antimicrobial peptides of multicellular organisms.* Nature, 2002. **415**(6870): p. 389-395.
51. Chertov, O., et al., *Identification of Defensin-1, Defensin-2, and CAP37/Azurocidin as T-cell Chemoattractant Proteins Released from Interleukin-8-stimulated Neutrophils.* J. Biol. Chem., 1996. **271**(6): p. 2935-2940.
52. Yang, D., et al., *Human neutrophil defensins selectively chemoattract naive T and immature dendritic cells.* J. Leukoc. Biol., 2000. **68**(1): p. 9-14.
53. Wang, Z. and G. Wang, *APD: the Antimicrobial Peptide Database.* Nucleic Acids Res, 2004. **32**(suppl 1): p. D590-D592.
54. Wang, G., *Tool developments for structure-function studies of host defense peptides.* Protein Pept. Lett., 2007. **14**(1): p. 57-69.
55. Wade, D. and J. Englund, *Synthetic antibiotic peptides database.* Protein Pept. Lett., 2002. **9**(1): p. 53-57.
56. Brahmachary, M., et al., *ANTIMIC: a database of antimicrobial sequences.* Nucleic Acids Res, 2004. **32**(suppl 1): p. D586-D589.
57. Seebah, S., et al., *Defensins knowledgebase: a manually curated database and information source focused on the defensins family of antimicrobial peptides.* Nucleic Acids Res, 2007. **35**(suppl 1): p. D265-D268.
58. Hammami, R., et al., *BACTIBASE: a new web-accessible database for bacteriocin characterization.* BMC Microbiol, 2007. **7**(1): p. 89.
59. Wang, G., X. Li, and Z. Wang, *APD2: the updated antimicrobial peptide database and its application in peptide design.* Nucleic Acids Res, 2009. **37**(suppl 1): p. D933-D937.
60. Jalian, H.R. and J. Kim, *Antimicrobial Peptides*, in *Clinical and Basic Immunodermatology*, A.A. Gaspari and S.K. Tyring, Editors. 2008, Springer London. p. 131-145.
61. Schroder, J.M. and J. Harder, *Antimicrobial skin peptides and proteins.* Cell Moll Life Sci, 2006. **63**(4): p. 469-86.

62. Royet, J. and R. Dziarski, *Peptidoglycan recognition proteins: pleiotropic sensors and effectors of antimicrobial defences.* Nat Rev Micro, 2007. **5**(4): p. 264-277.
63. Cash, H.L., et al., *Symbiotic Bacteria Direct Expression of an Intestinal Bactericidal Lectin.* Science, 2006. **313**(5790): p. 1126-1130.
64. Courselaud, B., et al., *C/EBPα Regulates Hepatic Transcription of Hepcidin, an Antimicrobial Peptide and Regulator of Iron Metabolism.* J. Biol. Chem., 2002. **277**(43): p. 41163-41170.
65. Hancock, R.E.W. and H.-G. Sahl, *Antimicrobial and host-defense peptides as new anti-infective therapeutic strategies.* Nat. Biotech., 2006. **24**(12): p. 1551-1557.
66. Hancock, R.E., *Peptide antibiotics.* Lancet, 1997. **349**: p. 418-442.
67. Andreu, D. and L. Rivas, *Animal antimicrobial peptides: An overview.* Biopolymers, 1998. **47**: p. 415-433.
68. van't Hof, W., et al., *Antimicrobial peptides: Properties and applicability.* J. Biol. Chem., 2001. **382**: p. 597-619.
69. Koczulla, A.R. and R. Bals, *Antimicrobial peptides: Current status and therapeutic potentials.* Drugs, 2003. **63**: p. 389-406.
70. Lehrer, R.I. and T. Ganz, *Defensins: Endogenous Antibiotic Peptides from Human Leukocytes*. Ciba Foundation Symposium 171 - Secondary Metabolites: their Function and Evolution. 2007: John Wiley & Sons, Ltd. 276-304.
71. Semple CA, G.P., Taylor K, Dorin JR., *The changing of the guard: Molecular diversity and rapid evolution of beta-defensins.* Mol Divers., 2006. **10**(4): p. 575-84.
72. Thomma, B.P., B.P. Cammue, and K. Thevissen, *Plant defensins.* Planta. **216(2)**: p. 193-202.
73. Aerts, A.M., et al., *The antifungal activity of RsAFP2, a plant defensin from raphanus sativus, involves the induction of reactive oxygen species in Candida albicans.* J Mol Microbiol Biotechnol, 2007. **13**(4): p. 243-247.
74. Lay, F.T. and M.A. Anderson, *Defensins--components of the innate immune system in plants.* Curr Protein Pept Sci, 2005. **6**(1): p. 85-101.
75. Hoffman J A, H.C., *Insect defensins: inducible antibacterial peptide.* Immunol. Today, 1992. **13**: p. 411-415.
76. Thevissen, K., et al., *Defensins from Insects and Plants Interact with Fungal Glucosylceramides.* J. Biol. Chem., 2004. **279**(6): p. 3900-3905.
77. Tincu, J.A. and S.W. Taylor, *Antimicrobial Peptides from Marine Invertebrates.* Antimicrob. Agents Chemother., 2004. **48**(10): p. 3645-3654.
78. Rodriguez de la Vega, R.C. and L.D. Possani, *On the evolution of invertebrate defensins.* Trends Genet., 2005. **21**(6): p. 330-332.
79. Hetru, C. and P. Bulet, *Strategies for the isolation and characterization of antimicrobial peptides of invertebrates.* Methods Mol. Biol., 1997. **78**: p. 35-49.
80. Lehrer, R.I. and T. Ganz, *Defensins of vertebrate animals.* Curr. Opin. Immunol., 2002. **14**(1): p. 96-102.
81. Ganz, T., *Defensins: antimicrobial peptides of innate immunity.* Nat Rev Immunol, 2003. **3**: p. 710 - 720.

82. Steinstraesser, L., et al., *Host defense peptides in burns.* Burns, 2004. **30**(7): p. 619-627.
83. Epand, R.M. and H.J. Vogel, *Biochem Biophys Acta.* Acta, 1999. **1462**: p. 11-28.
84. Lehrer, R.I., T. Ganz, and M.E. Selsted, *Defensins: endogenous antibiotic peptide of animal cells.* Cell, 1991. **64**: p. 229-30.
85. White, S.H., W.C. Wimly, and M.E. Selsted, *Structure, function and membrane integration of defensins.* Curr. Opin. Struct. Biol., 1995. **5**: p. 521-527.
86. Bowdish, D., D. Davidson, and R. Hancock, *Immunomodulatory Properties of Defensins and Cathelicidins*, in *Antimicrobial Peptides and Human Disease*, W.M. Shafer, Editor. 2006, Springer Berlin Heidelberg. p. 27-66.
87. Harder, J., et al., *Mucoid Pseudomonas aeruginosa, TNF-alpha, and IL-1beta, but not IL-6, induce human beta-defensin-2 in respiratory epithelia.* Am J Resp Cell Mol Biol, 2000. **22**(6): p. 714-721.
88. Krishnakumari, V., N. Rangaraj, and R. Nagaraj, *Antifungal activities of human beta-defensins HBD-1 to HBD-3 and their C-terminal analogs Phd1 to Phd3.* Antimicrob. Agents Chemother., 2009. **53**(1): p. 256-260.
89. Ganz, T., et al., *Defensins: natural peptide antibiotics of human neutrophils.* J Clin Invest, 1985. **76**: p. 1427-35.
90. Ganz, T. and R.I. Lehrer, *Defensins.* Pharmacol. Ther., 1995. **66**: p. 191-205.
91. Selsted, M.E., et al., *Enteric defensins. Antibiotic peptide components of intestinal host defense.* J. Cell Biol., 1992. **118**: p. 929.
92. Jones, D.E. and C.L. Bevins, *Defensin-6 mRNA in human Paneth cells: implications for antimicrobial peptides in host defense of the human bowel.* FEBS Lett., 1993. **315**(2): p. 187-192.
93. Jones, D.E. and C.L. Bevins, *Paneth cells of the human small intestine express an antimicrobial peptide gene.* J. Biol. Chem., 1992. **267**(32): p. 23216-23225.
94. Hancock, R.E. and G. Diamond, *The role of cationic antimicrobial peptides in innate host defences.* Trends Microbiol., 2000. **8**(9): p. 402-410.
95. Huttner, K.M. and C.L. Bevins, *Antimicrobial peptides as mediators of epithelial host defense.* Pediatr. Res., 1999. **45**(6): p. 785-794.
96. Zhao, C., I. Wang, and R.I. Lehrer, *Widespread expression of beta defensin hBD-1 in human secretory glands and epithelial cells.* FEBS Lett., 1996. **396**: p. 319-322.
97. Harder, J., et al., *A peptide antibiotic from human skin.* Nature, 1997. **387**(6636): p. 861.
98. Harder, J., et al., *Isolation and characterization of human beta -defensin-3, a novel human inducible peptide antibiotic.* J. Biol. Chem., 2001 Feb. **276**(8): p. 5707-5713.
99. Selsted, M.E., et al., *Primary structures of MCP-1 and MCP-2, natural peptide antibiotics of rabbit lung macrophages.* J. Biol. Chem., 1983. **258**(23): p. 14485-14489.
100. Lehrer, R.I., et al., *Antibacterial activity of microbicidal cationic proteins 1 and 2, natural peptide antibiotics of rabbit lung macrophages.* Infect. Immun., 1983. **42**(1): p. 10-14.

101. Cunliffe, R.N., *α-Defensins in the gastrointestinal tract.* Mol. Immunol., 2003. **40**(7): p. 463-467.
102. Selsted, M.E., et al., *Primary structures of three human neutrophil defensins.* J. Clin. Invest., 1985. **76**(4): p. 1436-1439.
103. Wilde, C.G., et al., *Purification and characterization of human neutrophil peptide 4, a novel member of the defensin family.* J. Biol. Chem., 1989. **264**(19): p. 11200-11203.
104. Hill, C.P., et al., *Crystal structure of defensin HNP-3, an amphiphilic dimer: mechanisms of membrane permeabilization.* Science, 1991. **251**(5000): p. 1481-1485.
105. Szyk, A., et al., *Crystal structures of human α-defensins HNP4, HD5 and HD6.* Protein Sci., 2006. **15**: p. 2749–2760.
106. Diamond, G., et al., *Tracheal antimicrobial peptide, a cystein rich peptide from mammalian tracheal mucosa: peptide isolation and cloning of a cDNA.* Proc Natl Acad Sci U. S. A, 1991. **88**: p. 3952-3956.
107. Selsted, M.E., et al., *Purification, primary structures, and antibacterial activities of beta-defensins, a new family of antimicrobial peptides from bovine neutrophils.* J. Biol. Chem., 1993. **268**(9): p. 6641-6648.
108. Bensch, K.W., et al., *hBD-1: a novel β-defensin from human plasma.* FEBS Lett., 1995. **368**(2): p. 331-335.
109. Valore, E.V., et al., *Human beta-defensin-1: an antimicrobial peptide of urogenital tissues.* J. Clin. Invest., 1998. **101**(8): p. 1633-1642.
110. McCray, P.B., Jr. and L. Bentley, *Human airway epithelia express a beta-defensin.* Am J Resp Cell Mol Biol, 1997. **16**(3): p. 343-349.
111. Tang, Y.-Q., et al., *A cyclic antimicrobial peptide produced in primate leukocytes by the ligation of two truncated α-defensins.* Science, 1999. **286**(5439): p. 498-502.
112. Garcia, A.E., et al., *Isolation, synthesis, and antimicrobial activities of naturally occurring theta-defensin isoforms from baboon leukocytes.* Infect. Immun., 2008. **76**(12): p. 5883-5891.
113. Leonova, L., et al., *Circular minidefensins and posttranslational generation of molecular diversity.* J. Leukoc. Biol., 2001. **70**(3): p. 461-464.
114. Tran, D., et al., *Homodimeric theta-defensins from rhesus macaque leukocytes: isolation, synthesis, antimicrobial activities, and bacterial binding properties of the cyclic peptides.* J. Biol. Chem., 2002 Feb. **277**(5): p. 3079-3084.
115. Nguyen, T.X., A.M. Cole, and R.I. Lehrer, *Evolution of primate [theta]-defensins: a serpentine path to a sweet tooth.* Peptides, 2003. **24**(11): p. 1647-1654.
116. Cole, A.M., et al., *Retrocyclin: a primate peptide that protects cells from infection by T- and M-tropic strains of HIV-1.* Proc. Natl. Acad. Sci. U. S. A., 2002. **99**(4): p. 1813-1818.
117. Venkataraman, N., et al., *Reawakening retrocyclins: Ancestral human defensins active against HIV-1.* PLoS Biol, 2009. **7**(4): p. e95.
118. Zanetti, M., R. Gennaro, and D. Romeo, *Cathelicidins: a novel protein family with a common proregion and a variable C-terminal antimicrobial domain.* FEBS Lett., 1995. **374**(1): p. 1-5.

119. Larrick, J.W., et al., *Human CAP18: a novel antimicrobial lipopolysaccharide-binding protein.* Infect. Immun., 1995. **63**(4): p. 1291-1297.
120. Sorensen, O., et al., *The human antibacterial cathelicidin, hCAP-18, is synthesized in myelocytes and metamyelocytes and localized to specific granules in neutrophils.* Blood, 1997. **90**(7): p. 2796-2803.
121. Ganz, T. and R.I. Lehrer, *Antimicrobial peptides of leucocytes.* Curr. Opin. Hematol., 1997. **4**: p. 53-8.
122. Abergerth, B., *The human antimicrobial and chemotactic peptides LL-37 and α-defensins are expressed by specific lymphocytes and monocytes populations.* Blood, 2000. **96**: p. 3086-3093.
123. Yang, D., *LL-37, the neutrophil granule- and epithelial cell-derived cathelicidin, utilyzes formyl peptide receptor-like 1 (FPRL1) as a good receptor to chemoattract human peripheral blood neutrophils, monocytes, and T-cells.* J. Exp. Med., 2000. **192**: p. 1064-1074.
124. Gallo, R.L. and V. Nizet, *Endogenous production of antimicrobial peptides in innate immunity and human disease.* Curr. Allergy Asthma Rep., 2003. **3**: p. 402-409.
125. Gallo, R.L., et al., *Biology and clinical reference of naturally occuring antimicrobial peptides.* J. Allergy Clin. Immunol., 2002. **110**: p. 823-831.
126. Ong, P.Y., et al., *Endogenous antimicrobial peptides and skin infections in atopic dermatitis.* N. Engl. J. Med., 2002. **347**(15): p. 1151-1160.
127. Dorschner, R.A., et al., *Cutaneous Injury Induces the Release of Cathelicidin Anti-Microbial Peptides Active Against Group A Streptococcus.* J. Invest. Dermatol., 2001. **117**(1): p. 91-97.
128. Turner, J., et al., *Activitities of LL-37, a cathelin-associated antimicrobial peptide of human neutrophils.* Antimicrob. Agents Chemother., 1998. **42**: p. 2206-14.
129. Sack, R.A., *Host defense mechanism of the ocular surface.* Biosci. Rep., 2001. **21**(4): p. 463-480.
130. Agerberth, B., et al., *FALL-39, a putative human peptide antibiotic, is cyctein-free and expressed in bone marrow and testis. .* Proc. Natl. Acad. Sci. U. S. A, 1995. **92**: p. 195-199.
131. Frohm, M., et al., *The expression of the gene coding for the antibacterial peptide LL-37 is induced in human keratinocytes during inflammatory disorders.* J. Biol. Chem., 1997. **272**: p. 15258-15263.
132. Travis, S.M., *Bactericidal activity of mammalian cathelicidin-derived peptides.* Infec Immunol, 2000. **68**: p. 2748-2755.
133. Zanetti, M., et al., *Cathelicidin peptides as candidates for a novel class of antimicrobials.* Curr. Pharm. Des., 2002. **8**: p. 779-793.
134. McManus, A.M., et al., *Three dimensional structure of RK-1: a novel α–defensin peptide.* Biochemistry, 2000. **39**: p. 15757-15764.
135. Jing, W., et al., *Solution structure of cryptdin-4, a mouse paneth cell α-defensin.* Biochemistry, 2004. **43**: p. 15759-15766.
136. Ganz, T., *The Role of Antimicrobial Peptides in Innate Immunity.* Integr. Comp. Biol., 2003. **43**(2): p. 300-304.
137. Ganz, T., et al., *Defensins. Natural peptide antibiotics of human neutrophils.* J. Clin. Invest., 1985. **76**(4): p. 1427-1435.

138. Lehrer, R.I., et al., *Direct inactivation of viruses by MCP-1 and MCP-2, natural peptide antibiotics from rabbit leukocytes.* J. Virol., 1985. **54**(2): p. 467-472.
139. Hiratsuka, T., et al., *Identification of Human β-Defensin-2 in Respiratory Tract and Plasma and Its Increase in Bacterial Pneumonia.* Biochem. Biophys. Res. Commun., 1998. **249**(3): p. 943-947.
140. Lehrer, R.I., et al., *Interaction of human defensins with Escherichia coli. Mechanism of bactericidal activity.* J. Clin. Invest., 1989. **84**(2): p. 553-561.
141. Schröder, J.M., *Epithelial antimicrobial peptides: innate local host response elements.* Cell. Mol. Life Sci., 1999. **56**(1): p. 32-46.
142. Sahl, H.-G., et al., *Mammalian defensins: structures and mechanism of antibiotic activity.* J. Leukoc. Biol., 2005. **77**(4): p. 466-475.
143. Hoover, D.M., et al., *The Structure of Human β-Defensin-2 Shows Evidence of Higher Order Oligomerization.* J. Biol. Chem., 2000. **275**(42): p. 32911-32918.
144. Hoover, D.M., O. Chertov, and J. Lubkowski, *The structure of human beta-defensin-1: new insights into structural properties of beta-defensins.* J. Biol. Chem., 2001 Oct 19. **276**(42): p. 39021-39026.
145. Niyonsaba, F., et al., *Evaluation of the effects of peptide antibiotics human β-defensins-1/-2 and LL-37 on histamine release and prostaglandin D(2) production from mast cells.* Eur. J. Immunol., 2001. **31**: p. 1066-75.
146. Niyonsaba, F., et al., *Epithelial cell-derived human β-defensin-2 acts as a chemotaxin for mast cells through a pertussis toxin sensitive and phospholipase C-dependant pathway.* Int. Immunol., 2002. **14**: p. 421-6.
147. Niyonsaba, F., H. Ogawa, and I. Nagaoka, *Human β-defensin-2 functions as a chemotactic agent for tumour necrosis factor-α-treated human neutrophils.* Immunology, 2004. **111**(3): p. 273-281.
148. Fellermann, K., et al., *A chromosome 8 gene-cluster polymorphism with low human beta-defensin 2 gene copy number predisposes to Crohn's disease of the colon.* Am. J. Hum. Genet., 2006. **79**(3): p. 439-448.
149. Wehkamp, J., et al., *NOD2 (CARD15) mutations in Crohn's disease are associated with diminished mucosal α-defensin expression.* Gut, 2004. **53**(11): p. 1658-1664.
150. Yang, D., et al., *Multiple roles of antimicrobial defensins, cathelicidins, and eosinophil-derived neurotoxin in host defense.* Annu. Rev. Immunol., 2004. **22**: p. 181-215.
151. Hancock, R.E., *Cation peptides: effectors in innate immunity and novel antimicrobials.* Lancet Infect Dis, 2001. **1**: p. 156-164.
152. Steinstraesser, L., *Protegrin-1 increases bacterial clearance in sepsis but decreases survival.* Crit. Care Med., 2003. **31**: p. 221-226.
153. Steinstraesser, L., *Activity of novispirin G10 against Pseudomonas aeruginosa in vitro and in infected burns.* Antimicrob. Agents Chemother., 2002. **46**: p. 1837-1844.
154. Singer, A.J. and R.A.F. Clark, *Cutaneous wound healing.* N. Engl. J. Med., 1999. **341**(10): p. 738-746.
155. Oono, T., et al., *Effects of human neutrophil peptide-1 on the expression of interstitial collagenase and type I collagen in human dermal fibroblasts.* Arch. Dermatol. Res., 2002. **294**(4): p. 185-189.

156. Yenegu, S., et al., *The androgen-regulated epididymal sperm-binding protein, human β-defensins 118 (DEFB118) (formerly ESC42), is an antimicrobial β-defensin.* Endocrinology, 2004. **145**: p. 3165-3173.
157. Zhou, C.X., et al., *An epididymis specific β-defensin is important for the inititation of sperm maturation.* Nat. Cell Biol., 2004. **6**: p. 458-464.
158. Koczulla, R., et al., *An angiogenic role for the human peptide antibiotic LL-37/hCAP-18.* J. Clin. Invest., 2003. **111**(11): p. 1665-1672.
159. Koczulla, R. and R. Bals, *Cathelicidin antimicrobial peptides modulate angiogenesis*, in *Therapeutic Neovascularization–Quo Vadis?*, E. Deindl and C. Kupatt, Editors. 2007, Springer Netherlands. p. 191-196.
160. Bullard, R.S., et al., *Functional analysis of the host defense peptide Human Beta Defensin-1: New insight into its potential role in cancer.* Mol. Immunol., 2008. **45**(3): p. 839-848.
161. Droin, N., et al., *Human defensins as cancer biomarkers and antitumour molecules.* J. Proteomics, 2009. **72**(6): p. 918-927.
162. Okumura, K., et al., *C-terminal domain of human CAP18 antimicrobial peptide induces apoptosis in oral squamous cell carcinoma SAS-H1 cells.* Cancer Lett., 2004. **212**: p. 185-194.
163. Candille, S.I., et al., *A β-defensin -defensin mutation causes black coat color in domestic dogs.* Science, 2007 Oct 18. **318**(5855): p. 1418-1423.
164. Gottsch, J.D., et al., *Defensin gene expression in the cornea.* Curr. Eye Res., 1998. **17**(11): p. 1082-1086.
165. Haynes, J.R., P.J. Tighe, and H.S. Dua, *Innate defense of the eye by antimicrobial defensin peptide.* Lancet, 1998. **352**: p. 451-452.
166. Hattenbach, L.-O., H. Gümbel, and S. Kippenberger, *Identification of beta-defensins in human conjunctiva.* Antimicrob. Agents Chemother., 1998. **42**(12): p. 3332.
167. Zhou, L., et al., *Proteomic analysis of human tears: defensin expression after ocular surface surgery.* J. Proteom. Res., 2004. **3**(3): p. 410-416.
168. Haynes, J.R., P.J. Tighe, and H.S. Dua, *Antimicrobial defensins peptides of the human ocular surface.* Br. J. Ophthalmol., 1999. **83**: p. 737-742.
169. Lehmann, O.J., I.R. Hussain, and P.J. Watt, *Investigation of beta defensin gene expression in the ocular anterior segment by semiquantitative RT-PCR.* Br. J. Ophthalmol., 2000. **84**(5): p. 523-526.
170. McDermott, A.M., et al., *Defensin expression by the cornea: multiple signalling pathways mediate IL-1beta stimulation of hBD-2 expression by human corneal epithelial cells.* Invest. Ophthalmol. Vis. Sci., 2003. **44**(5): p. 1859-1865.
171. McNamara, N.A., et al., *Ocular Surface Epithelia Express mRNA for Human Beta Defensin-2.* Exp. Eye Res., 1999. **69**(5): p. 483-490.
172. Narayanan, S., W.L. Miller, and A.M. McDermott, *Expression of human β-defensins in conjunctival epithelium: relevance to dry eye disease.* Invest. Ophthalmol. Vis. Sci., 2003. **44**: p. 3795-3801.
173. Matseva I, M.N., Fleiszig SMJ, Basbaum C, *NFKB is involved in Pseudomonas aeruginosa-mediated transcriptional regulation of the human beta defensin gene in human corneal epithelial cells.*, in *ARVO*. 2002: USA.

174. Wada, A., et al., *Helicobacter pylori-mediated transcriptional regulation of the human β-defensin 2 gene requires NF-κB.* Cell. Microbiol., 2001. **3**(2): p. 115-123.
175. O'Neil, D.A., et al., *Expression and regulation of the human beta-defensins hBD-1 and hBD-2 in intestinal epithelium.* J. Immunol., 1999. **163**(12): p. 6718-6724.
176. Birchler, T., et al., *Human Toll-like receptor 2 mediates induction of the antimicrobial peptide human beta-defensin 2 in response to bacterial lipoprotein.* Eur. J. Immunol., 2001. **31**(11): p. 3131-3137.
177. Wang, X., et al., *Airway epithelia regulate expression of human beta-defensin 2 through Toll-like receptor 2.* FASEB J., 2003 Jul. **17**(12): p. 1727-9.
178. McDermott, A.M., R.L. Redfern, and B. Zhang, *Human beta-defensin 2 is up-regulated during re-epithelialization of the cornea.* Curr. Eye Res., 2001. **22**(1): p. 64-67.
179. Nomura, I., et al., *Cytokine milieu of atopic dermatitis, as compared to psoriasis, skin prevents induction of innate immune response genes.* J. Immunol., 2003. **171**(6): p. 3262-3269.
180. García, J.-R., et al., *Identification of a novel, multifunctional β-defensin (human β-defensin 3) with specific antimicrobial activity.* Cell Tissue Res., 2001. **306**(2): p. 257-264.
181. Kawasaki, S., et al., *Up-Regulated Gene Expression in the Conjunctival Epithelium of Patients With Sjogren's Syndrome.* Exp. Eye Res., 2003. **77**(1): p. 17-26.
182. Stern, M.E. and S.C. Pflugfelder, *Inflammation in dry eye.* Ocul. Surf., 2004. **2**(2): p. 124-130.
183. Pflugfelder, S.C., et al., *Altered cytokine balance in the tear fluid and conjunctiva of patients with Sjogren's syndrome keratoconjunctivitis sicca.* Curr. Eye Res., 1999. **19**(3): p. 201-211.
184. Solomon, A., et al., *Pro- and anti-inflammatory forms of interleukin-1 in the tear fluid and conjunctiva of patients with dry-eye disease.* Invest. Ophthalmol. Vis. Sci., 2001. **42**(10): p. 2283-2292.
185. McIntosh, R.S., et al., *The spectrum of antimicrobial peptide expression at the ocular surface.* Invest. Ophthalmol. Vis. Sci., 2005 Apr. **46**(4): p. 1379-1385.
186. Garreis, F., et al., *Roles of human β-defensins in innate immune defence at the ocular surface: arming and alarming corneal and conjunctival epithelial cells.* Histochem. Cell Biol., 2010. **134**(1): p. 59-73.
187. Abedin, A., et al., *A novel antimicrobial peptide on the ocular surface shows decreased expression in inflammation and infection.* Invest. Ophthalmol. Vis. Sci., 2008 Jan. **49**(1): p. 28-33.
188. Premratanachai, P., et al., *Expression and regulation of novel human beta-defensins in gingival keratinocytes.* Oral Microbiol. Immunol., 2004. **19**(2): p. 111-117.
189. Islam, D., et al., *Downregulation of bactericidal peptides in enteric infections: A novel immune escape mechanism with bacterial DNA as a potential regulator.* Nat. Med., 2001. **7**(2): p. 180-185.
190. Nakatsuji, T. and R.L. Gallo, *Antimicrobial Peptides: Old Molecules with New Ideas.* J. Invest. Dermatol., 2012. **132**(3): p. 887-895.

191. Zhang, L. and T.J. Falla, *Antimicrobial peptides: therapeutic potential.* Expert Opin. Pharmacol., 2006. **7**(6): p. 653-663.
192. Loo, W.T., et al., *Clinical application of human beta-defensin and CD14 gene polymorphism in evaluating the status of chronic inflammation.* J. Transl. Med., 2012 Sep 19. **10**(Suppl 1): p. S1-S9.
193. Singh, P., *Integration of defensins: A promising clinical tool.* Int. J. Prev. Med., 2013. **4**(7): p. 861-862.
194. Zhang L, P.S., Harris SM, Falla TJ, *Broad spectrum antimicrobial and antiviral peptides for the prevention of sexually-transmitted diseases*, in *American society of Microbiology*. 2004: New Orleans, LA.
195. Kristensen, H., *Plectasin - systematic applications of an antimicrobial peptide.*, in *American Society of Microbiology*. 2004: New Orleans, LA.
196. Levin, M., *Recombinant bactericidal/permeability-increasing protein (rBPI21) as adjunctive treatment for treatment of children with severe meningococcal sepsis: a randomised clinical trial. rBPI21 Meningococcal Sepsis Study Group.* Lancet, 2000. **356**: p. 961-967.
197. Giroir, B.P., P.J. Scannon, and M. Levin, *Bactericidal/permeability-increasing protein--lessons learned from the phase III, randomized, clinical trial of rBPI21 for adjunctive treatment of children with severe meningococcemia.* Crit. Care Med., 2001. **29**(7 Suppl): p. S130-S135.
198. Nos-Barbera, S., et al., *Effect of Hybrid Peptides of Cecropin A and Melittin in an Experimental Model of Bacterial Keratitis.* Cornea, 1997. **16**(1): p. 101-106.
199. Mannis, M., *The use of antimicrobial peptides in ophthalmology: an experimental study in corneal preservation and the management of bacterial keratitis.* Trans. Am. Ophthalmol. Soc., 2002. **100**: p. 243-71.
200. McDermott, A.M., et al., *The in vitro activity of selected defensins against an isolate of Pseudomonas in the presence of human tears.* Br. J. Ophthalmol., 2006. **90**(5): p. 609-611.
201. Huang, L., et al., *Human Tears Inhibit the Antimicrobial Activity of Human beta-Defensin-2 In Vitro.* Invest. Ophthalmol. Vis. Sci., 2002. **43**(13): p. 82.
202. Singh, P.K., et al., *Synergistic and additive killing by antimicrobial factors found in human airway surface liquid.* Am. J. Physiol. Lung Cell. Mol. Physiol., 2000. **279**(5): p. L799-805.
203. Yan, H. and R.E.W. Hancock, *Synergistic Interactions between Mammalian Antimicrobial Defense Peptides.* Antimicrob. Agents Chemother., 2001. **45**(5): p. 1558-1560.
204. Pazgier, M., et al., *Human β–defensins.* Cell. Mol. Life Sci., 2006. **63**: p. 1294-1313.
205. Abiko, Y., et al., *Role of β-defensin in oral epithelial health and disease.* Med. Mol. Morphol., 2007. **40**: p. 179-184.
206. Human Genome Sequencing, C.I., *Finishing the euchromatic sequence of the human genome.* Nature, 2004. **431**(7011): p. 931-945.
207. Baca, A.M. and W.G. Hol, *Overcoming codon bias: a method for high-level overexpression of Plasmodium and other AT-rich parasite genes in Escherichia coli.* Int. J. Parasitol., 2000. **30**(2): p. 113-118.
208. Lee, S.F., Y.-J. Li, and S.A. Halperin, *Overcoming codon-usage bias in heterologous protein expression in Streptococcus gordonii.* Microbiology, 2009. **155**(11): p. 3581-3588.

209. Semple, C.A., et al., *The changing of the guard: Molecular diversity and rapid evolution of beta-defensins.* Mol. Divers., 2006. **10**(4): p. 575-584.
210. Radhakrishnan, Y., et al., *Identification, characterization, and evolution of a primate beta-defensin gene cluster.* Genes Immune., 2005. **6**(3): p. 203-210.
211. Patil, A., A.L. Hughes, and G. Zhang, *Rapid evolution and diversification of mammalian alpha-defensins as revealed by comparative analysis of rodent and primate genes.* Physiol. Genomics, 2004 Dec **20**(1): p. 1-11.
212. Patil, A., et al., *Cross-species analysis of the mammalian beta-defensin gene family: presence of syntenic gene clusters and preferential expression in the male reproductive tract.* Physiol. Genomics, 2005 Sep. **23**(1): p. 5-17.
213. Xiao, Y., et al., *A genome-wide screen identifies a single beta-defensin gene cluster in the chicken: implications for the origin and evolution of mammalian defensins.* BMC Genomics, 2004. **5**(1): p. 56.
214. Harder, J., et al., *Mapping of the Gene Encoding Human [beta]-Defensin-2 (DEFB2) to Chromosome Region 8p22-p23.1.* Genomics, 1997. **46**(3): p. 472-475.
215. Liu, L., et al., *Structure and mapping of the human [beta]-defensin HBD-2 gene and its expression at sites of inflammation.* Gene, 1998. **222**(2): p. 237-244.
216. Linzmeier, R., et al., *A 450-kb contig of defensin genes on human chromosome 8p23.* Gene, 1999. **233**(1-2): p. 205-211.
217. Ballana, E., et al., *Inter-population variability of DEFA3 gene absence: correlation with haplotype structure and population variability.* BMC Genomics, 2007. **8**(1): p. 14.
218. Taudien, S., et al., *Polymorphic segmental duplications at 8p23.1 challenge the determination of individual defensin gene repertoires and the assembly of a contiguous human reference sequence.* BMC Genomics, 2004. **5**: p. 92-92.
219. Ouellette, A.J., et al., *Localization of the cryptdin locus on mouse chromosome 8.* Genomics, 1989. **5**(2): p. 233-239.
220. Bevins, C.L., et al., *Human Enteric Defensin Genes: Chromosomal Map Position and a Model for Possible Evolutionary Relationships.* Genomics, 1996. **31**(1): p. 95-106.
221. Iannuzzi, L., et al., *High-resolution FISH mapping of beta-defensin genes to river buffalo and sheep chromosomes suggests a chromosome discrepancy in ffttle standard karyotypes.* Cytogenet. Cell Genet., 1996. **75**(1): p. 10-13.
222. Schutte, B.C., et al., *Discovery of five conserved beta -defensin gene clusters using a computational search strategy.* Proc. Natl. Acad. Sci. U. S. A., 2002. **99**(4): p. 2129-2133.
223. Radhakrishnan, Y., et al., *Comparative genomic analysis of a mammalian β-defensin gene cluster.* Physiol. Genomics, 2007. **30**(3): p. 213-222.
224. Rodríguez-Jiménez, F., et al., *Distribution of new human [beta]-defensin genes clustered on chromosome 20 in functionally different segments of epididymis.* Genomics, 2003. **81**(2): p. 175-183.

225. Kao, C.Y., et al., *ORFeome-Based Search of Airway Epithelial Cell-Specific Novel Human {beta}-Defensin Genes.* Am. J. Respir. Cell Mol. Biol., 2003. **29**(1): p. 71-80.
226. Semple, C., M. Rolfe, and J. Dorin, *Duplication and selection in the evolution of primate beta-defensin genes.* Genome Biol., 2003. **4**(Genome Biology): p. R31.
227. Abu Bakar, S., E.J. Hollox, and J.A. Armour, *Allelic recombination between distinct genomic locations generates copy number diversity in human beta-defensins.* Proc. Natl. Acad. Sci. U. S. A., 2009 Jan. **106**(3): p. 853-858.
228. Morrison, G.M., et al., *Signal Sequence Conservation and Mature Peptide Divergence Within Subgroups of the Murine β-Defensin Gene Family.* Mol. Biol. Evol., 2003. **20**(3): p. 460-470.
229. Lehrer, R.I., *Primate defensins. Nat. Rev. Microbiol*, 2004. **2**: p. 727-738.
230. Linzmeier, R.M. and T. Ganz, *Human defensin gene copy number polymorphisms: Comprehensive analysis of independent variation in [alpha]- and [beta]-defensin regions at 8p22-p23.* Genomics, 2005. **86**(4): p. 423-430.
231. Mohammed, I., et al., *Localization and Gene Expression of Human β-Defensin 9 at the Human Ocular Surface Epithelium.* Invest. Ophthalmol. Vis. Sci., 2010. **51**(9): p. 4677-4682.
232. Otri, A.M., et al., *Antimicrobial peptides expression by ocular surface cells in response to Acanthamoeba castellanii: an in vitro study.* Br. J. Ophthalmol., 2010. **94**(11): p. 1523-1527.
233. Hopkinson, A., et al., *Optimization of amniotic membrane (AM) denuding for tissue engineering.* Tissue Eng Part C Methods, (10): p. 2008 Dec;14(4):371-81.
234. Serganov, A., et al., *Do mRNA and rRNA binding sites of E.coli ribosomal protein S15 share common structural determinants?* J. Mol. Biol., 2002. **320**(5): p. 963-978.
235. Rosano, G.L. and E.A. Ceccarelli, *Rare codon content affects the solubility of recombinant proteins in a codon bias-adjusted Escherichia coli strain.* Microb. Cell Fact., 2009. **8**: p. 41.
236. Chen, H., et al., *Recent advances in the research and development of human defensins.* Peptides, 2006. **27**(4): p. 931-940.
237. Hu, X., et al., *Specific replacement of consecutive AGG codons results in high-level expression of human cardiac troponin T in Escherichia coli.* Protein Expr. Purif., 1996. **7**(3): p. 289-293.
238. Kane, J.F., *Effects of rare codon clusters on high-level expression of heterologous proteins in Escherichia coli.* Curr. Opin. Biotechnol., 1995. **6**(5): p. 494-500.
239. Puigbò, P., et al., *OPTIMIZER: a web server for optimizing the codon usage of DNA sequences.* Nucleic Acids Res., 2007. **35**(suppl 2): p. W126-W131.
240. Pearson, W.R., et al., *Comparison of DNA sequences with protein sequences.* Genomics, 1997. **46**(1): p. 24-36.

241. Terpe, K., *Overview of bacterial expression systems for heterologous protein production: from molecular and biochemical fundamentals to commercial systems.* Appl. Microbiol. Biotechnol., 2006 Sept. **72**(2): p. 211-222.
242. Xu, Z., et al., *High-Level Expression of a Soluble Functional Antimicrobial Peptide, Human β-Defensin 2, in Escherichia coli.* Biotechnol. Progr., 2006. **22**(2): p. 382-386.
243. Peng, L., et al., *High-level expression of soluble human β-defensin-2 in Escherichia coli.* Process Biochem., 2004. **39**(12): p. 2199-2205.
244. Peng, L., et al., *Preferential Codons Enhancing the Expression Level of Human Beta-Defensin-2 in Recombinant Escherichia Coli.* Protein Pept. Lett., 2004. **11**(4): p. 339-344.
245. Huang, L., et al., *Production of Bioactive Human β-defensin-3 in Escherichia coli by Soluble Fusion Expression.* Biotechnol. Lett., 2006. **28**(9): p. 627-632.
246. Demain, A.L. and P. Vaishnav, *Production of recombinant proteins by microbes and higher organisms.* Biotechnol. Adv. **27**(3): p. 297-306.
247. Idicula-Thomas, S. and P.V. Balaji, *Understanding the relationship between the primary structure of proteins and its propensity to be soluble on overexpression in Escherichia coli.* Protein Sci., 2005. **14**(3): p. 582-592.
248. Saida, F., et al., *Expression of highly toxic genes in E. coli: special strategies and genetic tools.* Curr Protein Pept Sci, 2006. **7**(1): p. 47-56.
249. Guzman, L.M., et al., *Tight regulation, modulation, and high-level expression by vectors containing the arabinose PBAD promoter.* J. Bacteriol., 1995. **177**(14): p. 4121-4130.
250. Wang, R.F. and S.R. Kushner, *Construction of versatile low-copy-number vectors for cloning, sequencing and gene expression in Escherichia coli.* Gene, 1991. **100**: p. 195-9.
251. LaVallie, E.R., et al., *A Thioredoxin Gene Fusion Expression System That Circumvents Inclusion Body Formation in the E. coli Cytoplasm.* Nat. Biotech., 1993. **11**(2): p. 187-193.
252. Terpe, K., *Overview of tag protein fusions: from molecular and biochemical fundamentals to commercial systems.* Appl. Microbiol. Biotechnol., 2003. **60**(5): p. 523-533.
253. Xu, Z., et al., *High-level production of bioactive human beta-defensin-4 in Escherichia coli by soluble fusion expression.* Appl. Microbiol. Biotechnol., 2006. **72**(3): p. 471-479.
254. Rosano, G.L. and E.A. Ceccarelli, *Recombinant protein expression in Escherichia coli: advances and challenges.* Front. Microbiol., 2014. **5**: p. 172.
255. Vera, A., et al., *The conformational quality of insoluble recombinant proteins is enhanced at low growth temperatures.* Biotechnol. Bioeng., 2007. **96**(6): p. 1101-1106.
256. San-Miguel, T., P. Pérez-Bermúdez, and I. Gavidia, *Production of soluble eukaryotic recombinant proteins in E. coli is favoured in early log-phase cultures induced at low temperature.* SpringerPlus, 2013. **2**: p. 89.

257. Strocchi, M., et al., *Low temperature-induced systems failure in Escherichia coli: Insights from rescue by cold-adapted chaperones.* Proteomics, 2006. **6**(1): p. 193-206.
258. Ferrer, M., et al., *Expression of a Temperature-Sensitive Esterase in a Novel Chaperone-Based Escherichia coli Strain.* Appl. Environ. Microbiol., 2004. **70**(8): p. 4499-4504.
259. Stewart, E.J., F. Aslund, and J. Beckwith, *Disulfide bond formation in the Escherichia coli cytoplasm: an in vivo role reversal for the thioredoxins.* EMBO J., 1998. **17**(19): p. 5543-5550.
260. Schneider, C.A., W.S. Rasband, and K.W. Eliceiri, *NIH Image to ImageJ: 25 years of image analysis.* Nat. Meth., 2012. **9**(7): p. 671-675.
261. Carter, J., et al., *Fusion partners can increase the expression of recombinant interleukins via transient transfection in 2936E cells.* Protein Sci., (10): p. 2010 Feb;19(2):357-62.
262. Porath, J., *Immobilized metal ion affinity chromatography.* Protein Expr. Purif., 1992. **3**(4): p. 263-281.
263. Porath, J., et al., *Metal chelate affinity chromatography, a new approach to protein fractionation.* Nature, 1975. **258**: p. 598-599.
264. Hochuli, E., H. Dobeli, and A. Schacher, *New metal chelate adsorbent selective for proteins and peptides containing neighbouring histidine residues.* J. Chromatogr., 1987. **411**: p. 177-84.
265. Chaga, G., J. Hopp, and P. Nelson, *Immobilized metal ion affinity chromatography on Co2+-carboxymethylaspartate-agarose Superflow, as demonstrated by one-step purification of lactate dehydrogenase from chicken breast muscle.* Biotechnol. Appl. Biochem., 1999. **29**(Pt 1): p. 19-24.
266. Bornhorst, J.A. and J.J. Falke, *[16] Purification of proteins using polyhistidine affinity tags*, in *Methods Enzymol.*, S.D.E.J.N.A. Jeremy Thorner, Editor. 2000, Academic Press. p. 245-254.
267. Schmitt, J., H. Hess, and H.G. Stunnenberg, *Affinity purification of histidine-tagged proteins.* Mol. Biol. Rep., 1993. **18**(3): p. 223-30.
268. Knecht, S., et al., *Oligohis-tags: mechanisms of binding to Ni2+-NTA surfaces.* J. Mol. Recogn., 2009. **22**(4): p. 270-279.
269. Lindeberg, G., H. Bennich, and A. Engstrom, *Purification of synthetic peptides. Immobilized metal ion affinity chromatography (IMAC).* Int. J. Pept. Protein Res., 1991. **38**(3): p. 253-259.
270. Khan, F., M. He, and M.J. Taussig, *Double-hexahistidine tag with high-affinity binding for protein immobilization, purification, and detection on ni-nitrilotriacetic acid surfaces.* Anal. Chem., 2006. **78**(9): p. 3072-3079.
271. Chaga, G.S., *Twenty-five years of immobilized metal ion affinity chromatography: past, present and future.* J. Biochem. Bioph. Meth., 2001. **49**(1): p. 313-334.
272. Jenny, R.J., K.G. Mann, and R.L. Lundblad, *A critical review of the methods for cleavage of fusion proteins with thrombin and factor Xa.* Protein Expr. Purif., 2003. **31**(1): p. 1-11s.
273. Parks, T.D., et al., *Expression and purification of a recombinant tobacco etch virus NIa proteinase: biochemical analyses of the full-length and a naturally occurring truncated proteinase form.* Virology, 1995. **210**(1): p. 194-201.

274. Charlton, A. and M. Zachariou, *Tag removal by site-specific cleavage of recombinant fusion proteins.* Methods Mol. Biol., 2011. **681**(10): p. 349-367.
275. Xu, M.Q., H. Paulus, and S. Chong, *Fusions to self-splicing inteins for protein purification.* Methods Enzymol., 2000. **326**: p. 376-418.
276. Collins-Racie, L.A., et al., *Production of recombinant bovine enterokinase catalytic subunit in Escherichia coli using the novel secretory fusion partner DsbA.* Biotechnol, 1995. **13**(9): p. 982-987.
277. Shahravan, S.H., et al., *Enhancing the specificity of the enterokinase cleavage reaction to promote efficient cleavage of a fusion tag.* Protein Expr. Purif., 2008. **59**(2): p. 314-319.
278. Kenig, M., et al., *Influence of the protein oligomericity on final yield after affinity tag removal in purification of recombinant proteins.* J. Chromatogr., 2005 Oct. **1101**(1-2): p. 293-306.
279. Tay, D.K.S., et al., *A new bioproduction route for a novel antimicrobial peptide.* Biotechnol. Bioeng., 2011. **108**(3): p. 572-581.
280. Malakhov, M.P., et al., *SUMO fusions and SUMO-specific protease for efficient expression and purification of proteins.* J. Struct. Funct. Genomics, 2004. **5**(1-2): p. 75-86.
281. Garcia, J.-R.C., et al., *Human β-defensin 4: a novel inducible peptide with a specific salt-sensitive spectrum of antimicrobial activity.* FASEB J., 2001. **15**(10): p. 1819-1821.
282. Huang, L., et al., *Production of bioactive human beta-defensin 5 and 6 in Escherichia coli by soluble fusion expression.* Protein Expr. Purif., 2008. **61**(2): p. 168-174.
283. Schulz, A., et al., *Engineering disulfide bonds of the novel human β-defensins hBD-27 and hBD-28: Differences in disulfide formation and biological activity among human β-defensins.* Pept. Sci., 2005. **80**(1): p. 34-49.
284. Chow, B.T., et al., *Antibacterial Activity of Four Human Beta-Defensins: HBD-19, HBD-23, HBD-27, and HBD-29.* Polymers, 2012. **4**(1): p. 747-758.
285. Tang, Y.Q. and M.E. Selsted, *Characterization of the disulfide motif in BNBD-12, an antimicrobial beta-defensin peptide from bovine neutrophils.* J. Biol. Chem., 1993. **268**(9): p. 6649-6653.
286. Schroder, J.M. and J. Harder, *Human beta-defensin-2.* Int. J. Biochem. Cell Biol., 1999. **31**: p. 645-651.
287. Yamaguchi, Y., et al., *Identification of Multiple Novel Epididymis-Specific β-Defensin Isoforms in Humans and Mice.* J. Immunol., 2002. **169**(5): p. 2516-2523.
288. Ishikawa, C., et al., *Precursor Processing of Human Defensin-5 Is Essential to the Multiple Functions in vitro and in vivo.* J. Innate. Immun., 2010. **2**(1): p. 66-76.
289. Diamond, G., et al., *The roles of antimicrobial peptides in innate host defense.* Curr. Pharm. Des., 2009. **15**(21): p. 2377-92.
290. Chaly, Y.V., et al., *Neutrophil α-defensin human neutrophil peptide modulates cytokine production in human monocytes and adhesion molecules expression in endothelial cells.* Eur. Cytokine Netw., 2000. **11**: p. 257-266.

291. Sahly, H., et al., *Activity of human beta-defensins 2 and 3 against ESBL-producing Klebsiella strains.* J. Antimicrob. Chemother., 2006. **57**(3): p. 562-565.
292. Wu, Z., et al., *Engineering disulfide bridges to dissect antimicrobial and chemotactic activities of human β-defensin 3.* Proc. Natl. Acad. Sci. U. S. A., 2003. **100**(15): p. 8880-8885.
293. Hoover, D.M., et al., *Antimicrobial Characterization of Human {beta}-Defensin 3 Derivatives.* Antimicrob. Agents Chemother., 2003. **47**(9): p. 2804-2809.
294. Kluver, E., et al., *Structure-activity relation of human beta-defensin 3: influence of disulfide bonds and cysteine substitution on antimicrobial activity and cytotoxicity.* Biochemistry (Mosc). 2005. **44**: p. 9804-9816.
295. Krishnakumari, V., S. Singh, and R. Nagaraj, *Antibacterial activities of synthetic peptides corresponding to the carboxy-terminal region of human β-defensins 1–3.* Peptides, 2006. **27**(11): p. 2607-2613.
296. Krishnakumari, V., et al., *Single disulfide and linear analogues corresponding to the carboxy-terminal segment of bovine beta-defensin-2: effects of introducing the beta-hairpin nucleating sequence d-pro-gly on antibacterial activity and Biophysical properties.* Biochemistry (Mosc). 2003. **42**(31): p. 9307-9315.
297. Mandal, M., M.V. Jagannadham, and R. Nagaraj, *Antibacterial activities and conformations of bovine beta-defensin BNBD-12 and analogs:structural and disulfide bridge requirements for activity.* Peptides, 2002. **23**(3): p. 413-418.
298. Bauer, F., et al., *Structure determination of human and murine beta-defensins reveals structural conservation in the absence of significant sequence similarity.* Protein Sci., 2001. **10**(12): p. 2470-2479.
299. Bai, Y., et al., *Structure-Dependent Charge Density as a Determinant of Antimicrobial Activity of Peptide Analogues of Defensin.* Biochemistry (Mosc). 2009. **48**(30): p. 7229-7239.
300. Wieprecht, T., et al., *Peptide Hydrophobicity Controls the Activity and Selectivity of Magainin 2 Amide in Interaction with Membranes.* Biochemistry (Mosc). 1997. **36**(20): p. 6124-6132.
301. Takahashi, D., et al., *Structural determinants of host defense peptides for antimicrobial activity and target cell selectivity.* Biochimie, 2010. **92**(25): p. 1236-1241.
302. Tossi, A., L. Sandri, and A. Giangaspero, *Amphipathic, α-helical antimicrobial peptides.* Pept. Sci., 2000. **55**(1): p. 4-30.
303. Scudiero, O., et al., *Novel Synthetic, Salt-Resistant Analogs of Human Beta-Defensins 1 and 3 Endowed with Enhanced Antimicrobial Activity.* Antimicrob. Agents Chemother., 2010. **54**(6): p. 2312-2322.
304. Goldman, M.J., et al., *Human beta-defensin-1 is a salt-sensitive antibiotic in lung that is inactivated in cystic fibrosis.* Cell, 1997. **88**(4): p. 553-60.
305. Bals, R., et al., *Human beta-defensin 2 is a salt-sensitive peptide antibiotic expressed in human lung.* J. Clin. Invest., 1998. **102**(5): p. 874-880.
306. Boniotto, M., et al., *A study of host defence peptide beta-defensin 3 in primates.* Biochem. J., 2003. **374**(Pt 3): p. 707-714.

307. Tomita, T., et al., *Effect of ions on antibacterial activity of human beta defensin 2.* Microbiol. Immunol., 2000. **44**(9): p. 749-754.
308. Schibli, D.J., et al., *The Solution Structures of the Human β-Defensins Lead to a Better Understanding of the Potent Bactericidal Activity of HBD3 against Staphylococcus aureus.* J. Biol. Chem., 2002. **277**(10): p. 8279-8289.
309. Kaye, M.G., et al., *The clinical spectrum of Staphylococcus aureus pulmonary infection.* Chest, 1990. **97**(4): p. 788-792.
310. Lipsky, B.A., *Medical Treatment of Diabetic Foot Infections.* Clin. Infect. Dis., 2004. **39**(Supplement 2): p. S104-S114.
311. Dart, J.K.G. and D.V. Seal, *Pathogenesis and therapy of pseudomonas aeruginosa keratitis.* Eye, 1988. **2**(S1): p. S46-S55.
312. Holmgren, A., *Thioredoxin and glutaredoxin systems.* J. Biol. Chem., 1989. **264**(24): p. 13963-13966.
313. Husbeck, B., M. Berggren, and G. Powis, *DNA Microarray Reveals Increased Expression of Thioredoxin Peroxidase in Thioredoxin-1 Transfected Cells and Its Functional Consequences*, in *Biological Reactive Intermediates VI*, P. Dansette, et al., Editors. 2001, Springer US. p. 157-168.
314. Powis, G. and W.R. Montfort, *Properties and biological activities of thioredoxins.* Ann. Rev. Pharmacol. Toxicol., 2001. **41**: p. 261-295.
315. Arner, E.S. and A. Holmgren, *Physiological functions of thioredoxin and thioredoxin reductase.* Eur. J. Biochem., 2000. **267**(20): p. 6102-6109.
316. Wu, J., et al., *Molecular analysis and recombinant expression of bovine neutrophil β-defensin 12 and its antimicrobial activity.* Mol. Biol. Rep., 2011. **38**(1): p. 429-436.
317. Yoshida, T., et al., *The involvement of thioredoxin and thioredoxin binding protein-2 on cellular proliferation and aging process.* Ann. N. Y. Acad. Sci., 2005 Dec. **1055**: p. 1-12.
318. Suresh, A. and C. Verma, *Modelling study of dimerization in mammalian defensins.* BMC bioinformatics, 2006. **7** (Suppl 5): p. S17.
319. Kuwano, K., et al., *Antimicrobial activity of inducible human beta defensin-2 against Mycoplasma pneumoniae.* Curr. Microbiol., 2006 Jun. **52**(6): p. 435-438.
320. Veldhuizen, E.J., et al., *Porcine beta-defensin 2 displays broad antimicrobial activity against pathogenic intestinal bacteria.* Mol. Immunol., 2008 Jan. **45**(2): p. 386-394.